

Award Number:  
W81XWH-09-2-0102

TITLE:  
**Traumatic Brain Injury Diffusion Magnetic Resonance Imaging  
Research Roadmap Development Project**

PRINCIPAL INVESTIGATOR:  
Michael W. Vannier, M.D.

CONTRACTING ORGANIZATION:  
University of Chicago

Chicago, IL 60637-5418

REPORT DATE:  
October 2012

TYPE OF REPORT:  
Annual

PREPARED FOR: U.S. Army Medical Research and Materiel Command  
Fort Detrick, Maryland 21702-5012

DISTRIBUTION STATEMENT:

☒ Approved for public release; distribution unlimited

The views, opinions and/or findings contained in this report are those of the author(s) and should not be construed as an official Department of the Army position, policy or decision unless so designated by other documentation.

<b>REPORT DOCUMENTATION PAGE</b>				<i>Form Approved</i> <b>OMB No. 0704-0188</b>	
<small>Public reporting burden for this collection of information is estimated to average 1 hour per response, including the time for reviewing instructions, searching existing data sources, gathering and maintaining the data needed, and completing and reviewing this collection of information. Send comments regarding this burden estimate or any other aspect of this collection of information, including suggestions for reducing this burden to Department of Defense, Washington Headquarters Services, Directorate for Information Operations and Reports (0704-0188), 1215 Jefferson Davis Highway, Suite 1204, Arlington, VA 22202-4302. Respondents should be aware that notwithstanding any other provision of law, no person shall be subject to any penalty for failing to comply with a collection of information if it does not display a currently valid OMB control number. <b>PLEASE DO NOT RETURN YOUR FORM TO THE ABOVE ADDRESS.</b></small>					
<b>1. REPORT DATE</b> October 2012		<b>2. REPORT TYPE</b> Annual		<b>3. DATES COVERED</b> 14 September 2011- 13 September 2012	
<b>4. TITLE AND SUBTITLE</b> Traumatic Brain Injury Diffusion Magnetic Resonance Imaging Research Roadmap Development Project				<b>5a. CONTRACT NUMBER</b>	
				<b>5b. GRANT NUMBER</b> W81XWH-09-2-0102	
				<b>5c. PROGRAM ELEMENT NUMBER</b>	
<b>6. AUTHOR(S)</b> Michael W. Vannier, M.D.  <b>E-Mail:</b> mvannier@radiology.bsd.uchicago.edu				<b>5d. PROJECT NUMBER</b>	
				<b>5e. TASK NUMBER</b>	
				<b>5f. WORK UNIT NUMBER</b>	
<b>7. PERFORMING ORGANIZATION NAME(S) AND ADDRESS(ES)</b>  University of Chicago Chicago, IL 60637-5418				<b>8. PERFORMING ORGANIZATION REPORT NUMBER</b>	
<b>9. SPONSORING / MONITORING AGENCY NAME(S) AND ADDRESS(ES)</b> U.S. Army Medical Research and Materiel Command Fort Detrick, Maryland 21702-5012				<b>10. SPONSOR/MONITOR'S ACRONYM(S)</b>	
				<b>11. SPONSOR/MONITOR'S REPORT NUMBER(S)</b>	
<b>12. DISTRIBUTION / AVAILABILITY STATEMENT</b> Approved for Public Release; Distribution Unlimited					
<b>13. SUPPLEMENTARY NOTES</b>					
<b>14. ABSTRACT</b> . Traumatic Brain Injury (TBI) is a public health problem of immense magnitude and immediate importance that has become endemic among military personnel and veterans. Imaging biomarkers of TBI are needed to support diagnosis and therapy and to predict TBI consequences while avoiding further injury. Diffusion magnetic resonance imaging has potential to become the non-invasive tool of choice for TBI structural assessment. Despite its potential, realizing the benefits of diffusion MRI in TBI requires a base of evidence for decision making that requires multi-organizational coordination and planning. The purpose of this proposed research is to synthesize a roadmap for diffusion MR imaging in brain traumatic injury that can advance the field and deliver the benefits most effectively in the shortest period of time. Essential steps toward implementation of the plan will be taken thereafter.					
<b>15. SUBJECT TERMS-</b> none provided					
<b>16. SECURITY CLASSIFICATION OF:</b>			<b>17. LIMITATION OF ABSTRACT</b>	<b>18. NUMBER OF PAGES</b>	<b>19a. NAME OF RESPONSIBLE PERSON</b>
<b>a. REPORT</b> U	<b>b. ABSTRACT</b> U	<b>c. THIS PAGE</b> U			USAMRMC
			UU	86	<b>19b. TELEPHONE NUMBER</b> (include area code)

## INTRODUCTION

Traumatic Brain Injury (TBI) is a public health problem of immense magnitude and immediate importance especially for military personnel and veterans. Imaging biomarkers of TBI are needed to support diagnosis and therapy and to predict TBI consequences while avoiding further injury. Diffusion magnetic resonance imaging has potential to become the non-invasive tool of choice for TBI structural assessment. Despite its potential, realizing the benefits of diffusion MRI in TBI requires a base of evidence for decision making that can only be assembled by multi-organizational coordination and planning.

The purpose of this research is to synthesize a roadmap for diffusion MR imaging in brain traumatic injury that can advance the field to deliver the benefits most effectively and accelerate translation of the technology into clinical practice.

This project has progressed in parallel with the new Federal Interagency Traumatic Brain Injury Research (FITBIR) informatics system ([fitbir.nih.gov](http://fitbir.nih.gov)), a web-based repository of TBI datasets. We met with the leadership and developers of FITBIR at the NIH Center for Information Technology on 15 February 2012 to introduce our work and learn their plans.

We applied for access to datasets in public repositories containing diffusion MR imaging scans to learn their procedures and practices and to obtain comparison datasets. Specifically, we obtained access to the National Database for Autism Research (NDAR) a secure research data repository promoting scientific data sharing and collaboration among autism spectrum disorder (ASD) investigators. The FITBIR is modeled after and uses the software infrastructure of NDAR.

To establish a test database of TBI data, the XNAT software from Washington University was chosen as the basis. This software was installed and modified to accommodate TBI data.

Specifically, the DoD/NINDS Common Data Elements

<http://www.commondataelements.ninds.nih.gov/> for Traumatic Brain Injury were adopted and implemented. Several test datasets were uploaded into a virtual server. The system is managed using Globus Online <https://www.globusonline.org/>, a technical infrastructure for secure e-science applications developed at the Argonne National Laboratory / University of Chicago by the Computation Institute.

Several D-MRI of TBI software tools were integrated into the XNAT framework, especially FSL and elements of DTI Studio. FSL is a comprehensive library of analysis tools for FMRI, MRI and DTI brain imaging data. FSL is written mainly by members of the [Analysis Group, FMRI, Oxford, UK](#). DTI Studio is developed by the [Laboratory of Brain Anatomical MRI](#) at Johns Hopkins University to process DTI data and reconstruct three-dimensional fiber trajectories. FSL and DTI Studio represent tools developed for brain diffusion MRI image analysis, but for applications other than TBI. These represent the type of tools that we seek to test and adapt to the specific requirements of TBI research and clinical applications. A data quality control procedure based on the DTIprep software from the University of North Carolina was implemented.

A DTI phantom study of reproducibility was done at 3T. This is reported in Appendix 12. Based on these experiments, it appears that phantom measurements are less reproducible than human

studies due to the construction of the phantom, where widely variant fiber bundles with relatively low cross section are placed adjacent to one another. High resolution image registration can be used to greatly improve the measured reproducibility. These observations were used to construct the protocol for the human reproducibility trial.

We performed a reproducibility study – both immediate and short term – on human subjects using 3T MRI of DTI. We are in the midst of analyzing the results, and include a summary of our preliminary findings with this report.

### **Travel Report: Visit to Johns Hopkins University (JHU) by Kyle Chard, software engineer**

The purpose of this trip to JHU was to attend a DTIStudio tutorial and meet with Prof. Susumu Mori and his team to learn about the latest algorithms and tools used in Diffusion Tensor Imaging (DTI) processing, get access to the underlying DTI studio code for use in our automated pipelines, and look for collaboration opportunities. This took place on 6-9 August 2012.

The tutorial covered the basics of using DTIStudio as well as more advanced topics such as quality control, registration and fiber tracking. The second day of the tutorial explored the use of DifeoMap and ROIEditor including detailed examples of using the LDDMM remote processing registration service hosted at JHU. As a result of these tutorials Kyle Chard learned to use the various tools following the worked examples presented, Kyle Chard also gained a much deeper understanding of DTI and many of the algorithms we use in our processing pipeline. We discussed the limitations of some of these approaches (e.g. reviewing FA values in isolation without considering fiber size is potentially misleading), that we will need to consider with respect to our work. In the class Kyle Chard also met with other researchers using DTI, for example Dr. Atul Kalanuria at JHU is using DTI Studio to study ICU patients whose injuries are not visible in other modalities. The basis of his work is comparison between “normal” and injured brains – he is therefore very interested in our current work on reproducibility and we have agreed to swap publications in the future as this presents a potential collaboration partner for the processes we develop.

One of the major lessons learned in these tutorials was the difficulty using the tools appropriately especially for users with a non-technical background, this therefore, further motivates our decision to abstract complexities through automated pipelines for non-expert users.

Kyle Chard spent the following 2 days working with Susumu’s team to learn about their code base and the algorithms being developed. Briefly, some of the key areas of discussion were: their new LDDMM algorithm, how we could programmatically invoke the LDDMM service using a service-enabled architecture, how it could use Globus based solutions for reliably transferring large data sets, and how we could use it with identified information. We discussed approaches to quality control and improvement, for example by using pixel based detection and removal. Kyle Chard experimented with their new Quality Control algorithm using a custom DTI, they have agreed to give us access to the C++ code for inclusion in our automated pipelines when it is complete. They gave us access to their fiber tracking and DTI mapping C++ code, which we have since started integrating in our pipelines. Finally, they gave us a set of atlases and explained their experiences with using different atlases.



As a result of this visit we have identified several followup opportunities.

- 1) Integrate their quality control code in our pipelines when it is complete.
- 2) Integrate DTI studio fiber tracking and DTI mapping code into our pipelines.
- 3) Add additional Atlases and compare the accuracy of our pipelines on our dataset.
- 4) Integrate the LDDMM registration service into our pipelines.

We concentrated this year on building and testing an informatics infrastructure to manage and analyze diffusion MRI data for TBI clinical applications. We adopted an archive manager (XNAT) and integrated it with widely used post-processing image analysis tools (FSL and others). This work was done in a virtual environment with grid-based storage and servers using GLOBUS technology. The work was done in anticipation of FITBIR, the Federal Interagency Traumatic Brain Injury Registry, sponsored by NIH and DoD. Since FITBIR won't be available and fully functional until 2013 and later, we registered to use NDAR, the National D Autism Registry. NDAR serves as the model and shares architectural and software elements with FITBIR.

At present, an established medical method for quantitative, sensitive and specific evaluation of closed head traumatic brain injury does not exist. Many technologies are being utilized such as blood work, X-ray, computed tomography scan (CT), magnetic resonance imaging (MRI), and electroencephalogram (EEG), but perhaps the most promising technology on the horizon is the Diffusion Tensor Imaging (DTI). Diffusion tensor imaging (DTI) is a magnetic resonance imaging (MRI)-based technique that allows the visualization, location, and orientation, of the brain's white matter tracts to determine changes in the brain due to blast, contact and related traumatic brain injuries. There is a critical and immediate need to use these tools to measure and track long term changes in the brain. The potential for DTI to improve our understanding of TBI has not been fully explored and challenges associated with non-existent standard practices amongst researchers and manufacturers remain a major challenge that this award will attempt to address through the design of a roadmap. Ultimately, imaging biomarkers for TBI may be identified, qualified and validated as a result of the roadmap.

We applied for a no-cost extension to this contract, with the principal goal of finishing a clinical trial of DTI reproducibility and conducting a workshop on DTI image analysis tools applied to TBI subjects. We expect to complete this work in 2013 as this contract terminates.

## **BODY:**

There is need to develop D-MRI into a qualified and validated biomarker by adapting methods and using best practices for other neuroimaging biomarkers. We are engaged in identifying the barriers to progress, especially for multidisciplinary (MRI physics, computer science/image processing, and especially TBI clinical practice) collaboration.

### **TBI Database**

According to NIH, more than 1.7 million Americans sustain a TBI each year, mostly from common causes. This includes the more than 200,000 service members who have been diagnosed with TBI over the last 12 years — most of those injuries being combat-related. No two brain injuries look or act exactly alike. The damage to the brain and its location is unique, as are the mix of symptoms that go with it. For example, research has shown that blast-related TBI, such as that suffered in combat, can present very differently than other types of TBI.

With this variability in mind, DoD and NIH are partnering on the creation of a central TBI database. The hope is that by collecting uniform data on as many types of these injuries as possible, the database will be useful for research into the injury and help accelerate comparative effectiveness research on brain injury treatment and diagnosis.

The Federal Interagency Traumatic Brain Injury (FITBIR) database was announced in September 2011, and will be funded at \$10 million over the next four years. NIH's Center for Information Technology is building FITBIR (through a subcontractor), based on experience with the National Database on Autism Research.

The National Institute of Neurological Disorders and Stroke and the U.S. Army Medical Research and Materiel Command will partner in providing program support for the project and help fill the database with useful information. Researchers will be provided with exactly what kind of information FITBIR is looking for and will be encouraged to participate at the time they submit proposals for new TBI studies.

### **DTI Post-Processing Software Tools Evaluation**

Many groups worldwide have developed software tools for the pre-processing, visualization, and analysis of diffusion MRI datasets. Often these tools are developed for a single project at the authors' institution, and then offered in the public domain for general applications. In many instances, there are open source public domain tools that offer functionality that is superior to any available commercial product.

We intend to organize a workshop this year so the key developers of DTI software tools can meet to consider how best to handle TBI datasets and solve the difficult and unique problems that they present.

## **D-MRI of TBI Data Acquisition Protocol**

Diffusion Tensor Imaging (DTI) is a promising MRI imaging technique that has significant potential to serve as a biomarker for diagnosis and assessment of patients with brain trauma. In the past one year, we have focused our efforts to develop DTI techniques dedicated to the efficient study of TBI patients. Data acquisition pulse sequence development was done with the expectation that they will be tested in conjunction with manufacturer-supplied sequences to evaluate test-retest reproducibility on a variety of platforms.

In order to efficiently acquire DTI data for a reproducibility study and to test the feasibility of the 3T MRI protocol for our Philips scanner in human subjects, we adopted a 7 minute data acquisition protocol (Appendix 1).

DTI pulse sequence with 30 diffusion gradient directions: TR/TE = 11097/54 ms, FA = 90°, b = 1000 s/mm<sup>2</sup>. Seventy axial slices, FOV = 240 x 240, matrix = 108 x 108, voxel size = 2.22 x 2.22 x 2.22 mm<sup>3</sup>, reconstructed to 1 x 1 x 2.22 mm<sup>3</sup>. Total scanning time is 6 minutes 51 seconds. Five averages for b=0 image.

We have tested various correction schemes for EPI data acquisition, applicable to fMRI as well, and reported the results at the OHBM 2012 meeting in Beijing (Appendix 11).

This year we completed the work on phantom testing and implemented the standard DTI pulse sequences for a clinical trial in 20 normal subjects. The results of this work are briefly summarized in Appendices 8 and 9.

## **Progress**

To best explain the progress we made in the current year, we provide a set of appendices with detailed results and related information. The first appendix is the 7 minute Philips 3T MRI protocol used for our human studies of reproducibility (Appendix 1).

The automated data analysis pipeline that we developed parcellates the brain into 48 selected regions based on a JHU deformable atlas. The list of ROIs (n=48) of the brain are given in Appendix

We performed pilot experiments in several subjects at first and generated scatter plots to show variation from day-to-day and session-to-session (Appendix 3). For example, we performed the same data acquisition on each individual volunteer 4 times; twice on each day. The intra-day variation is considered an immediate test-retest paradigm, while the two sessions provide a measure of short term variability in data acquisition of D-MRI.

Each ROI has an associated volume and overall (3D) perimeter or surface area. Since the ROIs vary greatly in size or volume, we sorted them and compared the variation in ROI measurements related to perimeter (area) and volume in Appendix 4.

A detailed compilation of ROIs and the measured volumes associated with two sessions are given in tabular form (Appendix 5).

For a cohort of 8 subjects studied with D-MRI taken from Mbirn and stored at NAMIC ([http://www.namimic.org/Wiki/index.php/Mbirn: Diffusion MRI calibration data dissemination](http://www.namimic.org/Wiki/index.php/Mbirn:_Diffusion_MRI_calibration_data_dissemination)), we were able to derive the mean diffusivity - MD (Appendix 6) and fractional anisotropy – FA (Appendix 7) results.

Our own reproducibility study in human volunteers was performed in 20 subjects yielding the results for mean diffusivity – MD (Appendix 8) and fractional anisotropy – FA (Appendix 9).

A product line review of this and related projects was performed on 12 June 2012 in Frederick, MD. A presentation was given to explain the current progress, and copies of the slides are included (Appendix 10).

Two publications resulted from this work in the current year, and copies are included as Appendices 11 and 12.

## **Challenges**

Among the most important challenges that we faced this year were general unavailability, incompleteness, and overall low quality of data received from Dr. Little in Texas. We presume that her other duties have made it difficult or impossible to provide the data we require in a timely manner. As a consequence, we decided to terminate discussions of future subcontracting for data acquisition through this route. We found alternative data source and in the long term expect that FITBIR will provide abundant data. Finally, the diffusion phantom received from Brain Innovation BV, Maastricht, NL was damaged in shipping and required a complex repair procedure. The company has agreed to provide us a replacement phantom, and we await delivery.

## Next Funding Period

The goals for the next year include preparations for a sponsored workshop of D-MRI software toolbuilders who should undertake the analysis of TBI datasets and evaluation of the results. To accomplish this, a suitable on-line archive is required to manage data distribution and results collection. In preparation for evaluation of various software tools, we plan to take D-MRI of TBI datasets from studies published in the peer-reviewed literature and place them in the repository. Software tools have been downloaded and installed on local host computers which are capable of implementing the measurements used in the published studies. Having access to the datasets and automated tools will enable us to independently reproduce the results from the publications. Comparison of the published and independently processed data will allow us to verify the reports. If there are discrepancies, the root cause will be sought.

The long term focus of the TBI project is to host a workshop focused on tool development for analyzing DTI images for TBI (Q4 2013). As part of this workshop, we would like to present the system we have developed and offer one or more datasets that will allow DTI tool developers to experiment with TBI datasets. The main requirements are therefore the ability to securely publish a dataset for tool developers; provide access to a set of core tools (e.g., registration); provide the ability to run tools in the Cloud; and support the ability to store user submitted results for comparison. We have briefly mentioned automated tool comparison however we consider this future work beyond the initial workshop deliverable

Rather than focus on a single class of tool we will aim to support a wide range of tools that include: quality control, quality correction, artifact removal, registration, image analysis, visualization and other automated DTI processing.

The requirements for providing this infrastructure are as follows:

**Image repository:** Secure storage of DTI datasets, providing configurable and auditable access to users and developers, and providing the ability to organize and annotate (with structured data) raw and processed datasets. The repository should accept results published from tools along with associated metadata/provenance information that describes the processing performed.

**Image analysis platform:** Generic platform to provide an interface and infrastructure to run analysis tools. The platform must support orchestration of different tool combinations and provide some form of infrastructure to execute, potentially computationally intensive, processing tools. It must also integrate with the image repository to retrieve input and automatically store output.

**Data transfer:** Ability to transfer datasets between the repository, third party repositories (e.g., FITBIR), user machines, and the analysis platform.

**Tool repository and core tools:** An interface to publish access and share tools, such that users can easily utilize core tools in their processing. In addition, it should be easy for developers to upload tools so that they can be shared with others.

In addition to the workshop we are currently completing the DTI reproducibility study using automated image analysis. We have created an initial set of CDEs and pipelines capable of representing and processing TBI datasets. In the short term we will continue to run these analyses, we will also need to extend the pipelines to include additional algorithms (DTI studio fiber tracking), tools, services (JHU LDDMM) and atlases (JHU), while simultaneously exploring a Galaxy based approach that has parity with our current implementation.

The major focus of the past year has been developing the core infrastructure on which to experiment with different analysis workflows on internal datasets. Briefly, in this time we have evaluated different repositories, developed TBI-specific CDEs, wrapped various DTI tools, created TBI pipelines, and deployed a service for processing both internal and collaborators' DTI datasets. In somewhat tangential work we have also created a website for the project with information on the domain and progress of the project.

The evaluation of repositories focused on those that could meet both the image and metadata storage requirements of the project. We evaluated several leading repositories (XNAT, HID), PACS systems, and DICOM servers (including a custom DICOM server developed at ISI). After an extensive evaluation we selected XNAT as it provides an extensible storage mechanism for both image and metadata, exposes a well-defined service API, and includes support for creating automated pipelines.

To reduce the complexity of heterogeneous user accounts, we added Globus Online (GO) support to XNAT by developing a custom XNAT authentication module. This integration allows GO identities to be used to authenticate with the running XNAT service, we have also shared this code with the CVRG group at JHU for use in their portal. While XNAT provides considerable metadata support, it did not include many of the core data models required for analyzing TBI (e.g., injury information). To enhance XNAT's suitability for TBI data we developed a set of TBI-specific Common Data Elements (CDEs) that describe patient, family history, TBI assessment and diagnosis, and injury information. These CDEs are based on those proposed by IMPACT (International Mission for Prognosis and Analysis of Clinical Trials in TBI). We have also developed mechanisms to input and associate this metadata with image sessions.

After establishing a repository platform we investigated tools that provide value for DTI-TBI researchers. We investigated both GUI and CLI based tools and selected a subset that provided the functionality required. The final tools that have been integrated into the platform include DICOM header extraction, quality control (DTI Prep), Eddy current correction, registration, brain extraction, DTI fitting (Camino and FSL), FA/MD calculations, ROI-based calculations, and format conversion (e.g., DICOM to NIfTI and DICOM to NRRD). After exposing these tools in the platform we created a number of pipelines to perform common tasks, for example an automated pipeline to report on quality, and an end to end pipeline that performs quality control, eddy current correction, registration, brain extraction, tensor fitting, and ROI-based FA/MD calculations. The major focus of this development is to increase automation and ease of use, to do so we standardized the core tools' input and output.

Finally, after local testing we have deployed an instance of XNAT with DTI tools and TBI pipelines. As part of this deployment we created a Globus Online transfer endpoint and, combined with a local repository upload script, we use this as our primary mechanism to move datasets into the repository. After deploying the service we have used the developed pipelines and tools to process several real world datasets, including our own reproducibility study, our collaborator's dataset, and a published reproducibility study (kriby).

We have also prototyped the main DTI workflow in Galaxy as proof-of-concept deployment. The instance includes integrated Globus Online user accounts and authentication.

### **Requirements to Support a DTO Software Tools Workshop**

To meet the requirements outlined above we intend to do the following:

1. Image repository:
  - a. Extend the current access control to make it easier for users to be granted access to datasets (ideally through GO Groups and Globus OAuth).
  - b. Develop a model for developers and users to contribute result sets to the repository; this will involve defining new reconstruction/analysis schemas in XNAT and providing an interface to use them.
2. Tool Platform:

Continue developing XNAT (or Galaxy) to prototype different pipelines and deploy an instance for use at the workshop.

After experimenting with pipelines in XNAT we don't think they are suitably flexible or user friendly for our scenarios. We believe that Galaxy will provide a more intuitive and convenient mechanism to create, use and share workflows.

Develop a distributed execution platform that will allow simultaneous use of computationally intensive tools. Both Galaxy and XNAT support DRMAA execution, however we still need to obtain resources for execution.

We could potentially utilize an auto-scaling Cloud-based approach to delivering appropriate resources, we could also investigate the feasibility and cost of doing this on a commercial Cloud platform such as EC2 - we could submit an AWS grant to fund this experiment.
3. Transfer:

Standard XNAT mechanisms are probably sufficient for the workshop, however, if time permits, we could investigate integrating GO transfer in XNAT as a model for high performance and reliable data transfer.
4. Tool Repository and core tools:

Create a model for uploading, storing and sharing different tools. The Galaxy tool shed model may provide a suitable approach for doing this.

### **KEY RESEARCH ACCOMPLISHMENTS:**

In the third year, we were able to complete the following:

1. Implementation of an XNAT on-line traumatic brain injury database was completed, with linkage to FSL. This virtualized system was tested using datasets acquired locally and from various image repositories.
2. Dr. Farid Dahi, post-doctoral research associate departed and he was replaced by Xia Jiang.
3. Globus Online ([www.globus.org](http://www.globus.org)) and automated image quality control were integrated into the image workflow for secure communication of large datasets.
4. The D-MRI reproducibility study was performed using 20 human volunteers to evaluate sources of variability and stability in MRI scanners. Both immediate and short term reproducibility evaluations were done using a Philips 3T MRI scanner.
5. A no-cost one year extension of the project was requested.



## **REPORTABLE OUTCOMES:**

1. Xia Jiang, Xiaodong Guo, Fang Zhu, Michael Vannier, Jia-Hong Gao. Slice Timing Correction in Volume Selective z-shim fMRI Acquisition. Organization for Human Brain Mapping, Beijing, CN (2012).
2. Xia Jiang, Kyle Chard, Jia-Hong Gao, Michael Vannier. Partial Volume Effect in Diffusion Tensor Imaging: a Phantom Study, manuscript draft.

## **CONCLUSION:**

Diffusion MRI of neurological/neuropsychiatric disorders (chronic TBI, PTSD, and related disorders) is an important potential market for the imaging industry. Virtually all individuals with traumatic brain injuries – including all ages are potential candidates – whether injury is due to auto, sports, combat, falls or other. Serum protein changes after trauma, optical imaging methods, PET/SPECT with radioisotope agents, and other technologies are less generally available or have known limitations. No “one size fits all”, given the diversity of patients and injuries. By preparing the infrastructure needs and facilitating interactions among diverse experts in TBI and related disciplines, the translation of promising D-MRI technology into clinical practice based on a solid body of evidence can be accomplished.

## **REFERENCES:**

1. Federal Interagency Traumatic Brain Injury Research (FITBIR) database, August 29, 2011, <http://www.nih.gov/news/health/aug2011/ninds-29.htm>
2. The National Database for Autism Research, <http://www.hhs.gov/open/initiatives/hhsinnovates/round3/ndarpage.html>

## **APPENDICES:**

1. Philips 3T MRI DTI protocol (acquisition time: 7 minutes)
2. Sorted ROI list (n=48)
3. Scatter plots – Day 1:2, Session 1:2
4. ROI perimeter vs volume comparison in subjects 1-8
5. Session comparison (5/15/2012)
6. Subject 1-8: MD vs ROI; MD stddev/mean vs ROI
7. Subject 1-8: FA vs ROI; FA stdev/mean vs ROI
8. All 20 subjects: MD vs ROI; MD stddev/mean vs ROI
9. All 20 subjects: FA vs ROI; FA stdev/mean vs ROI
10. Traumatic Brain Injury D-MRI Research Roadmap Development Project. Product Line Review (PLR) meeting, Medical Imaging Technologies. 12 June 2012.
11. Xia Jiang, et al. Slice Timing Correction in Volume Selective z-shim fMRI Acquisition. Organization for Human Brain Mapping, Beijing, CN (2012).
12. Xia Jiang, et al. Partial Volume Effect in Diffusion Tensor Imaging: a Phantom Study (manuscript)

Appendix 1:  
Philips 3T MRI DTI protocol  
(acquisition time: 7 minutes)

# Philips MRI Protocol Dump

**Philips MRI Protocol Dump****Created on**

5/29/2012 5:09:20 PM




**Comment**


Created by ExamCard\_to\_XML with inputs: "G:\DTITBI-41-7min.ExamCard" on system ( :: )


**Software Stream**


3.2.1.0


[Expand All](#) | [Collapse All](#)


 (2)  (1)  (4)


 Hospital (2)


 DTITBI-41-7min (4) 06:40.6

 (1) Survey 00:37.5

 (2) RefScan 00:44.4

 DTI\_41\_FOV25

 T1W\_3D\_TFE SENSE 05:18.7

 {B1860723-4F8F-476e-8075-D42C65706693} (0)

This is a summary of the protocol used with the Philips 3T MRI scanner to acquire diffusion tensor image (DTI) and related information with a scan time of 7 minutes total. This protocol was the basis for reproducibility testing and the human subject examinations in the clinical trial.

Hospital (2) | DTITBI-41-7min (4) 06:40.6 | (1) Survey 00:37.5

INFO PAGE		GEOMETRY		CONTRAST	
Total scan duration	00:37.5	Multi-transmit	no	Scan type	Imaging
Rel. signal level (%)	100	Nucleus	H1	Scan mode	M2D
Act. TR/TE (ms)	18 / 4.6	Coil selection	SENSE-Head-8	technique	FFE
ACQ matrix M x P	256 x 128	element selection	SENSE	Contrast enhancement	T1
ACQ voxel MPS (mm)	0.98 / 1.95 / 10.0	connection	d	Acquisition mode	cartesian
REC voxel MPS (mm)	0.98 / 0.98 / 10.0	Dual coil	no	Fast Imaging mode	TFE
Scan percentage (%)	50	Multi coil	no	shot mode	multishot
TFE shots	2	Homogeneity correction	none	TFE factor	64
TFE dur. shot / acq (ms)	1389.3 / 1152.0	CLEAR	no	startup echoes	default
TFE shot interval (ms)	1389.329	FOV FH (mm)	250	shot interval	shortest
Min. TI delay	645.2518	AP (mm)	250	profile order	linear
Act. WFS (pix) / BW (Hz)	3.100 / 140.1	stack RL (mm)	50	Echoes	1
Min. WFS (pix) / Max. BW (Hz)	0.556 / 781.3	Voxel size FH (mm)	0.976563	partial echo	no
Min. TR/TE (ms)	9.4 / 3.7	AP (mm)	1.953125	shifted echo	no
SAR / head	< 9 %	Slice thickness (mm)	10	TE	in-phase
Whole body / level	0.0 W/kg / normal	Recon voxel size (mm)	0.9765625	(ms)	4.605324
B1 rms	0.69 uT	Fold-over suppression	no	Flip angle (deg)	15
PNS / level	51 % / normal	Reconstruction matrix	256	TR	user defined
Sound Pressure Level (dB)	9.813315	SENSE	no	(ms)	18
MOTION		Z Shim	no	Halfscan	no
Cardiac synchronization	no	k-t BLAST	no	Water-fat shift	user defined
Heart rate > 250 bpm	no	Stacks	3	(pixels)	3.5
Respiratory compensation	no	current	A	Shim	default
Navigator respiratory comp	no	type	parallel	mDIXON	no
Flow compensation	no	slices	3	Fat suppression	no
fMRI echo stabilisation	no	slice gap	user defined	Water suppression	no
Motion smoothing	no	gap (mm)	10	TFE prepulse	invert
NSA	1	slice orientation	sagittal	slice selection	no
DYN/ANG		fold-over direction	AP	shared	no
Angio / Contrast enh.	no	fat shift direction	F	delay	user defined
Quantitative flow	no	Slice scan order	default	(ms)	800
Manual start	no	Stack scan order	ascend	PSIR	no
Dynamic study	no	Move table per stack	no	MTC	no
Arterial Spin labeling	no	Stack alignment	no	T2prep	no
POST/PROC		Stack display order	no	Research prepulse	no
Preparation phases	auto	PlanAlign	no	Diffusion mode	no
Interactive F0	no	REST slabs	0	Elastography mode	no
SmartPlan survey	no	Catheter tracking	no	SAR mode	high
B0 field map	no	Interactive positioning	no	B1 mode	default
B1 field map	no	Allow table movement	no	SAR Patient data	auto
MIP/MPR	no	OFFC/ANG		PNS mode	low
Images	M, no, no, no	Stacks	3	Gradient mode	default
Autoview image	M	current	A	SoftTone mode	no
Calculated images	no, no, no, no	Stack Offc. AP (P=+mm)	-20		
Reference tissue	White matter	RL (L=+mm)	0		
Preset window contrast	soft	FH (H=+mm)	0		
Reconstruction mode	immediate	Ang. AP (deg)	0		
Save raw data	no	RL (deg)	0		
Hardcopy protocol	no	FH (deg)	0		
Ring filtering	default				
Geometry correction	default				

Hospital (2) | DTITBI-41-7min (4) 06:40.6 | (2) RefScan 00:44.4

INFO PAGE		GEOMETRY		CONTRAST	
Total scan duration	00:44.4	Multi-transmit	no	Multi-transmit	no
Rel. signal level (%)	100	Coil selection	SENSE-Head-8	Coil selection	SENSE-Head-8
Act. TR/TE (ms)	4.0 / 0.75	element selection	SENSE	element selection	SENSE
ACQ matrix M x P	96 x 75	connection	d	connection	d
ACQ voxel MPS (mm)	5.52 / 7.07 / 6.00	Dual coil	no	Dual coil	no
REC voxel MPS (mm)	5.52 / 5.52 / 3.00	Fold-over suppression	no	Fold-over suppression	no
Scan percentage (%)	78.125	Stack Offc. AP (P=+mm)	-19.91691	Stack Offc. AP (P=+mm)	-19.91691
Packages	1	RL (L=+mm)	-2.090301	RL (L=+mm)	-2.090301
Act. WFS (pix) / BW (Hz)	0.210 / 2071.3	FH (H=+mm)	5.474554	FH (H=+mm)	5.474554
Min. WFS (pix) / Max. BW (Hz)	0.208 / 2083.3	Respiratory compensation	no	Respiratory compensation	no
SAR / local torso	< 2 %	NSA	3	NSA	3
Whole body / level	0.0 W/kg / normal	Manual start	no	Manual start	no
B1 rms	0.25 uT	OFFC/ANG			
PNS / level	28 % / normal	Multi-transmit	no		
Sound Pressure Level (dB)	18.02323	Coil selection	SENSE-Head-8		
MOTION		element selection	SENSE		
Multi-transmit	no	connection	d		
Coil selection	SENSE-Head-8	Dual coil	no		
element selection	SENSE	Fold-over suppression	no		
connection	d	Stack Offc. AP (P=+mm)	-19.91691		
Dual coil	no	RL (L=+mm)	-2.090301		
Fold-over suppression	no	FH (H=+mm)	5.474554		
Stack Offc. AP (P=+mm)	-19.91691	Respiratory compensation	no		
RL (L=+mm)	-2.090301	NSA	3		
FH (H=+mm)	5.474554	Manual start	no		
Respiratory compensation	no	DYN/ANG			
NSA	3	Multi-transmit	no		
Manual start	no	Coil selection	SENSE-Head-8		
DYN/ANG		element selection	SENSE		
Multi-transmit	no	connection	d		
Coil selection	SENSE-Head-8	Dual coil	no		
element selection	SENSE	Fold-over suppression	no		
connection	d	Stack Offc. AP (P=+mm)	-19.91691		
Dual coil	no	RL (L=+mm)	-2.090301		
Fold-over suppression	no	FH (H=+mm)	5.474554		
Stack Offc. AP (P=+mm)	-19.91691	Respiratory compensation	no		
RL (L=+mm)	-2.090301	NSA	3		
FH (H=+mm)	5.474554	Manual start	no		
Respiratory compensation	no	POST/PROC			
NSA	3	Multi-transmit	no		
Manual start	no	Coil selection	SENSE-Head-8		
POST/PROC		element selection	SENSE		
Multi-transmit	no	connection	d		
Coil selection	SENSE-Head-8	Dual coil	no		
element selection	SENSE	Fold-over suppression	no		
connection	d	Stack Offc. AP (P=+mm)	-19.91691		
Dual coil	no	RL (L=+mm)	-2.090301		
Fold-over suppression	no	FH (H=+mm)	5.474554		
Stack Offc. AP (P=+mm)	-19.91691	Respiratory compensation	no		
RL (L=+mm)	-2.090301	NSA	3		
FH (H=+mm)	5.474554	Manual start	no		
Respiratory compensation	no				
NSA	3				
Manual start	no				

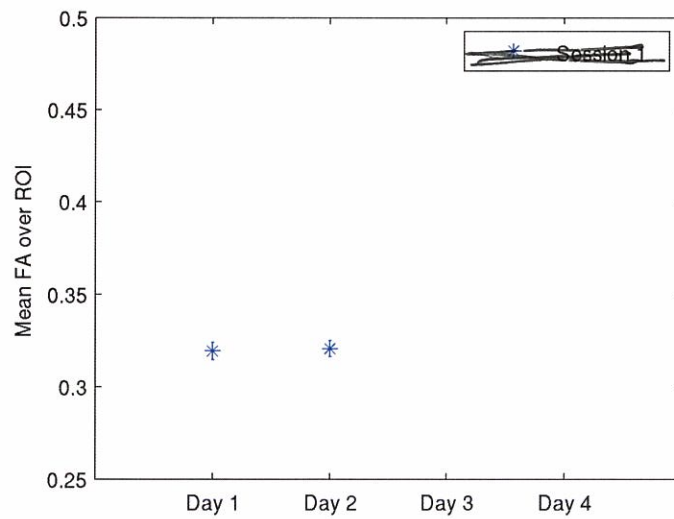
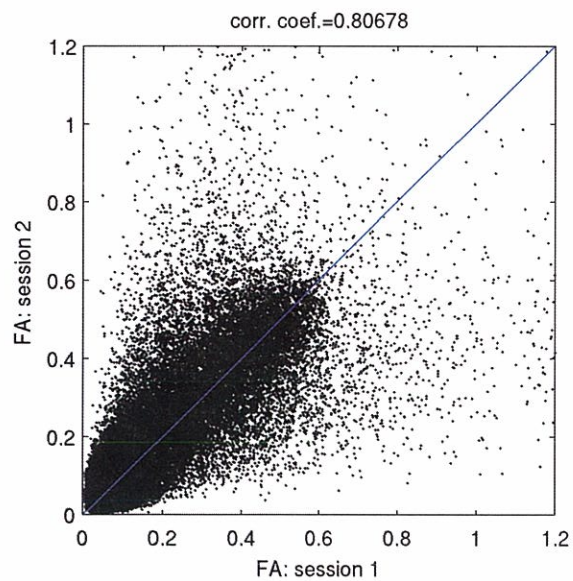
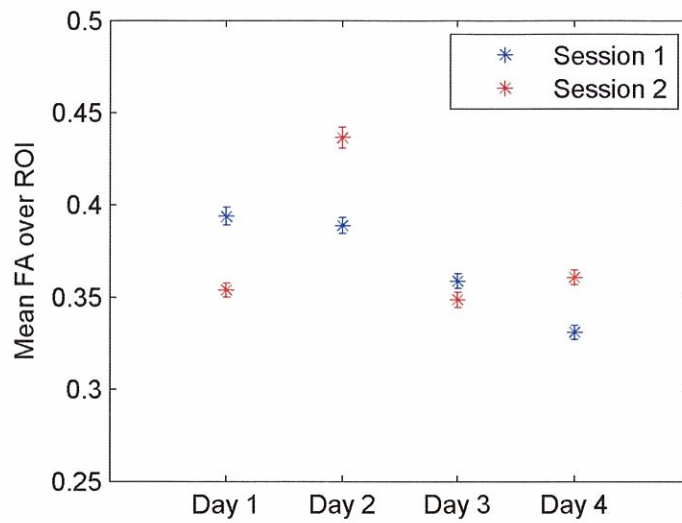
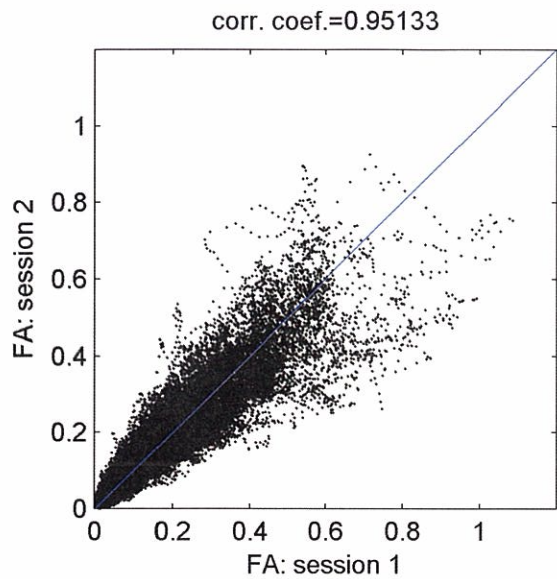
## Appendix 2:

### Sorted ROI list (n=48)

#	ROI name	# of voxels
1	Uncinate fasciculus L	376
2	Uncinate fasciculus R	380
3	Superior fronto-occipital fasciculus (could be a part of anterior internal capsule) R	507
4	Superior fronto-occipital fasciculus (could be a part of anterior internal capsule) L	507
5	Tapetum R	596
6	Tapetum L	600
7	Fornix (column and body of fornix)	659
8	Medial lemniscus R	690
9	Medial lemniscus L	699
10	Inferior cerebellar peduncle R	968
11	Inferior cerebellar peduncle L	968
12	Superior cerebellar peduncle R	992
13	Superior cerebellar peduncle L	992
14	Fornix (cres) / Stria terminalis (can not be resolved with current resolution) R	1124
15	Fornix (cres) / Stria terminalis (can not be resolved with current resolution) L	1125
16	Cingulum (hippocampus) L	1155
17	Cingulum (hippocampus) R	1236
18	Corticospinal tract R	1362
19	Corticospinal tract L	1370
20	Pontine crossing tract (a part of MCP)	1500
21	Sagittal stratum (include inferior longitudinal fasciculus and inferior fronto-occipital fasciculus) R	2228
22	Sagittal stratum (include inferior longitudinal fasciculus and inferior fronto-occipital fasciculus) L	2231
23	Cerebral peduncle R	2278
24	Cerebral peduncle L	2278
25	Cingulum (cingulate gyrus) R	2342
26	Retrolenticular part of internal capsule L	2469
27	Retrolenticular part of internal capsule R	2515
28	Cingulum (cingulate gyrus) L	2751
29	Anterior limb of internal capsule L	3018
30	Anterior limb of internal capsule R	3138
31	Posterior corona radiata L	3714
32	Posterior corona radiata R	3728
33	Posterior limb of internal capsule L	3752
34	Posterior limb of internal capsule R	3754
35	Posterior thalamic radiation (include optic radiation) R	3972
36	Posterior thalamic radiation (include optic radiation) L	3978
37	External capsule L	5587
38	External capsule R	5611
39	Superior longitudinal fasciculus L	6605
40	Superior longitudinal fasciculus R	6607
41	Anterior corona radiata R	6849
42	Anterior corona radiata L	6852
43	Superior corona radiata R	7500
44	Superior corona radiata L	7508
45	Genu of corpus callosum	8851
46	Splenium of corpus callosum	12729
47	Body of corpus callosum	13711
48	Middle cerebellar peduncle	15644

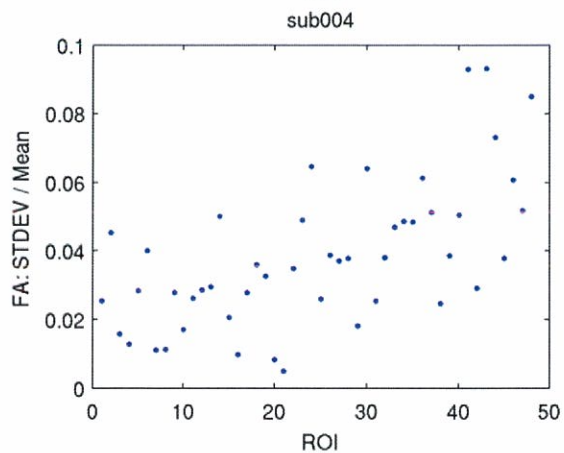
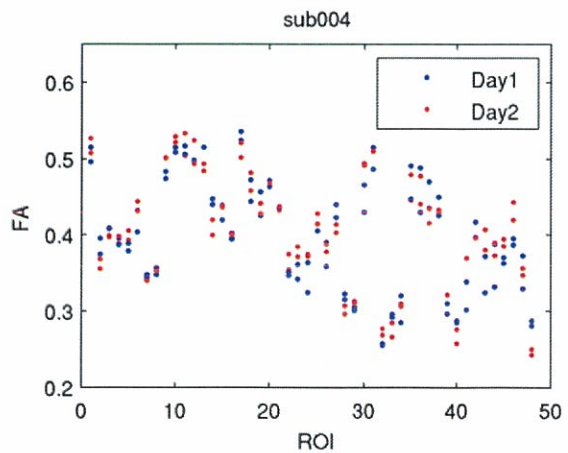
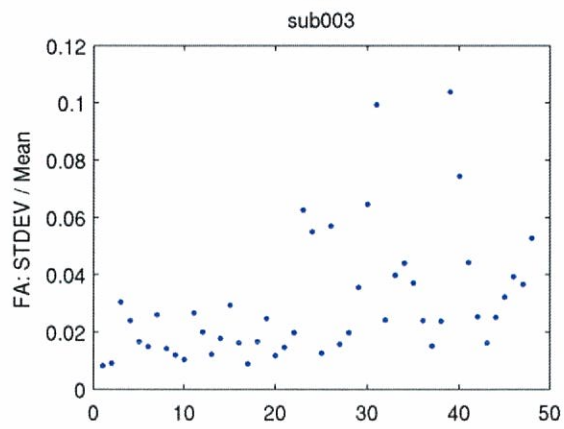
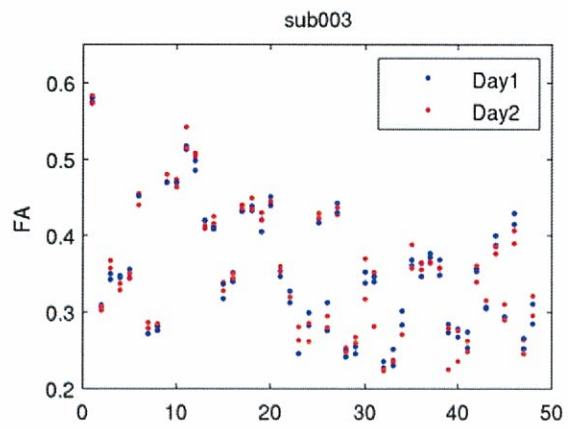
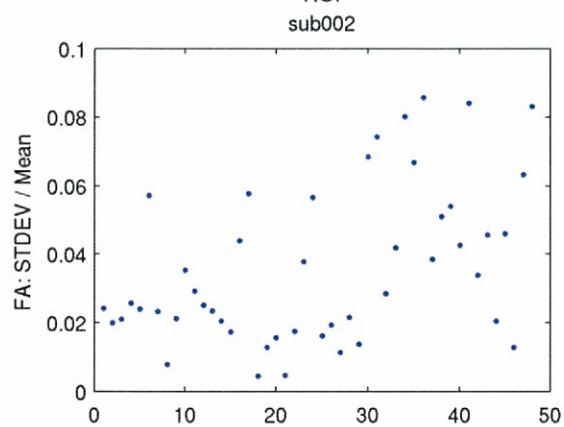
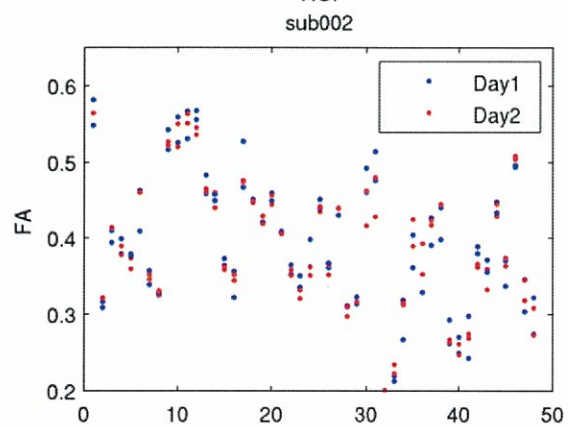
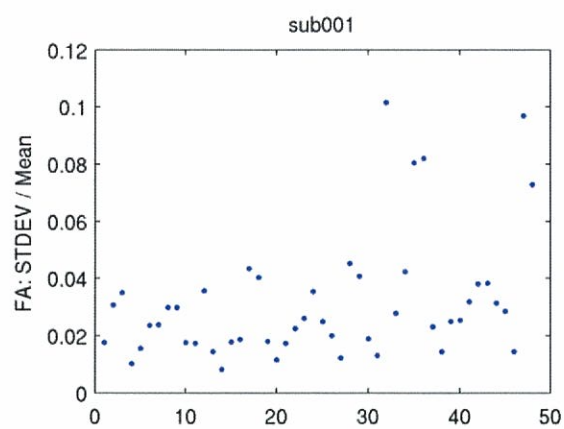
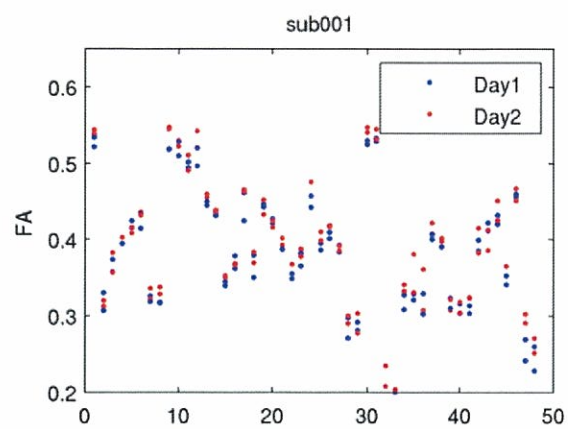
Appendix 3:  
Scatter plots – Day 1:2,  
Session 1:2

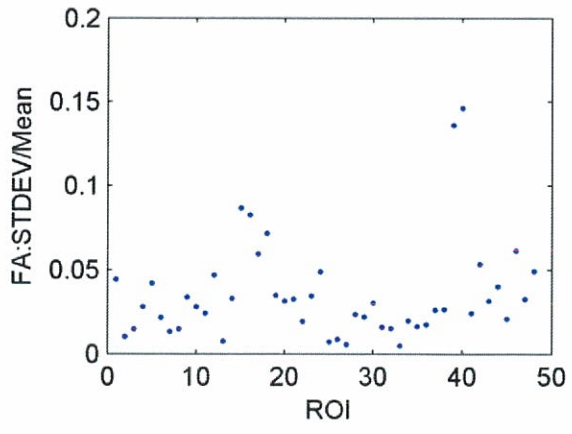
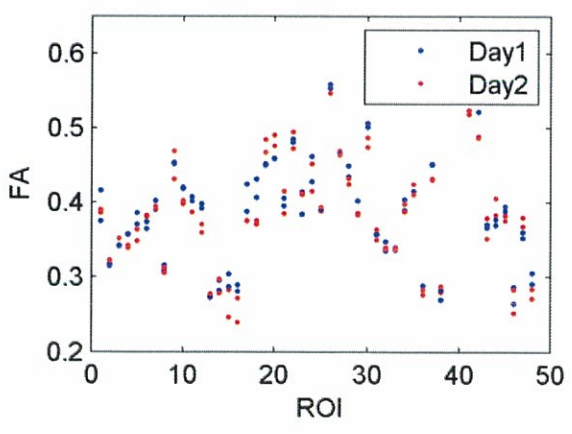
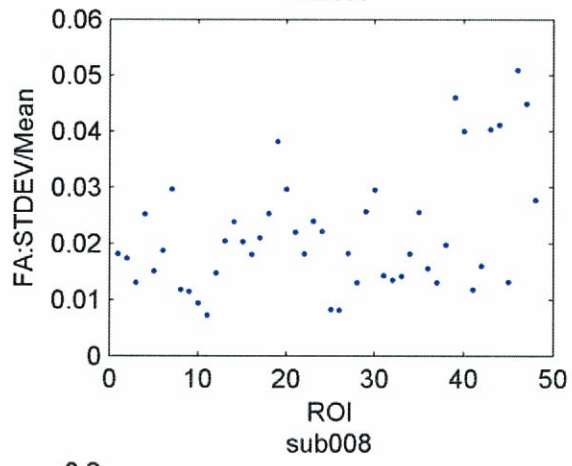
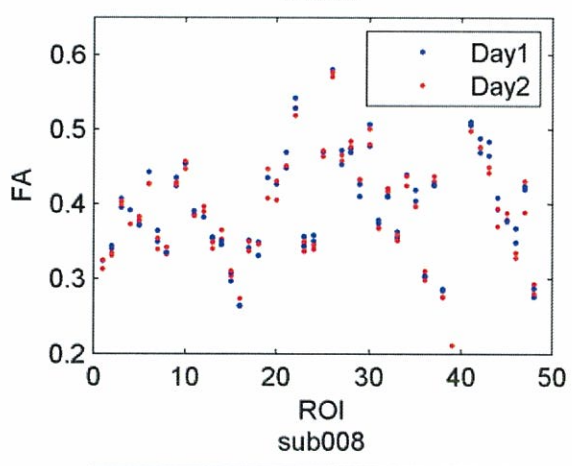
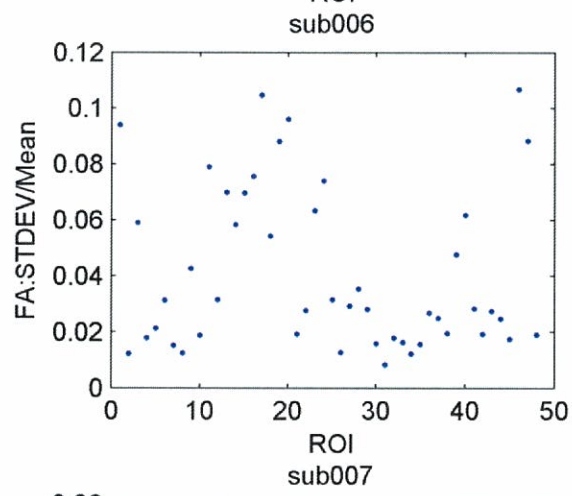
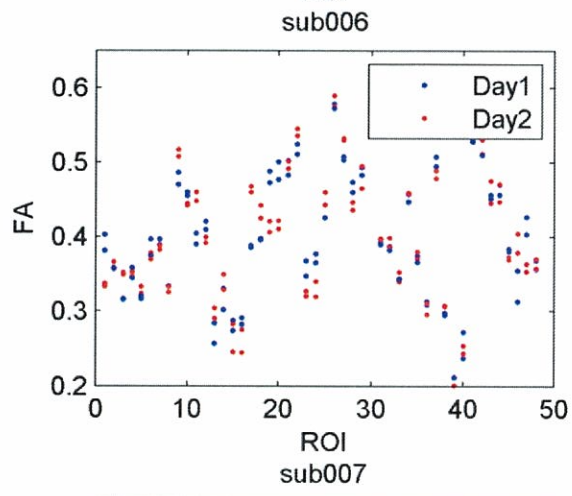
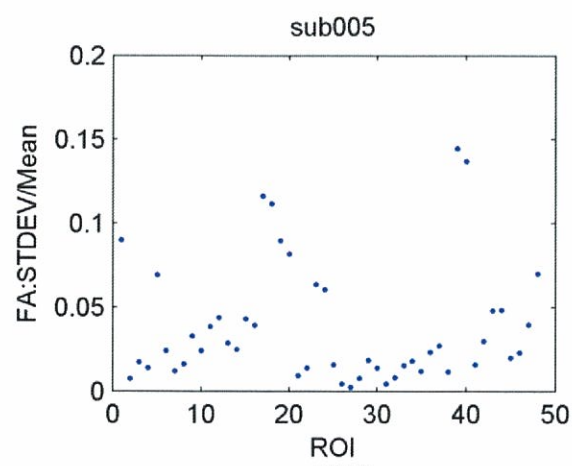
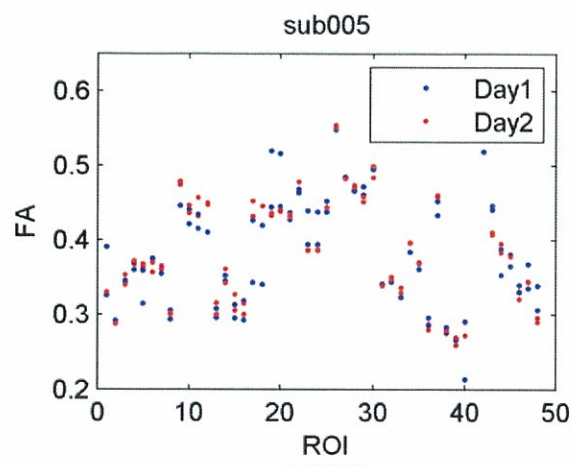




Appendix 4:  
ROI perimeter vs volume  
comparison in subjects 1-8

X axis from left to right: the ratio of # of perimeter voxels to ROI volume increases





Appendix 5:  
Session comparison  
(5/15/2012)



## Sessions Comparison

3115112

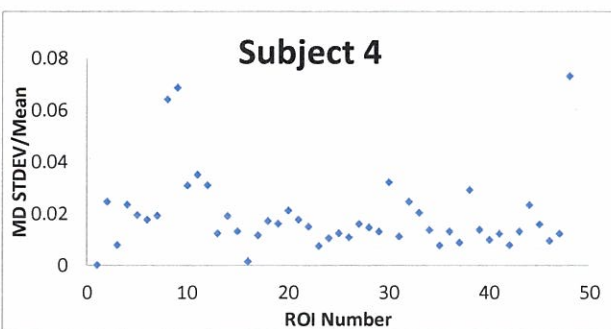
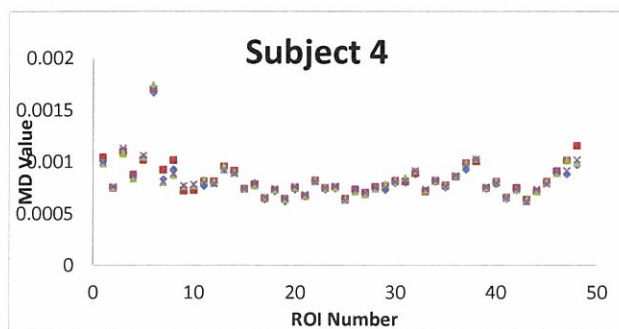
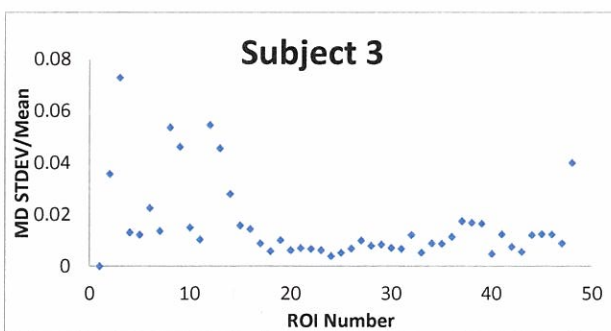
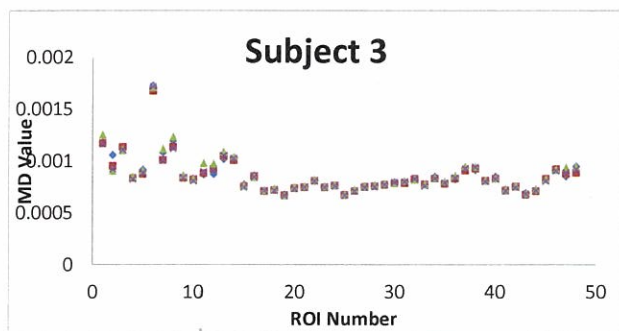
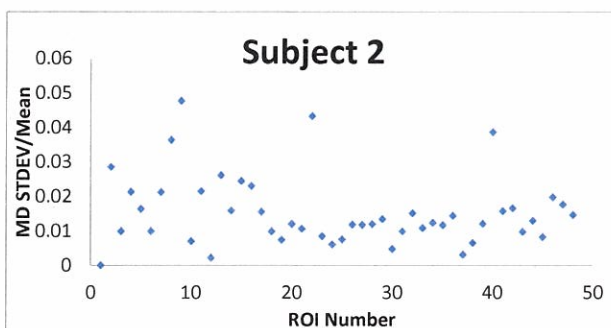
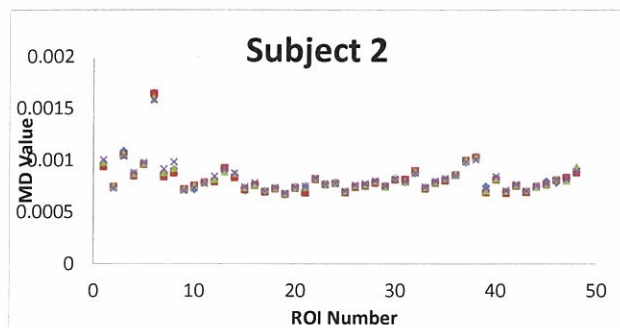
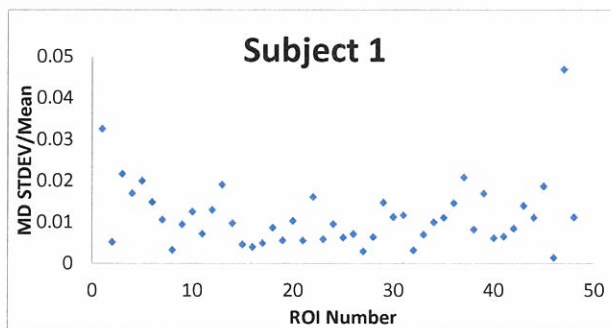
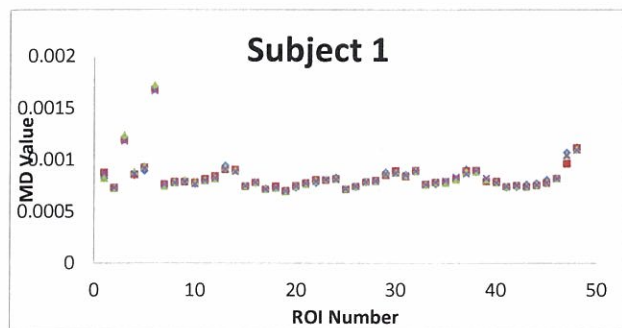
	ROI	# of voxels (1 voxel=1mm <sup>3</sup> )	DAY 1				DAY 2				Inter_days changes(%)
			Session1	Session2	Intra_day changes(%)	FA average in day1	Session3	Session4	Intra_day changes(%)	FA average in day2	
1	Middle cerebellar peduncle	15644	0.316813	0.31958	0.9	0.3181955	0.310097	0.314366	1.4	0.3122315	-1.9
2	Pontine crossing tract (a part of MCP)	1500	0.247581	0.28046	13.3	0.26402	0.262966	0.280864	6.8	0.271915	3.0
3	Genu of corpus callosum	8851	0.370317	0.36082	-2.6	0.3655685	0.377601	0.367219	-2.7	0.37241	1.9
4	Body of corpus callosum	13711	0.432428	0.42464	-1.8	0.428534	0.441599	0.424711	-3.8	0.433155	1.1
5	Splenium of corpus callosum	12729	0.579098	0.56653	-2.2	0.5728145	0.581093	0.569262	-2.0	0.5751775	0.4
6	Fornix (column and body of fornix)	659	0.297665	0.29903	0.5	0.2983455	0.311871	0.291662	-6.5	0.3017665	1.1
7	Corticospinal tract R	1362	0.276122	0.31316	13.4	0.294641	0.280052	0.296244	5.8	0.288148	-2.2
8	Corticospinal tract L	1370	0.28731	0.30525	6.2	0.2962775	0.265325	0.288927	8.9	0.277126	-6.5
9	Medial lemniscus R	690	0.347032	0.35214	1.5	0.3495875	0.282421	0.357118	26.4	0.3197695	-8.5
10	Medial lemniscus L	699	0.34406	0.36005	4.6	0.352054	0.320886	0.375508	17.0	0.348197	-1.1
11	Inferior cerebellar peduncle R	968	0.290149	0.2768	-4.6	0.2834755	0.224906	0.284081	26.3	0.2544935	-10.2
12	Inferior cerebellar peduncle L	968	0.276671	0.27362	-1.1	0.275144	0.240993	0.281529	16.8	0.261261	-5.0
13	Superior cerebellar peduncle R	992	0.362724	0.36899	1.7	0.3658555	0.390546	0.357518	-8.5	0.374032	2.2
14	Superior cerebellar peduncle L	992	0.359558	0.35984	0.1	0.3596975	0.371745	0.358305	-3.6	0.365025	1.5
15	Cerebral peduncle R	2278	0.500034	0.50455	0.9	0.502293	0.535283	0.505485	-5.6	0.520384	3.6
16	Cerebral peduncle L	2278	0.495001	0.4773	-3.6	0.486149	0.500466	0.503641	0.6	0.5020535	3.3
17	Anterior limb of internal capsule R	3138	0.404926	0.40706	0.5	0.4059915	0.399807	0.396245	-0.9	0.398026	-2.0
18	Anterior limb of internal capsule L	3018	0.42281	0.41689	-1.4	0.419849	0.433083	0.428456	-1.1	0.4307695	2.6
19	Posterior limb of internal capsule R	3754	0.456082	0.4477	-1.8	0.451891	0.460012	0.446932	-2.8	0.453472	0.3
20	Posterior limb of internal capsule L	3752	0.466561	0.45156	-3.2	0.459058	0.459563	0.469501	2.2	0.464532	1.2
21	Retrolenticular part of internal capsule R	2515	0.445485	0.44182	-0.8	0.443654	0.447052	0.441081	-1.3	0.4440665	0.1
22	Retrolenticular part of internal capsule L	2469	0.437467	0.43101	-1.5	0.43424	0.448171	0.435983	-2.7	0.442077	1.8
23	Anterior corona radiata R	6849	0.275038	0.28331	3.0	0.2791755	0.281726	0.284081	0.8	0.2829035	1.3
24	Anterior corona radiata L	6852	0.280617	0.27697	-1.3	0.278791	0.289913	0.28554	-1.5	0.2877265	3.2
25	Superior corona radiata R	7500	0.34581	0.3467	0.3	0.346255	0.328028	0.336833	2.7	0.3324305	-4.0
26	Superior corona radiata L	7508	0.360935	0.34829	-3.5	0.3546145	0.354327	0.347582	-1.9	0.3509545	-1.0
27	Posterior corona radiata R	3728	0.35219	0.35382	0.5	0.353007	0.361556	0.354046	-2.1	0.357801	1.4
28	Posterior corona radiata L	3714	0.331606	0.31699	-4.4	0.3242975	0.323121	0.323124	0.0	0.3231225	-0.4

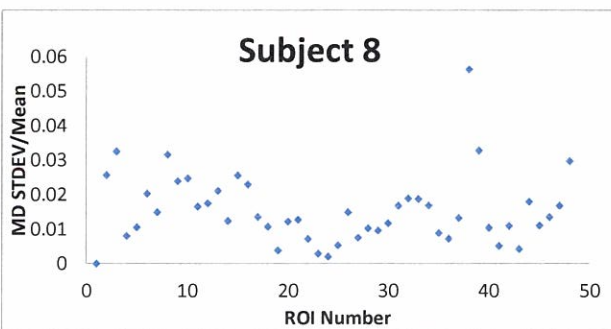
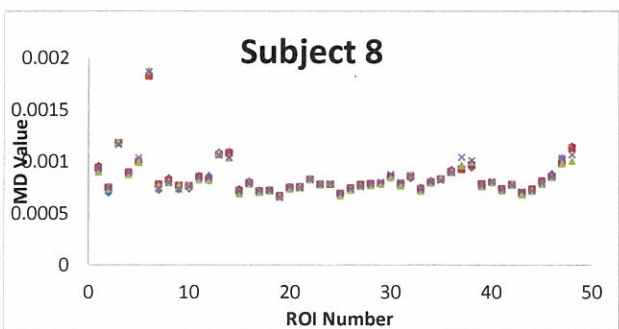
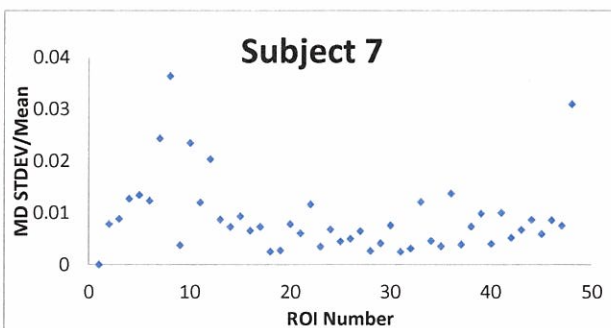
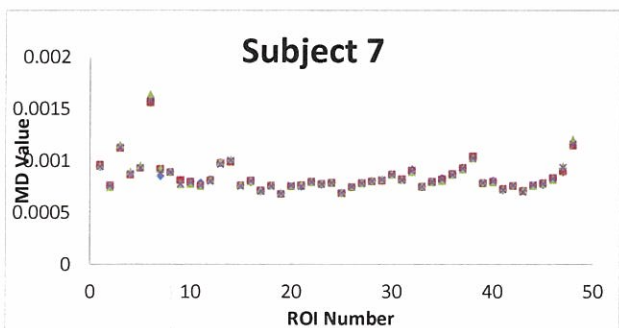
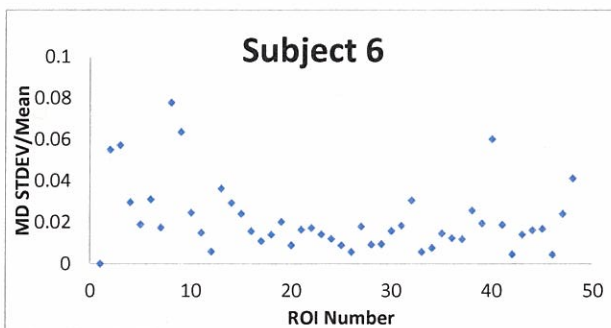
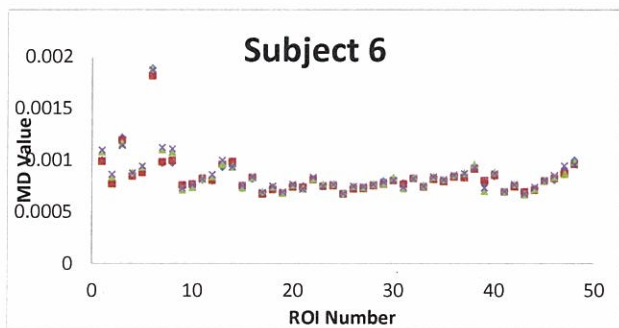
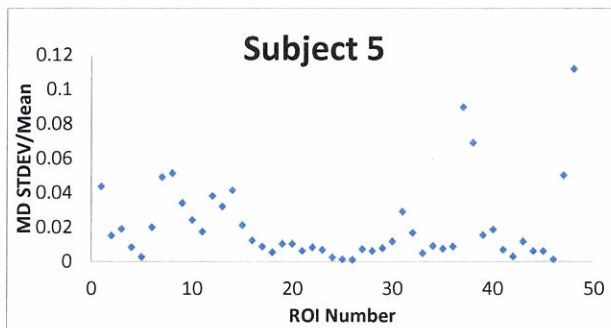
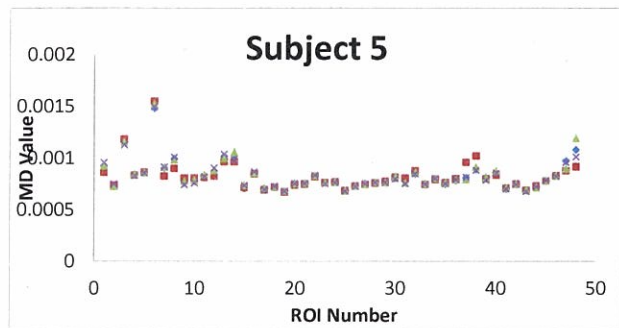


	ROI	# of voxels (1 voxel=1mm <sup>3</sup> )	DAY 1				DAY 2				Inter_days changes(%)
			Session1	Session2	Intra_day changes(%)	FA average in day1	Session3	Session4	Intra_day changes(%)	FA average in day2	
29	Posterior thalamic radiation (include optic radiation) R	3972	0.449908	0.44531	-1.0	0.4476075	0.456428	0.442477	-3.1	0.4494525	0.4
30	Posterior thalamic radiation (include optic radiation) L	3978	0.453857	0.4493	-1.0	0.451579	0.450636	0.450095	-0.1	0.4503655	-0.3
31	Sagittal stratum (include inferior longitudinal fasciculus and inferior fronto-occipital fasciculus) R	2228	0.432669	0.43318	0.1	0.4329255	0.426318	0.42953	0.8	0.427924	-1.2
32	Sagittal stratum (include inferior longitudinal fasciculus and inferior fronto-occipital fasciculus) L	2231	0.438775	0.43005	-2.0	0.4344115	0.427403	0.433604	1.5	0.4305035	-0.9
33	External capsule R	5611	0.239792	0.24889	3.8	0.2443385	0.248474	0.243921	-1.8	0.2461975	0.8
34	External capsule L	5587	0.263777	0.25476	-3.4	0.2592665	0.274292	0.266008	-3.0	0.27015	4.2
35	Cingulum (cingulate gyrus) R	2342	0.237055	0.23654	-0.2	0.2367985	0.240321	0.228286	-5.0	0.2343035	-1.1
36	Cingulum (cingulate gyrus) L	2751	0.261754	0.24212	-7.5	0.251938	0.26053	0.247519	-5.0	0.2540245	0.8
37	Cingulum (hippocampus) R	1236	0.233106	0.23078	-1.0	0.2319445	0.220252	0.222685	1.1	0.2214685	-4.5
38	Cingulum (hippocampus) L	1155	0.242824	0.24402	0.5	0.243421	0.244947	0.244322	-0.3	0.2446345	0.5
39	Fornix (cres) / Stria terminalis (can not be resolved with current resolution) R	1124	0.365999	0.35525	-2.9	0.3606265	0.361162	0.356986	-1.2	0.359074	-0.4
40	Fornix (cres) / Stria terminalis (can not be resolved with current resolution) L	1125	0.373948	0.36728	-1.8	0.3706125	0.363586	0.362881	-0.2	0.3632335	-2.0
41	Superior longitudinal fasciculus R	6607	0.321687	0.33137	3.0	0.326529	0.335341	0.327109	-2.5	0.331225	1.4
42	Superior longitudinal fasciculus L	6605	0.339853	0.33595	-1.1	0.3379035	0.347002	0.340741	-1.8	0.3438715	1.8
43	Superior fronto-occipital fasciculus (could be a part of anterior internal capsule) R	507	0.225951	0.22584	0.0	0.225895	0.242426	0.226699	-6.5	0.2345625	3.8
44	Superior fronto-occipital fasciculus (could be a part of anterior internal capsule) L	507	0.286081	0.25876	-9.5	0.2724225	0.312929	0.283851	-9.3	0.29839	9.5
45	Uncinate fasciculus R	380	0.350347	0.36083	3.0	0.3555885	0.334599	0.357861	7.0	0.34623	-2.6
46	Uncinate fasciculus L	376	0.326881	0.33072	1.2	0.3288005	0.323917	0.327799	1.2	0.325858	-0.9
47	Tapetum R	596	0.381061	0.39329	3.2	0.3871735	0.359049	0.382778	6.6	0.3709135	-4.2
48	Tapetum L	600	0.392576	0.37548	-4.4	0.3840295	0.364666	0.380967	4.5	0.3728165	-2.9

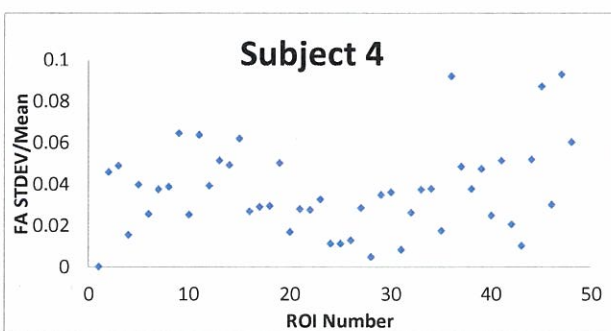
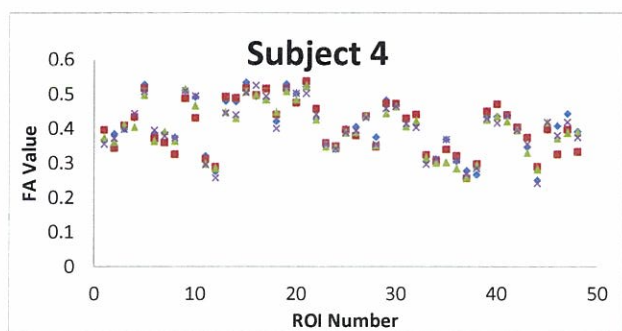
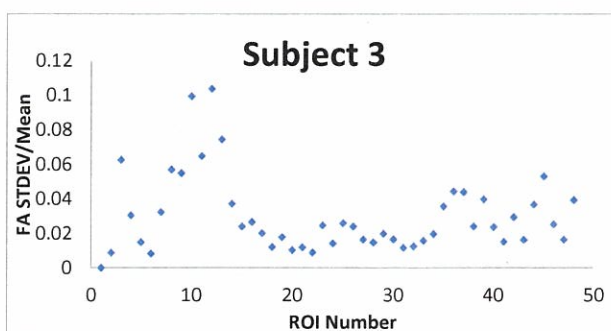
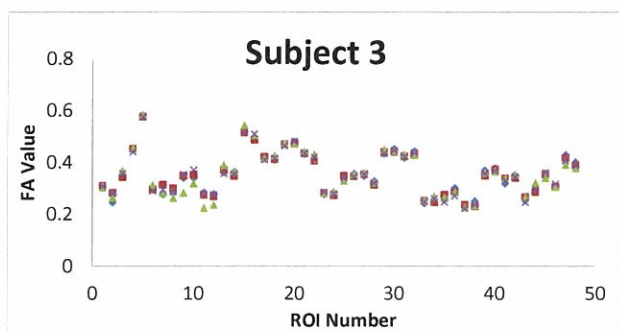
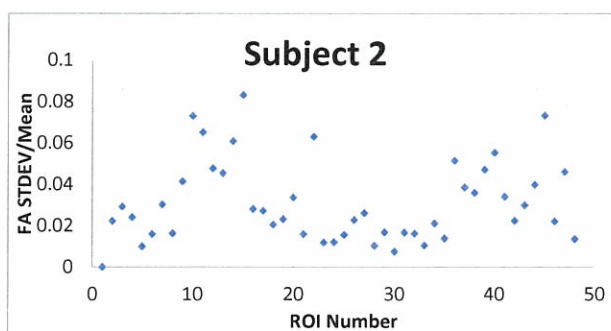
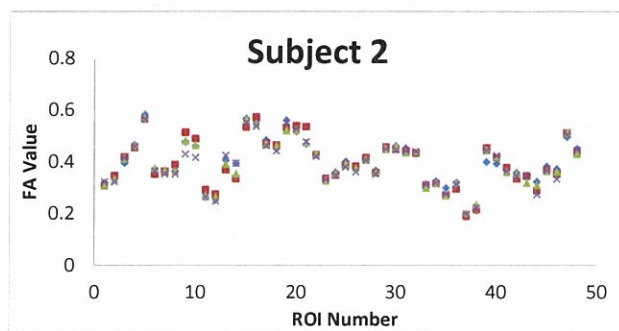
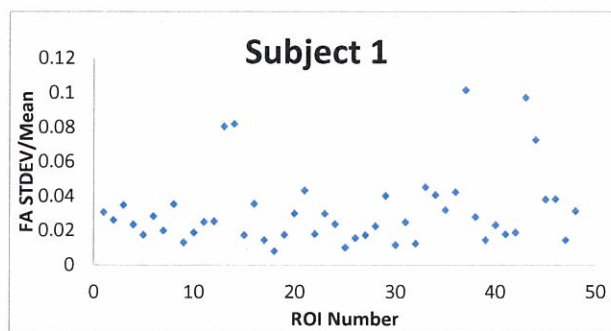
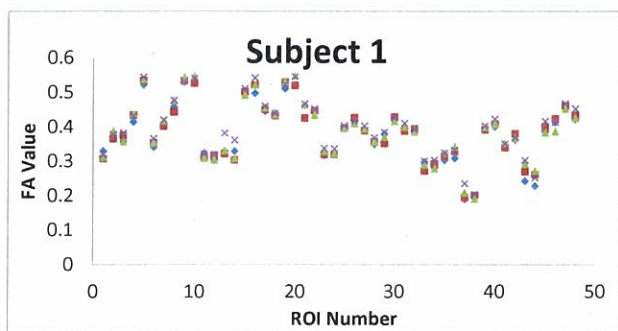
Appendix 6:  
Subject 1-8: MD vs ROI; MD  
stddev/mean vs ROI

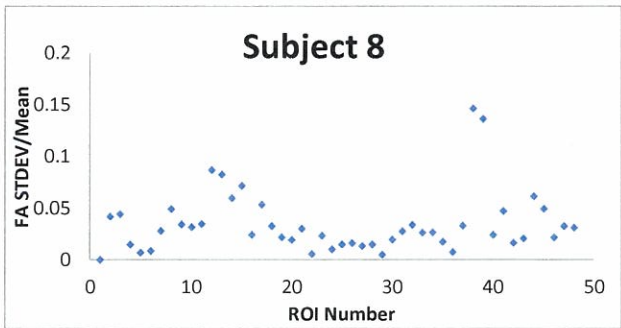
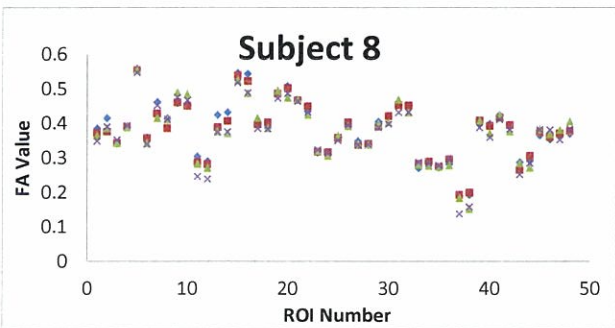
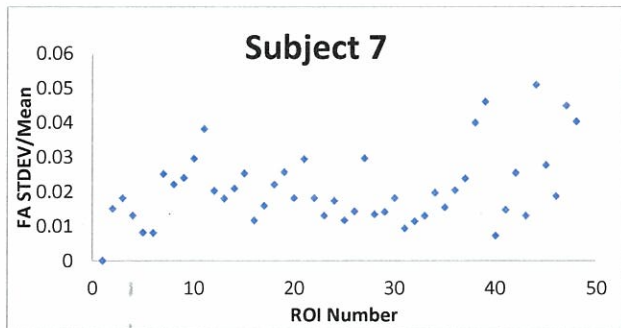
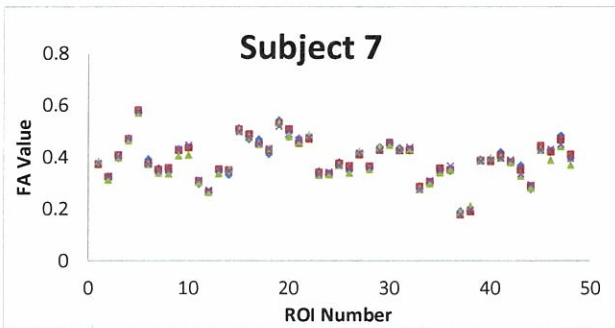
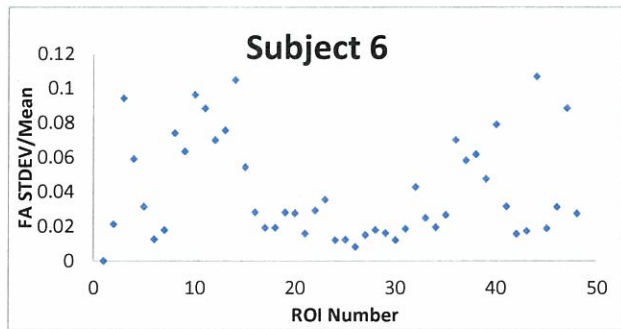
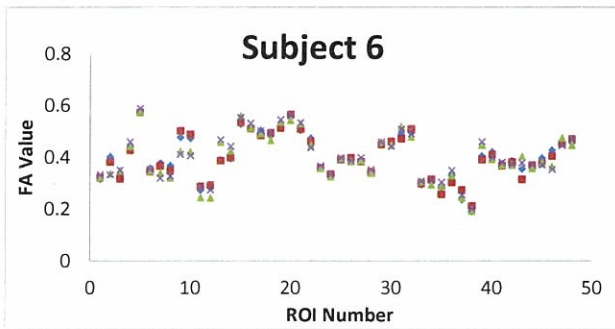
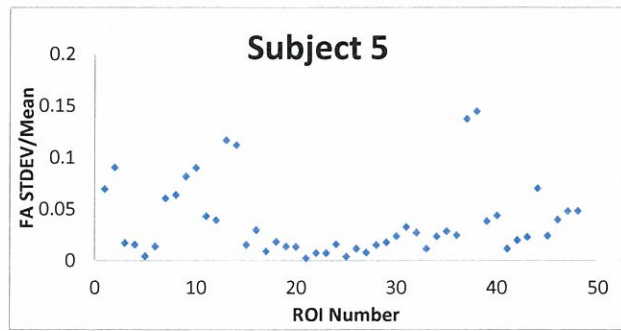
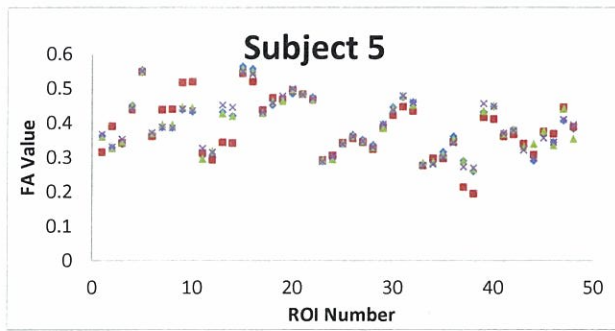






Appendix 7:  
Subject 1-8: FA vs ROI; FA  
stdev/mean vs ROI

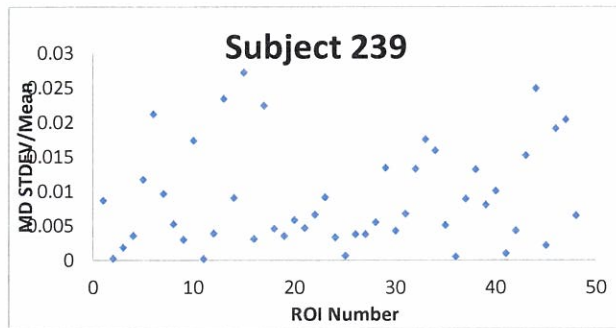
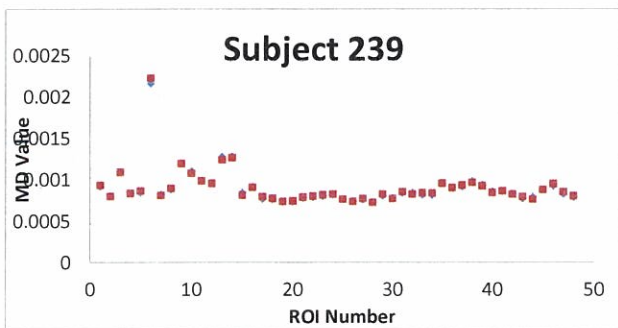
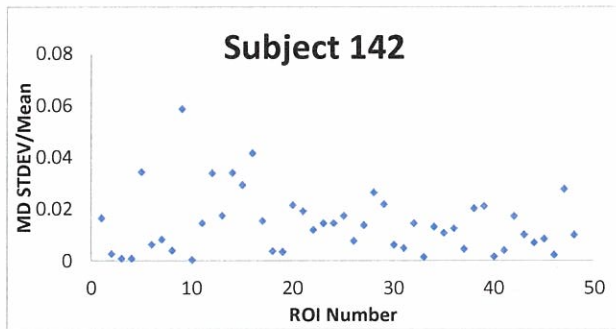
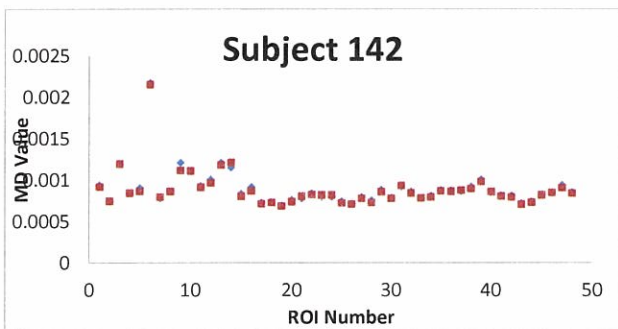
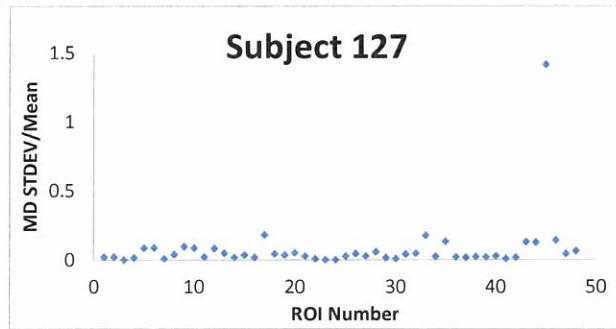
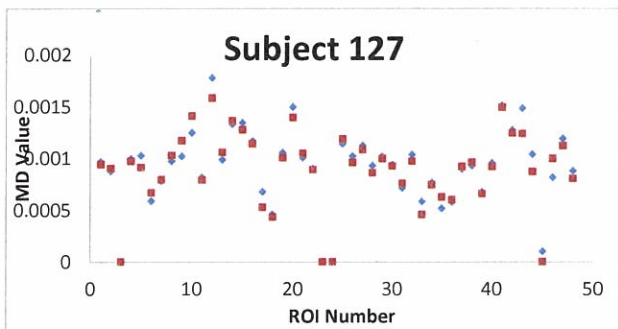
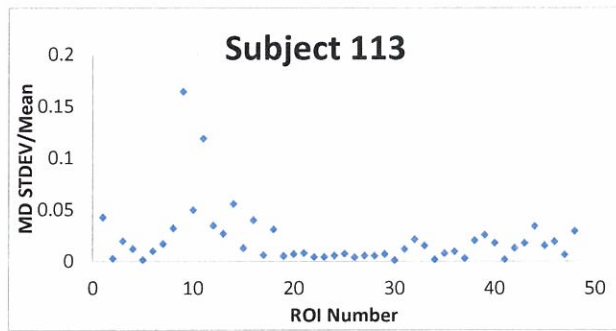
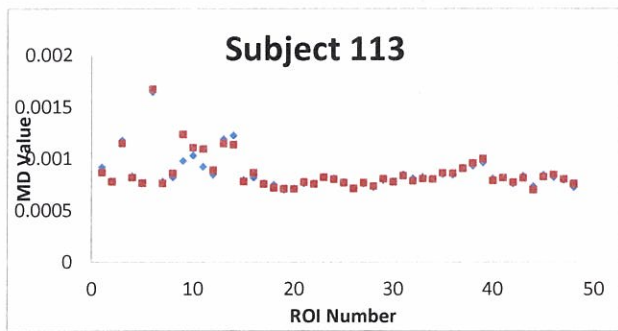




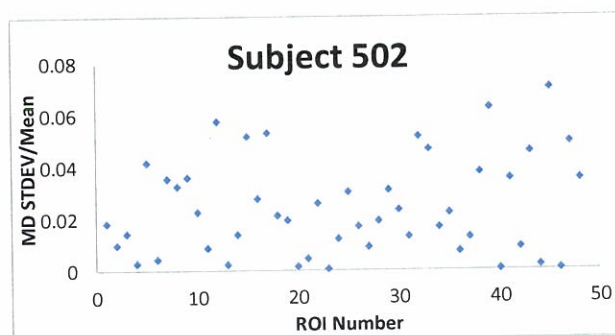
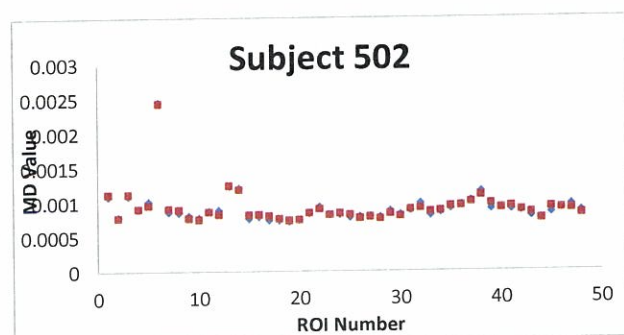
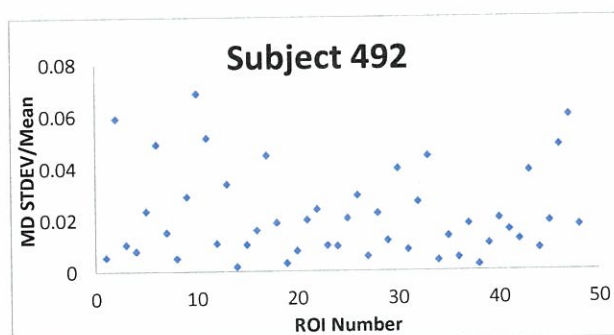
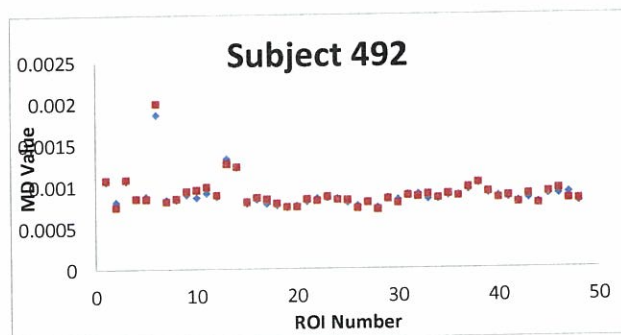
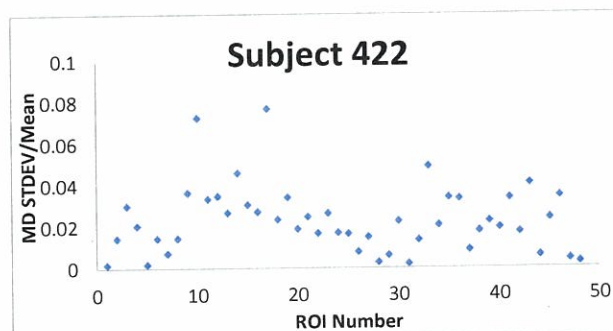
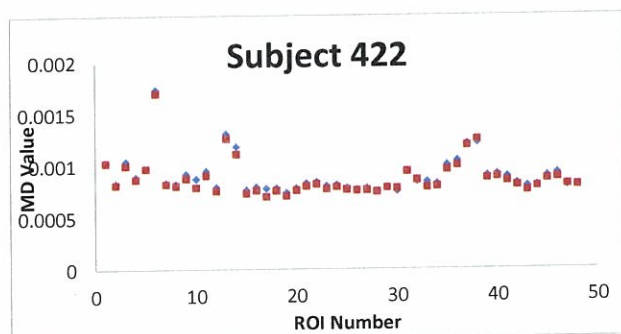
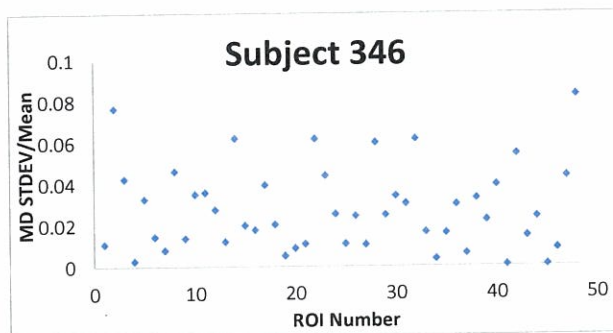
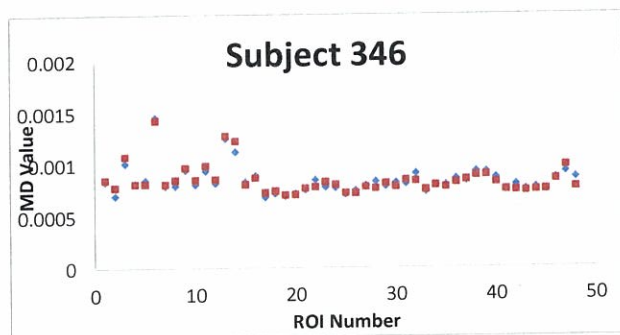
Appendix 8:  
All 20 subjects: MD vs ROI;  
MD stddev/mean vs ROI

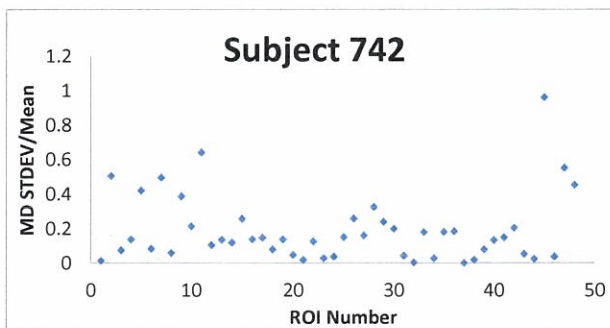
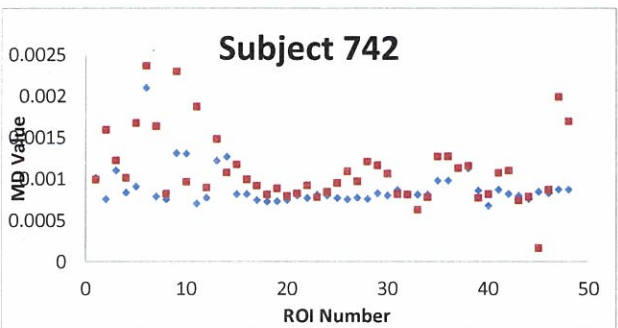
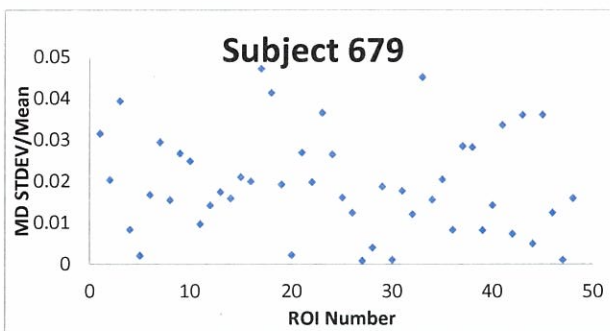
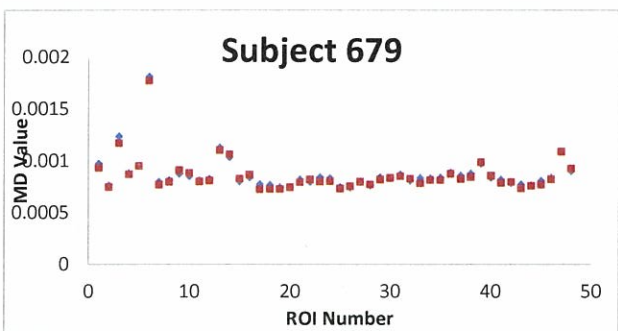
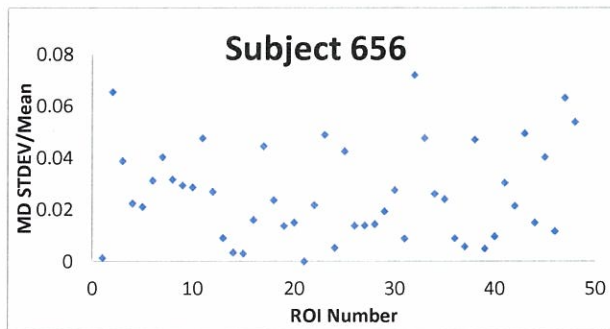
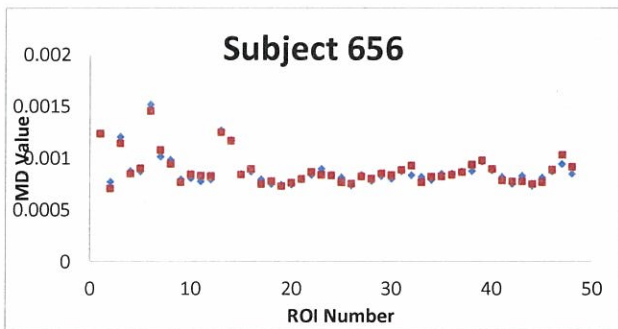
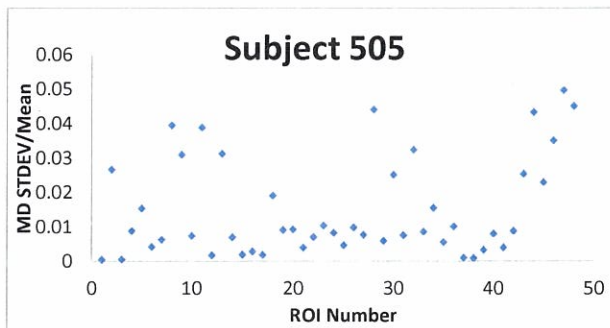
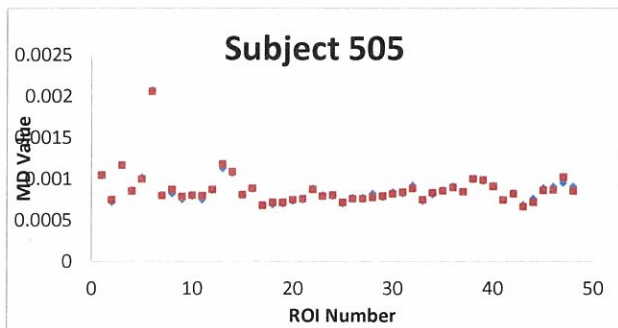
## 3T MRI - DTI Reproducibility - Human Study

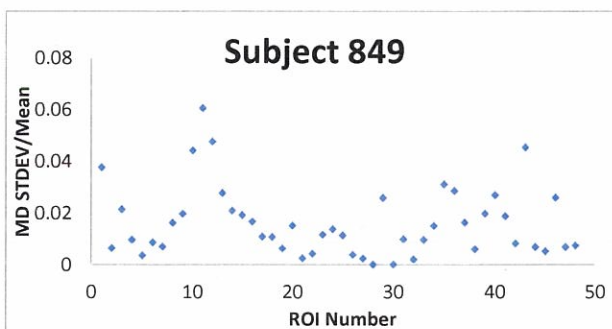
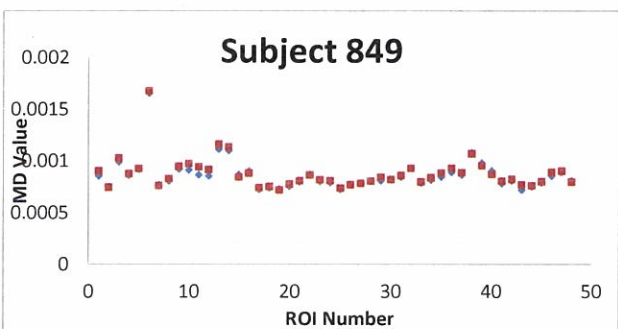
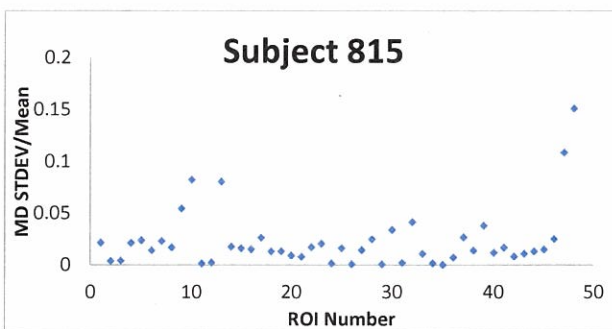
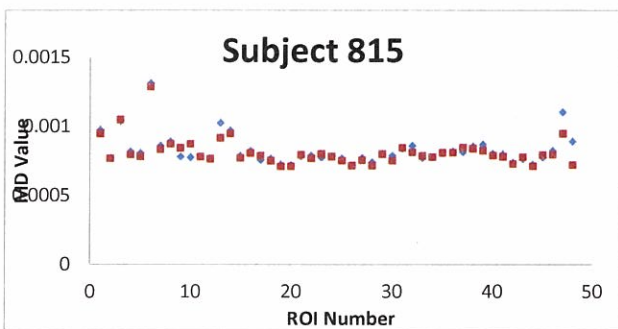
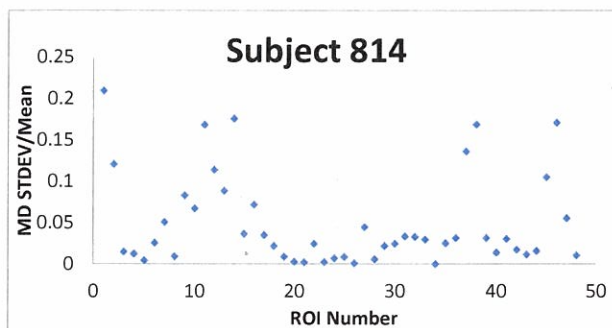
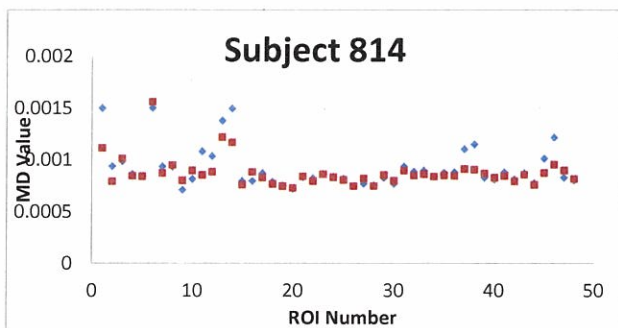
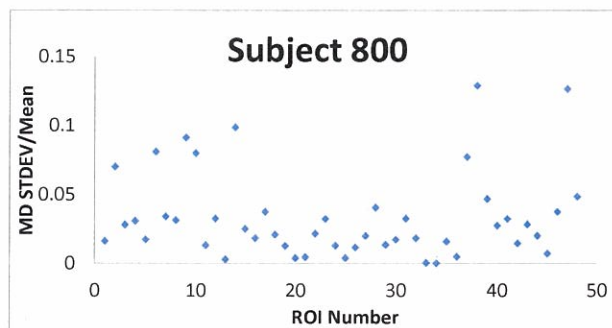
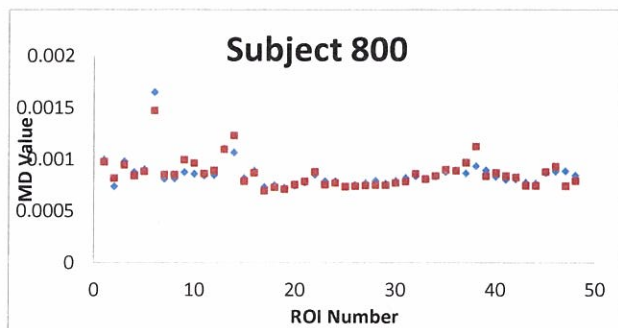
Index	Subject #
1	113
2	127
3	142
4	239
5	346
6	422
7	492
8	502
9	505
10	656
11	679
12	742
13	800
14	814
15	815
16	849
17	906
18	913
19	916
20	934

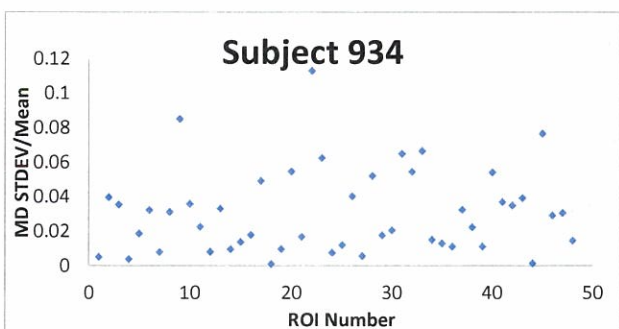
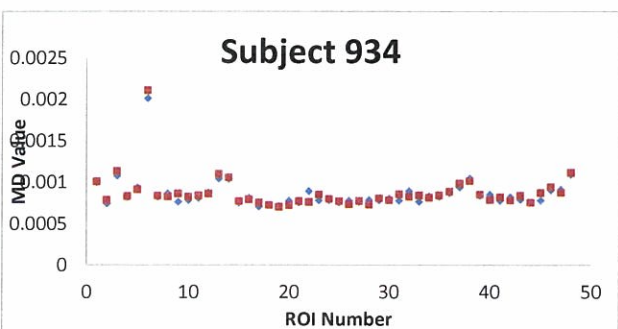
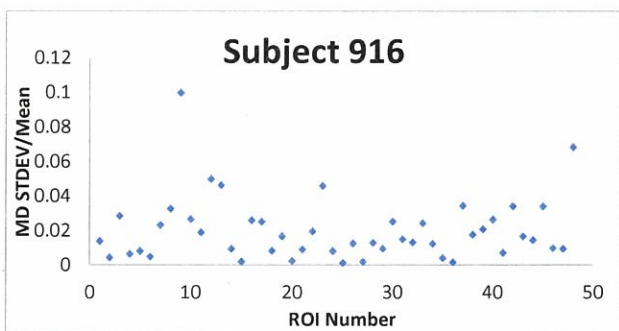
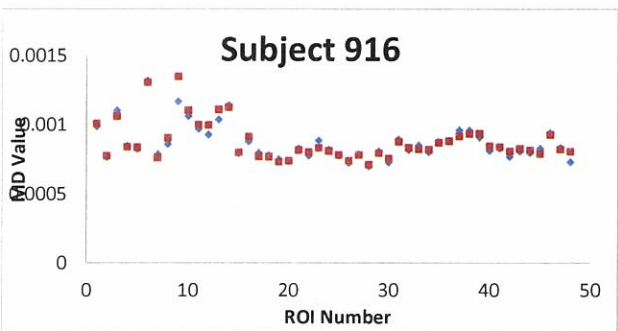
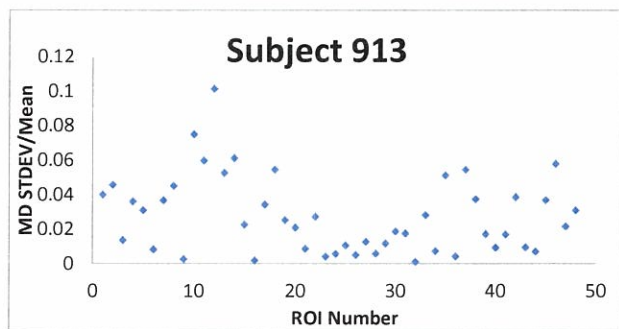
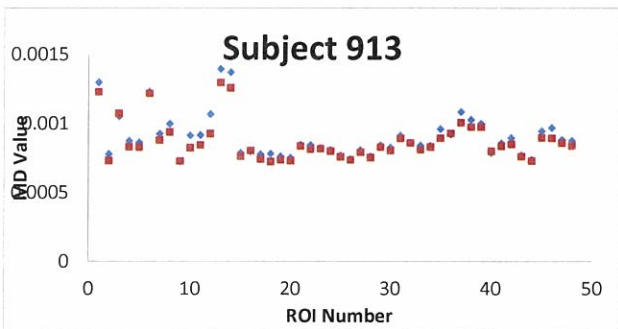
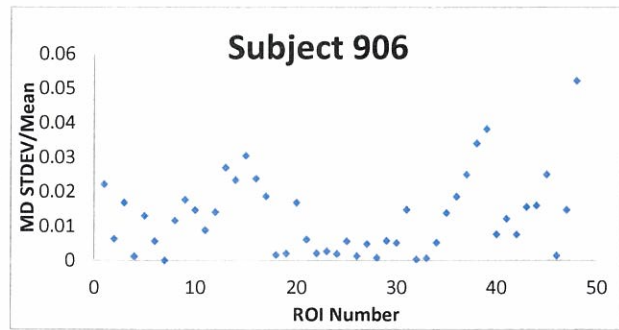
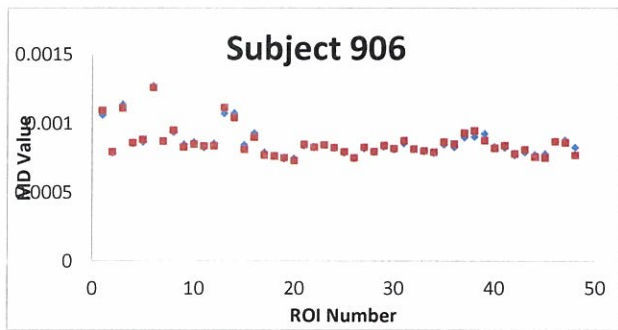




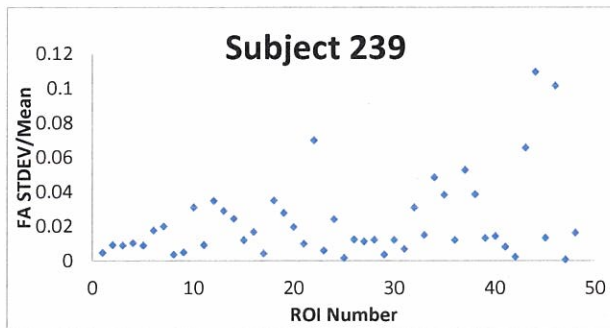
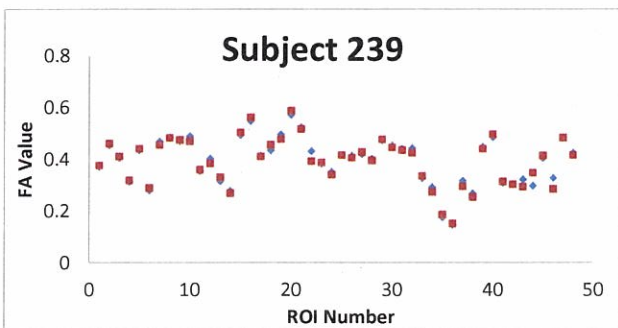
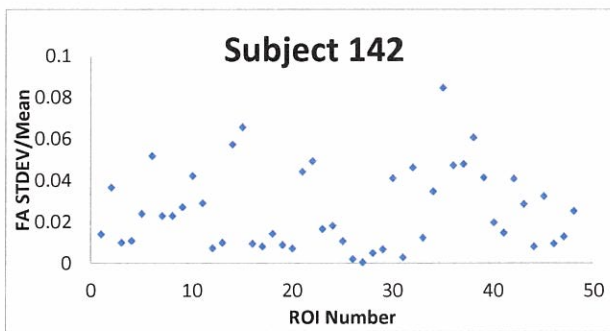
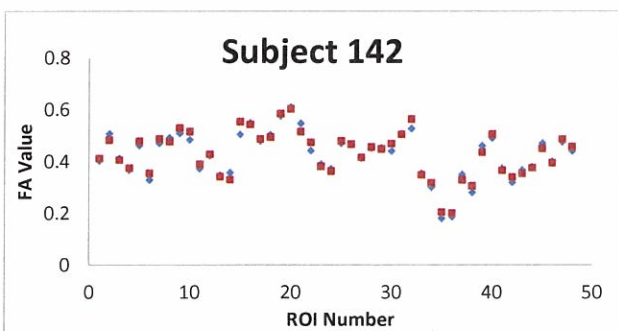
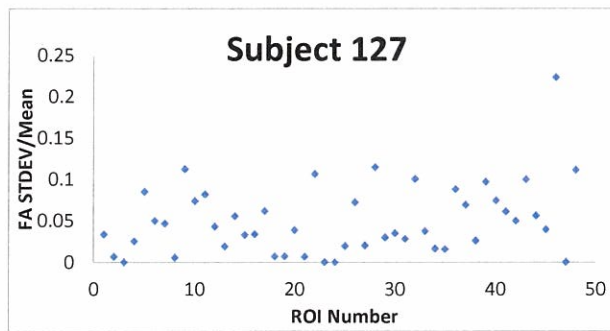
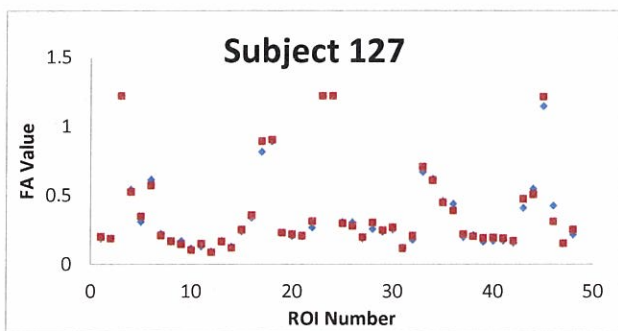
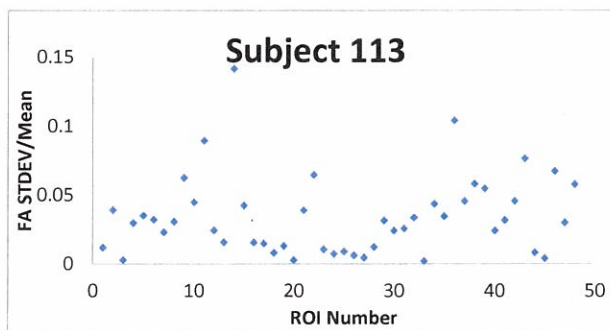
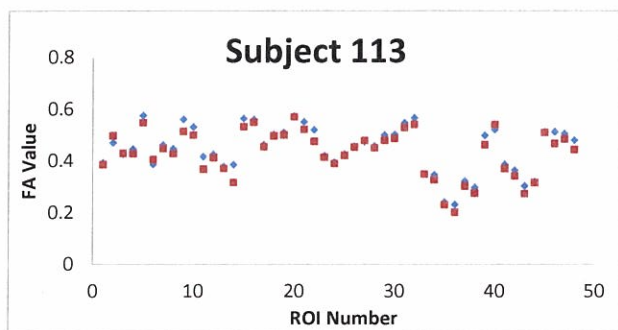




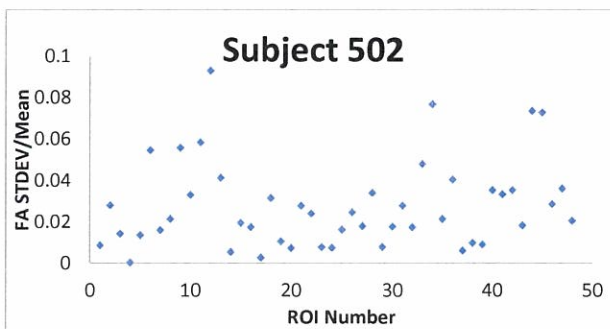
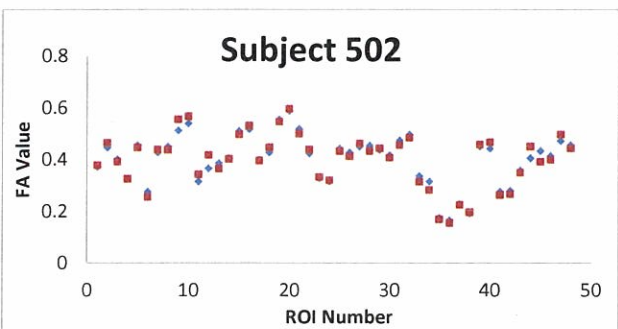
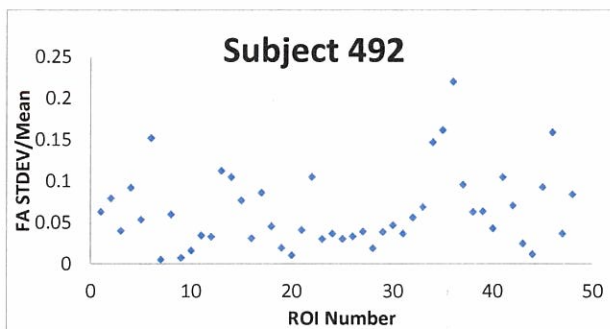
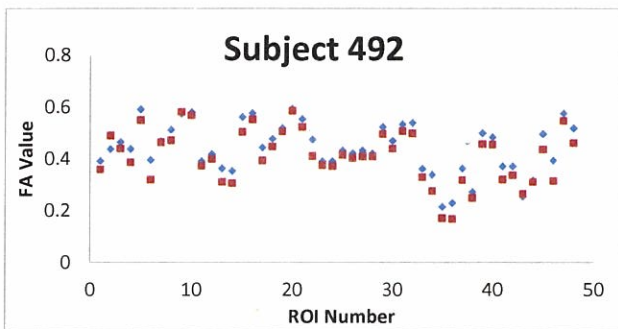
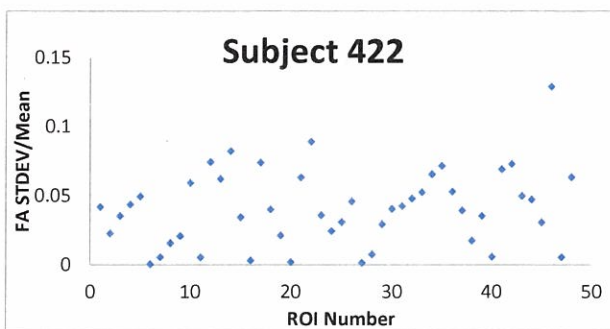
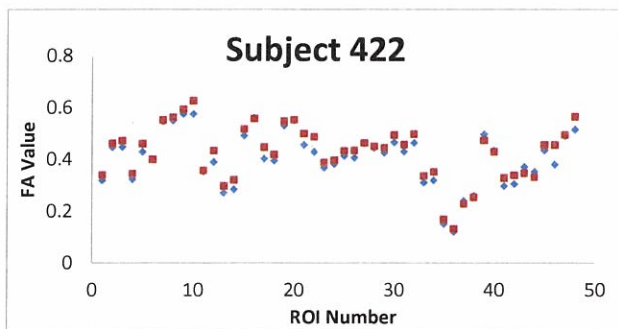
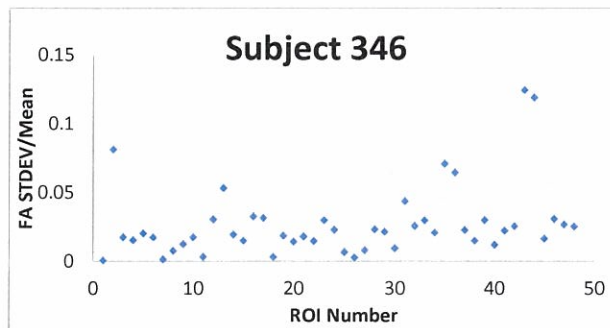
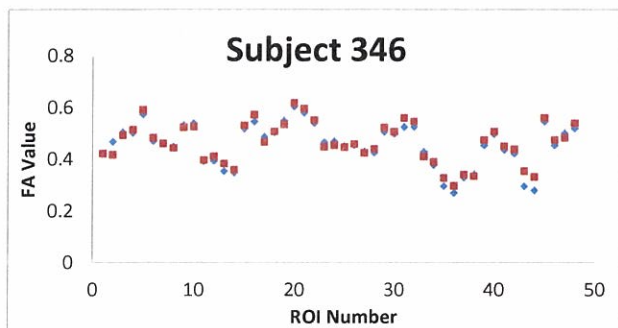


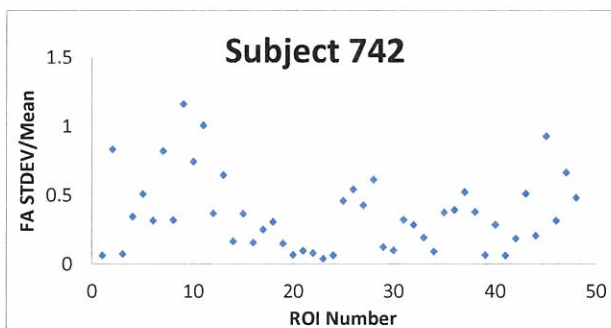
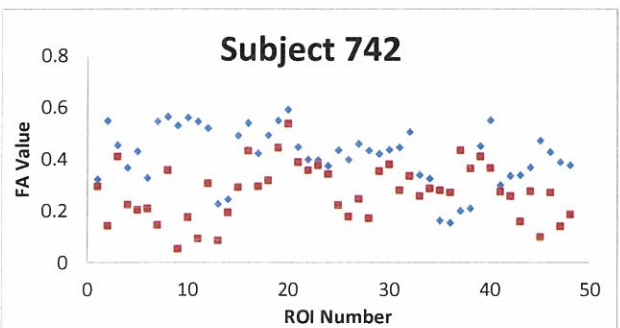
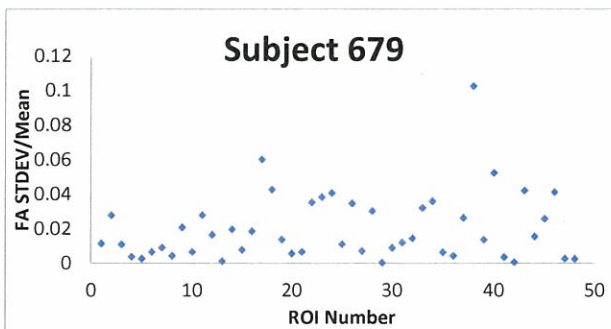
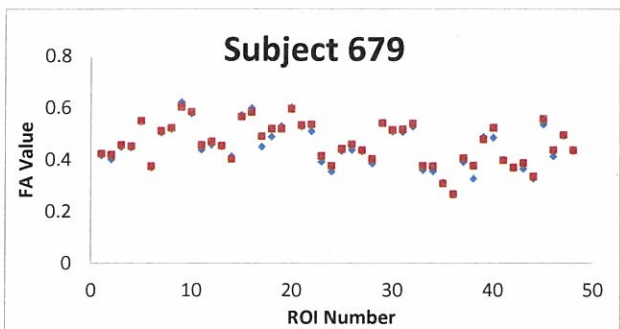
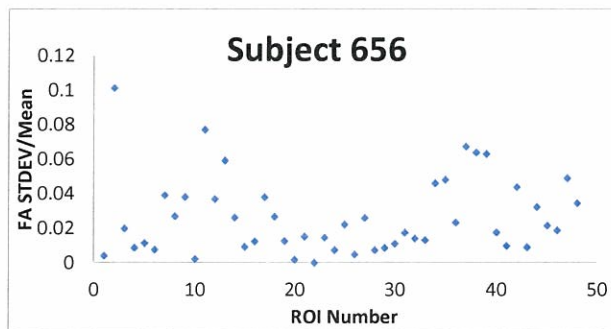
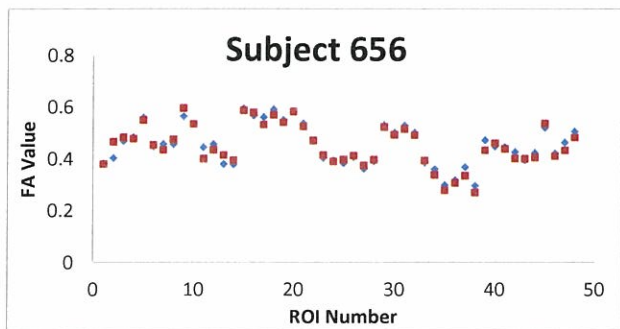
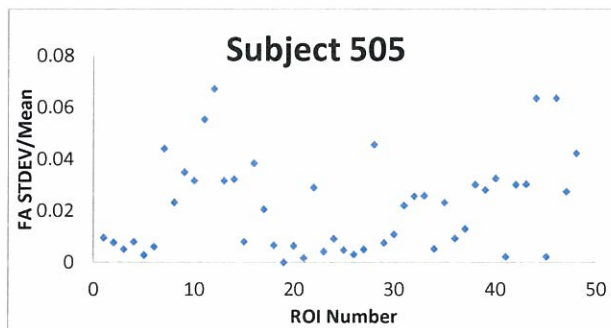
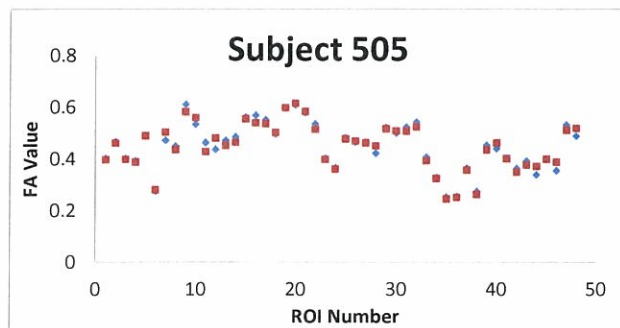


Appendix 9:  
All 20 subjects: FA vs ROI;  
FA stdev/mean vs ROI

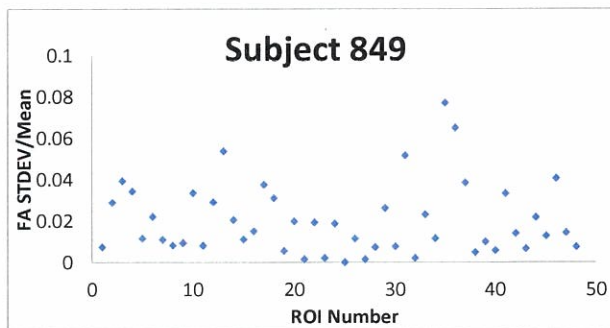
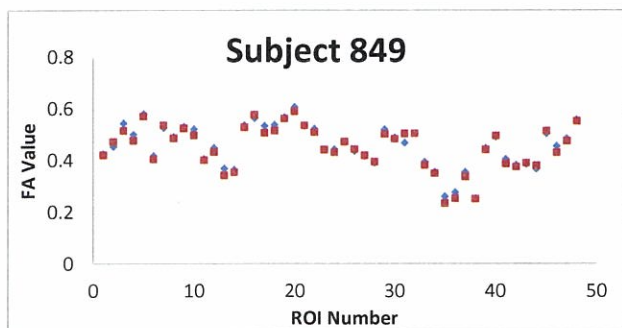
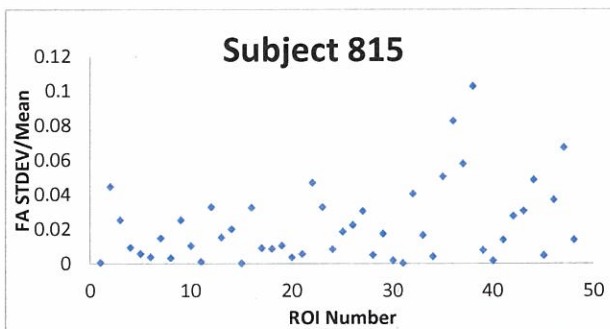
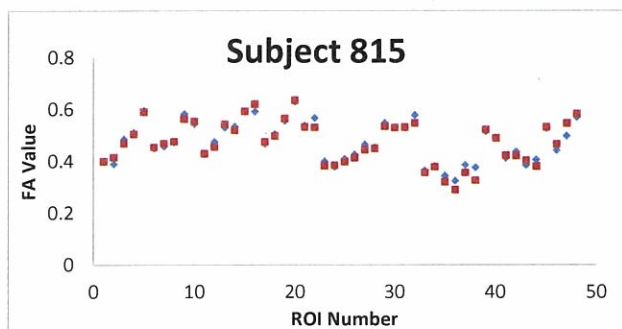
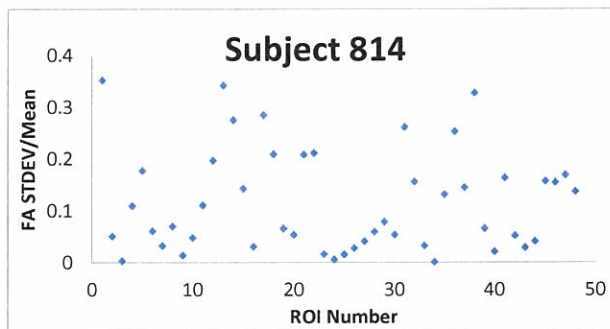
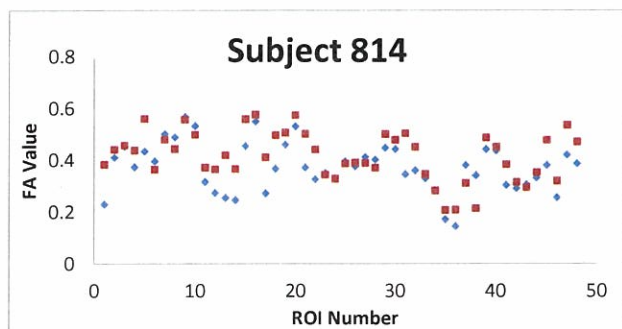
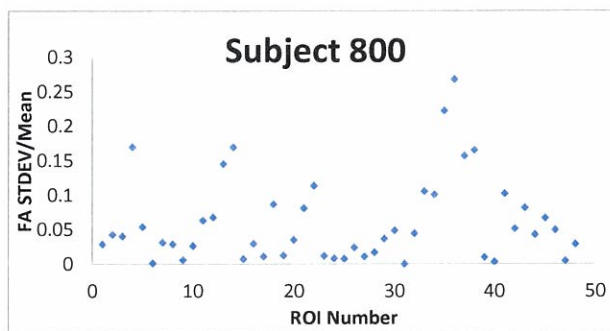
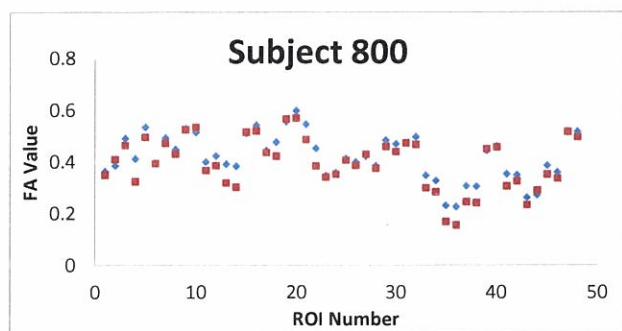


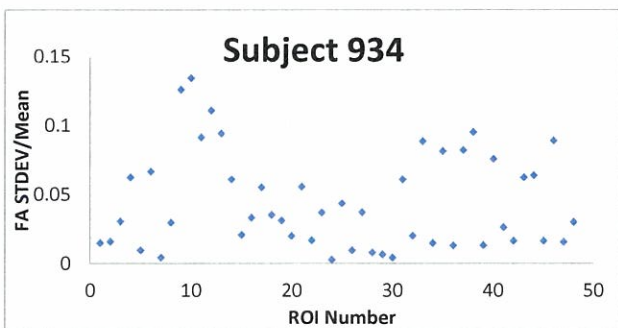
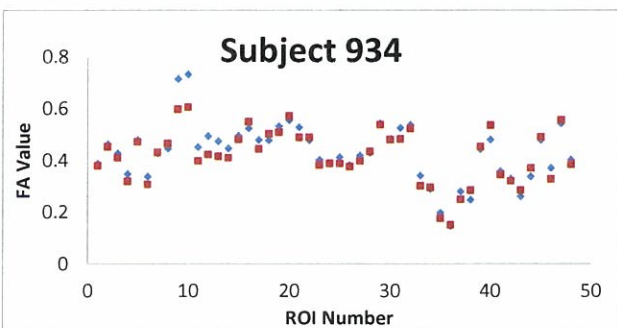
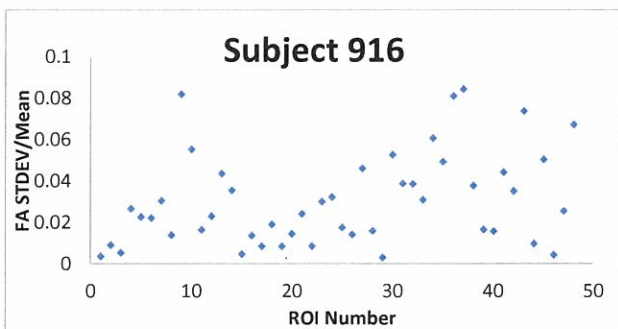
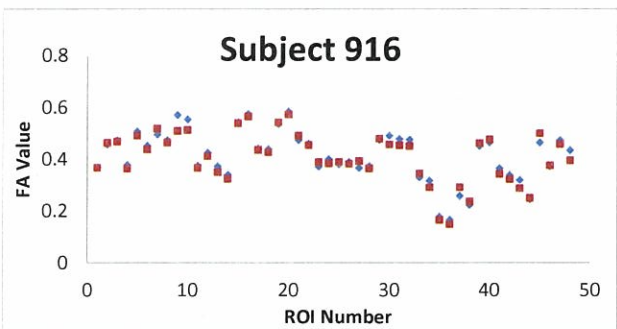
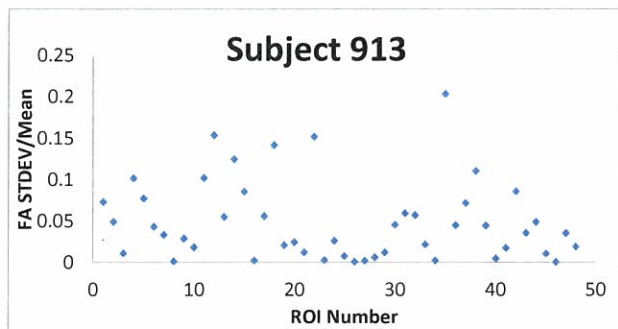
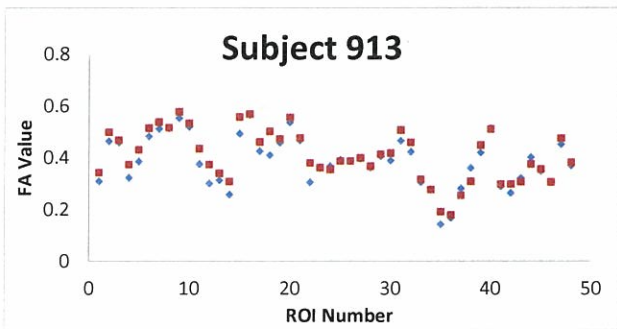
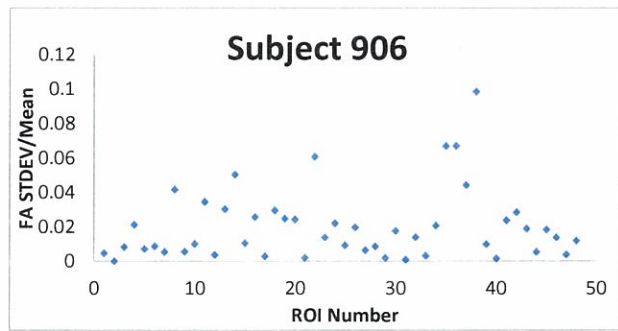
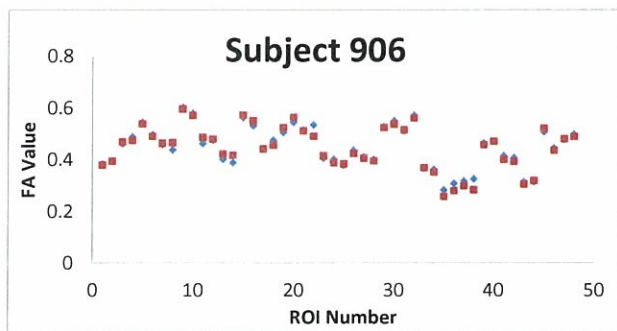













Appendix 10:  
Traumatic Brain Injury  
Diffusion Magnetic  
Resonance Imaging  
Research Roadmap  
Development Project.  
Product Line Review (PLR)  
meeting, Medical Imaging  
Technologies. Presentation  
slides. 12 June 2012.



Product Line  
Review  
(PLR)  
Meeting

Medical  
Imaging  
Technologies

12 June 2012


1

# Traumatic Brain Injury Diffusion Magnetic Resonance Imaging Research Roadmap Development Project

## Michael W. Vannier, MD

### 14 September 2009 – 13 October 2012

Type of Funding - CSI



Product Line  
Review  
(PLR)  
Meeting

Medical  
Imaging  
Technologies

12 June 2012

2

## Military relevant issue to be solved

- **Goal:** Translate diffusion MRI for TBI into a qualified clinical imaging biomarker
- **Aims:**
  - Develop consensus roadmap for diffusion MRI physics and image processing methods to provide sensitive and specific marker for mild to moderate traumatic brain injury (TBI)
  - Automate post-processing of D-MRI for TBI and conduct workshop(s) on comparative evaluation of methods
  - Design, develop and test infrastructure to support Phase 3 multicenter clinical trials of D-MRI for TBI (protocols, site qualification, quality control, record-keeping, ...)
  - Develop web-based image archive and support data sharing of D-MRI database



Product Line  
Review  
(PLR)  
Meeting

Medical  
Imaging  
Technologies

12 June 2012

3

## Solution

Develop D-MRI into a qualified and validated biomarker

- by adapting methods and using best practices for other neuroimaging biomarkers
- identifying the barriers to progress, especially for multidisciplinary (MRI physics, computer science/image processing, and especially TBI clinical practice) collaboration
- vanguard project to conduct multicenter trial and establish infrastructure needed for Phase 3 studies of TBI using D-MRI



Product Line  
Review  
(PLR)  
Meeting

Medical  
Imaging  
Technologies

12 June 2012

4

## Project Description

2010 workshop on D-MRI of TBI was held

Recommendations in 3 areas:

- TBI application of D-MRI (clinical)
- MR physics (protocol / quality control)
- Informatics (tool development / integration)

We developed on-line archive with integrated analysis tools; website on D-MRI of TBI

CDE – common data elements were implemented

Ongoing evaluation of D-MRI reproducibility and human trial of data acquisition protocol



Product Line  
Review  
(PLR)  
Meeting

Medical  
Imaging  
Technologies

12 June 2012

5

## Goals

- Archiving, quality control and automated analysis of Diffusion MRI (especially DTI) data for traumatic brain injury (TBI)
- Translate D-MRI into a clinical reality
  - Standardization of examinations
  - Automated analysis
  - Quality control
  - Reference database – independently validated

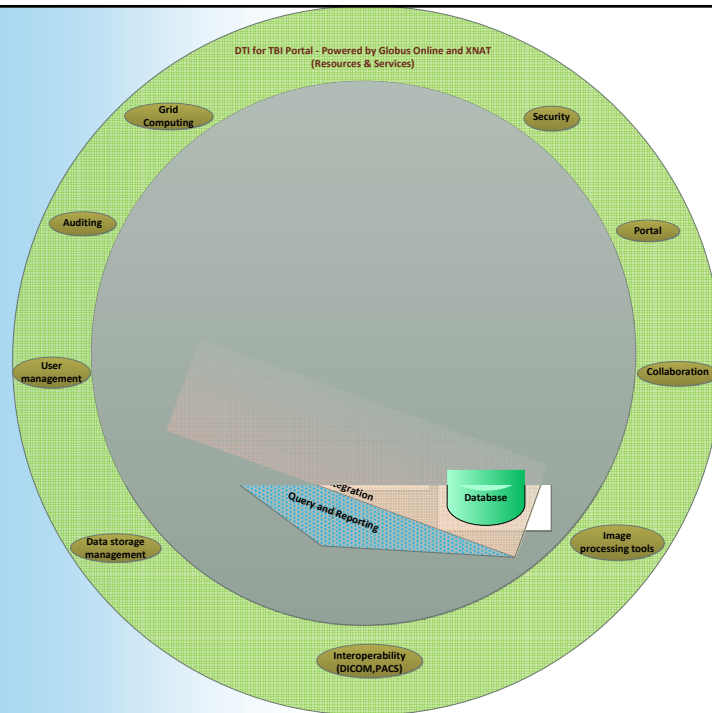


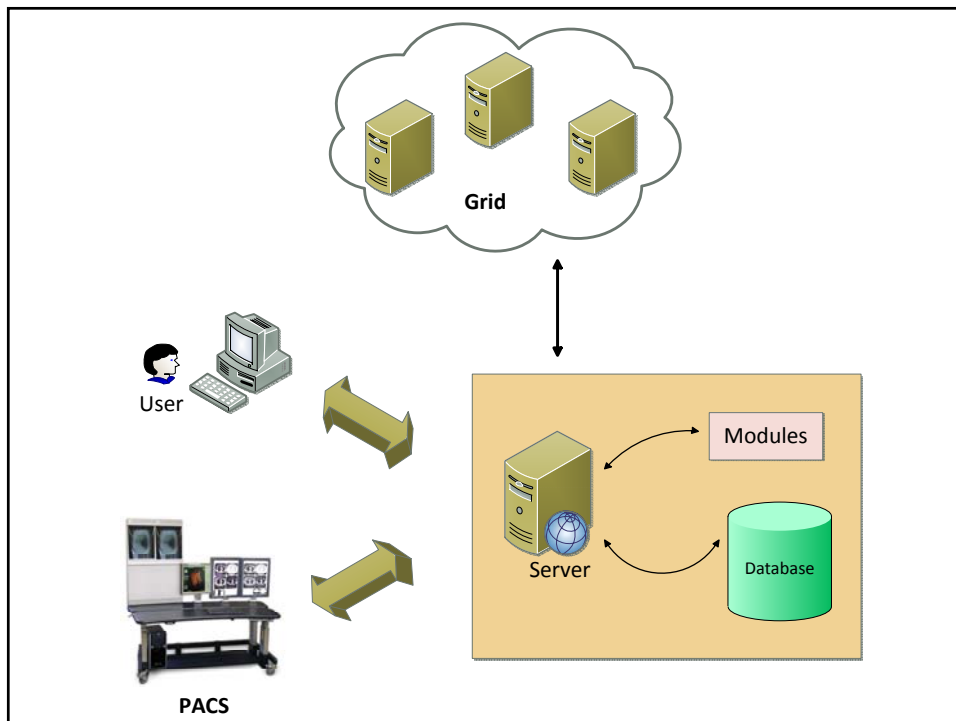
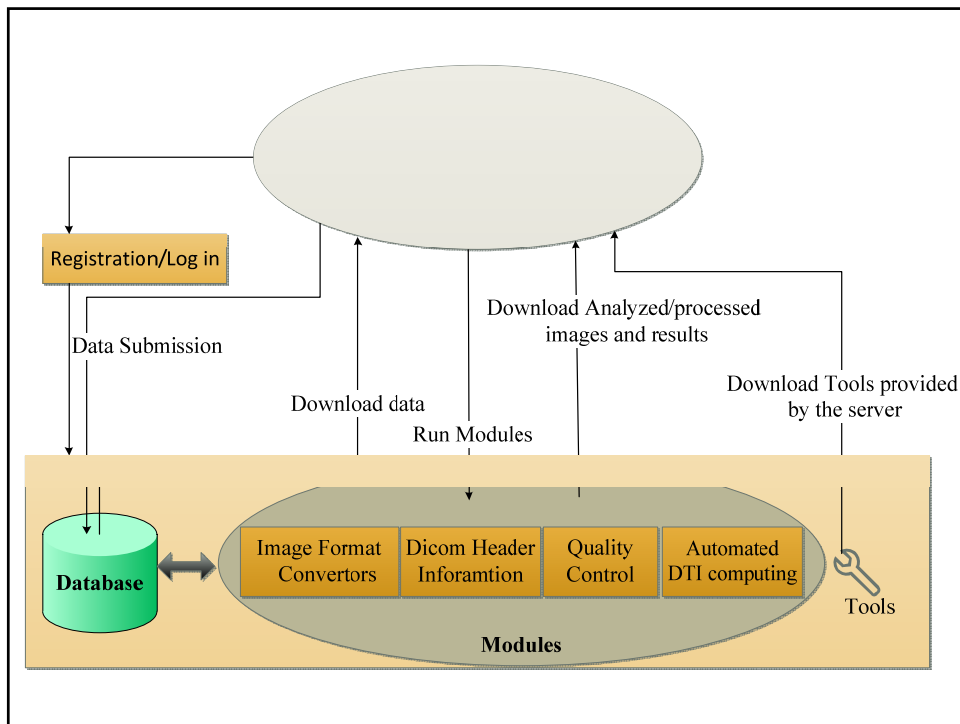
Product Line  
Review  
(PLR)  
Meeting

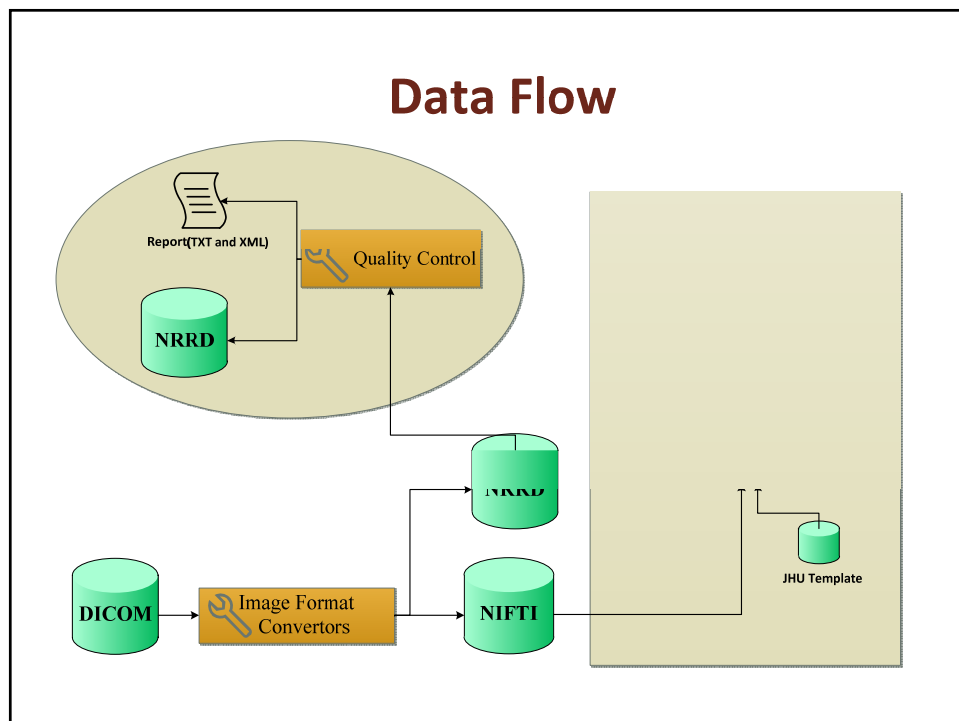
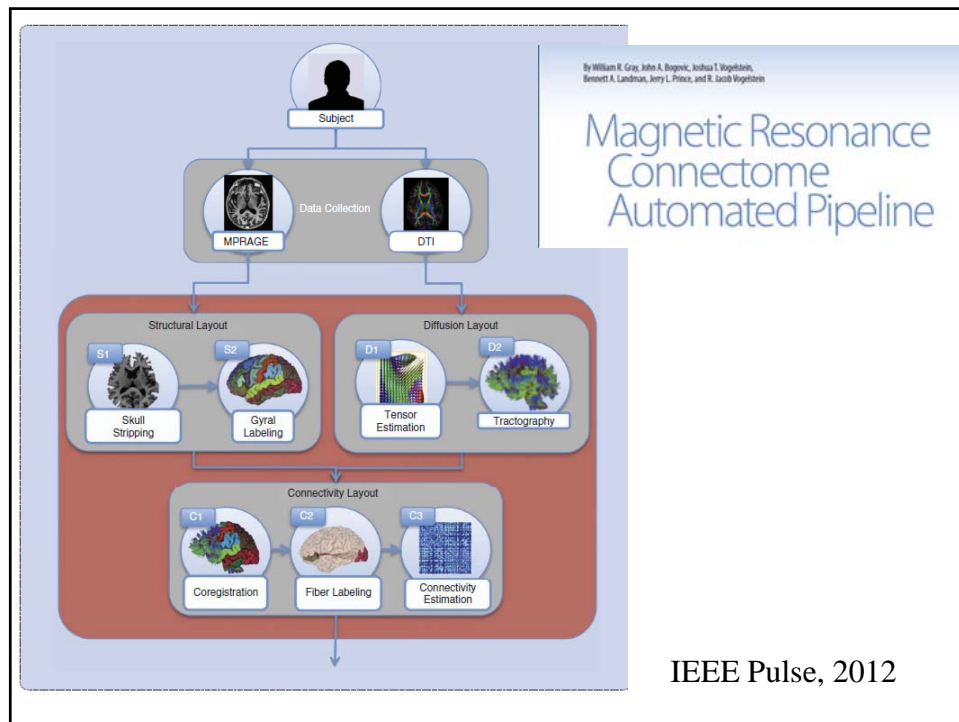
Medical  
Imaging  
Technologies

12 June 2012

6











# Computation Institute – University of Chicago and Argonne National Lab



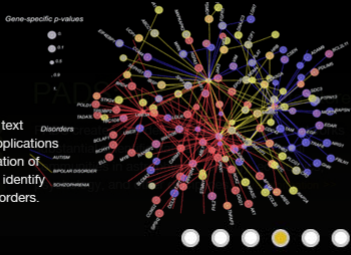
[jobs](#) | [contact us](#) | [computing resources](#) | [help desk](#)

[Home](#) | [About CI](#) | [People](#) | [Research](#) | [Collaborators](#) | [Facilities](#) | [Education](#) | [News](#) | [Events](#)

## Text Mining

Researchers at the CI are using text mining in a host of innovative applications including, among others, population of genetic models that are used to identify genetic overlaps in complex disorders.

[more information >>](#)



### Upcoming events

**JUN 13**

LANS Informal Seminar  
**Towards the Quantum Machine: Fast and accurate modeling of quantum chemical properties using machine learning**

### News



Computation Institute scientists receive honors  
 Computation Institute scientists at the University of Chicago and Argonne National Laboratory are accruing multiple honors this year, including two by CI director Ian Foster...

The Computation Institute is an intellectual nexus and resource center for scholars from multiple disciplines building and applying computational platforms for science.



# Globus Online - <https://www.globusonline.org/>



[Manage Data](#) | [News & Events](#) | [About](#) | [Support](#) | [Log In](#) | [Sign Up](#)

Reliable, high-performance, secure file transfer.

## Move files fast. No IT required.






[+ WATCH A VIDEO](#)  
 Globus Online in a nutshell



[> GET STARTED](#)  
 Sign up and get moving

**5,148,831,148 MB** TRANSFERRED

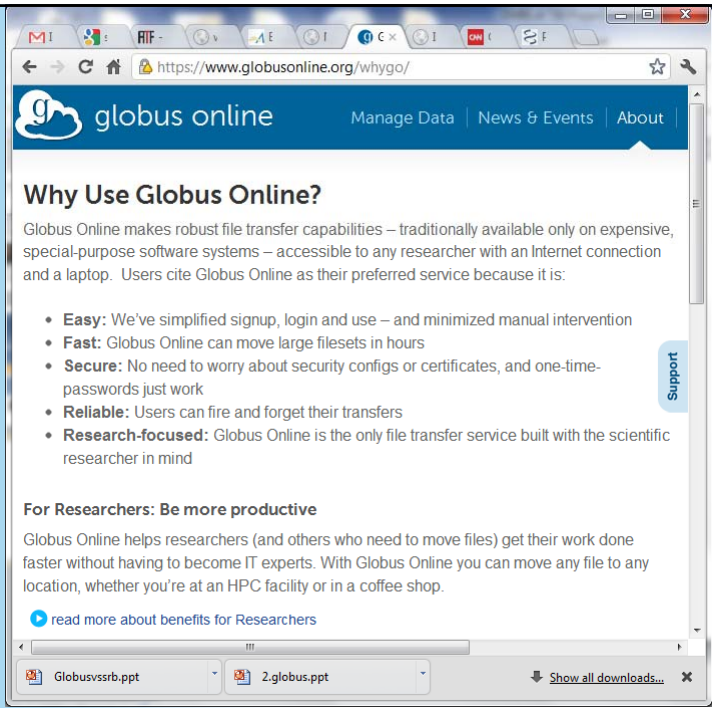


**Product Line  
Review  
(PLR)  
Meeting**


**Medical  
Imaging  
Technologies**

**12 June 2012**

13



The screenshot shows the Globus Online website with the URL <https://www.globusonline.org/whygo/>. The page title is "Why Use Globus Online?". The text describes Globus Online as a robust file transfer service accessible to researchers with an Internet connection and a laptop. It lists four key features: Easy (simplified signup/login), Fast (moving large filesets in hours), Secure (no security configs/certificates), and Reliable (fire-and-forget transfers). It also mentions it is research-focused. A section for researchers states it helps get work done faster. At the bottom, there are download links for "Globusvssrb.ppt" and "2.globus.ppt", and a "Show all downloads..." link.

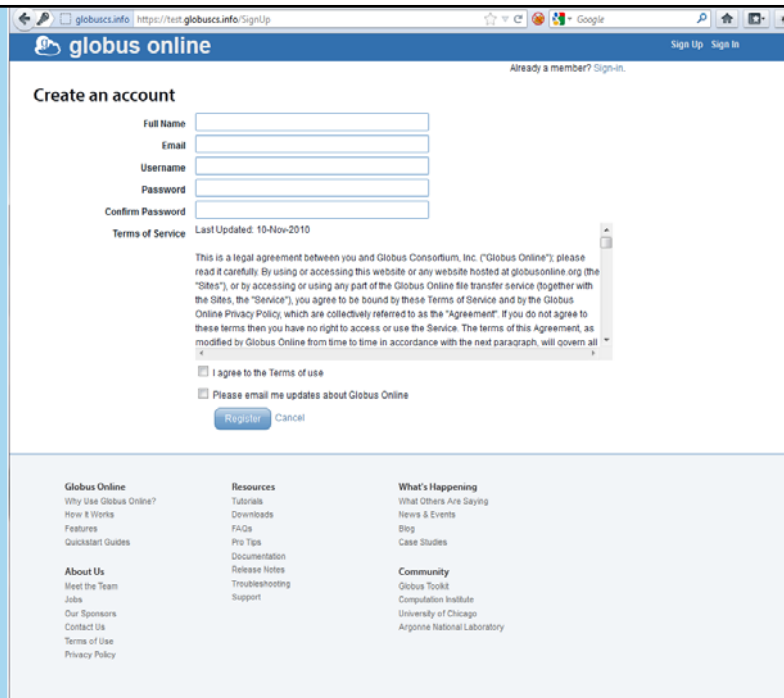


**Product Line  
Review  
(PLR)  
Meeting**

**Medical  
Imaging  
Technologies**

**12 June 2012**

14



The screenshot shows the Globus Online website with the URL <https://test.globusinfo.org/SignUp>. The page title is "Create an account". It includes a "Sign Up" link and a "Sign In" link. The "Create an account" section has input fields for Full Name, Email, Username, Password, and Confirm Password. Below these is a "Terms of Service" section with a "Last Updated: 10-Nov-2010" note. There are checkboxes for "I agree to the Terms of use" and "Please email me updates about Globus Online". At the bottom, there are "Register" and "Cancel" buttons. The footer contains links for "Globus Online", "Resources", "What's Happening", "About Us", and "Community".

Computed snapshots of the session.

Some information extracted from DICOM header

15

Product Line Review (PLR) Meeting

Medical Imaging Technologies

12 June 2012

Screen shot of DTI FA color map created by DTI-Computation tool (Visualized by FSL View)

16



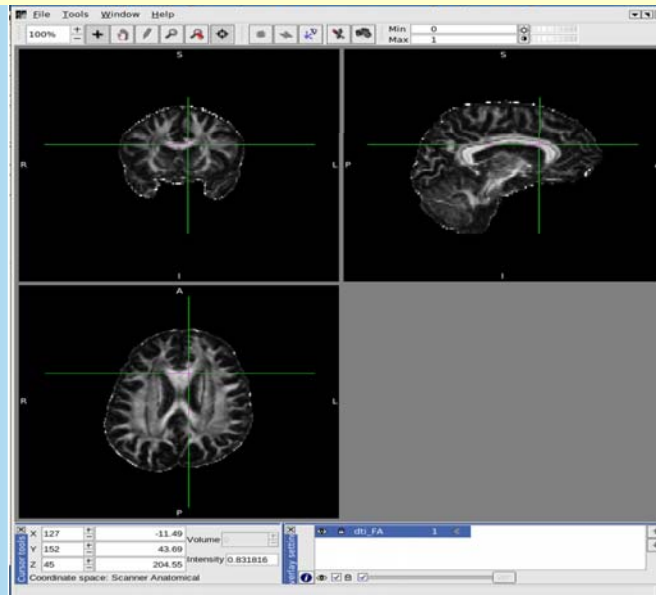
Product Line  
Review  
(PLR)  
Meeting

Medical  
Imaging  
Technologies

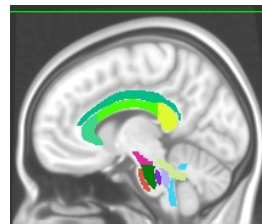
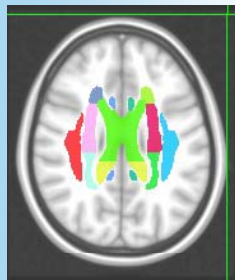
12 June 2012

17

## Screen shot of DTI FA map created by DTI-Computation tool



## Johns Hopkins ROI Template



**Tool : FSL**

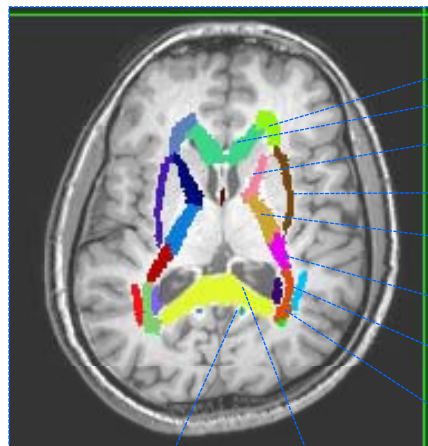
18



## Brain Substructures

index	label
1	Middle cerebellar peduncle
2	Pontine crossing tract (a part of MCP)
3	Genu of corpus callosum
4	Body of corpus callosum
5	Splenium of corpus callosum
6	Fornix (column and body of fornix)
7	Corticospinal tract R
8	Corticospinal tract L
9	Medial lemniscus R
10	Medial lemniscus L
11	Inferior cerebellar peduncle R
12	Inferior cerebellar peduncle L
13	Superior cerebellar peduncle R
14	Superior cerebellar peduncle L
15	Cerebral peduncle R
16	Cerebral peduncle L
17	Anterior limb of internal capsule R
18	Anterior limb of internal capsule L
19	Posterior limb of internal capsule R
20	Posterior limb of internal capsule L
21	Retrolecticular part of internal capsule R
22	Retrolecticular part of internal capsule L
23	Anterior corona radiata R
24	Anterior corona radiata L
25	Superior corona radiata R
26	Superior corona radiata L
27	Posterior corona radiata R
28	Posterior corona radiata L
29	Posterior thalamic radiation (include optic radiation) R
30	Posterior thalamic radiation (include optic radiation) L

index	label
31	Sagittal stratum (include inferior longitudinal fasciculus and inferior fronto-occipital fasciculus) R
32	Sagittal stratum (include inferior longitudinal fasciculus and inferior fronto-occipital fasciculus) L
33	External capsule R
34	External capsule L
35	Cingulum (cingulate gyrus) R
36	Cingulum (cingulate gyrus) L
37	Cingulum (hippocampus) R
38	Cingulum (hippocampus) L
39	Fornix (cres) / Stria terminalis (can not be resolved with current resolution) R
40	Fornix (cres) / Stria terminalis (can not be resolved with current resolution) L
41	Superior longitudinal fasciculus R
42	Superior longitudinal fasciculus L
43	Superior fronto-occipital fasciculus (could be a part of anterior internal capsule) R
44	Superior fronto-occipital fasciculus (could be a part of anterior internal capsule) L
45	Uncinate fasciculus R
46	Uncinate fasciculus L
47	Tapetum R
48	Tapetum L



Cingulum (cingulate gyrus) L

Splenium of corpus callosum

Anterior corona radiata L

Genu of corpus callosum

Anterior limb of internal capsule L

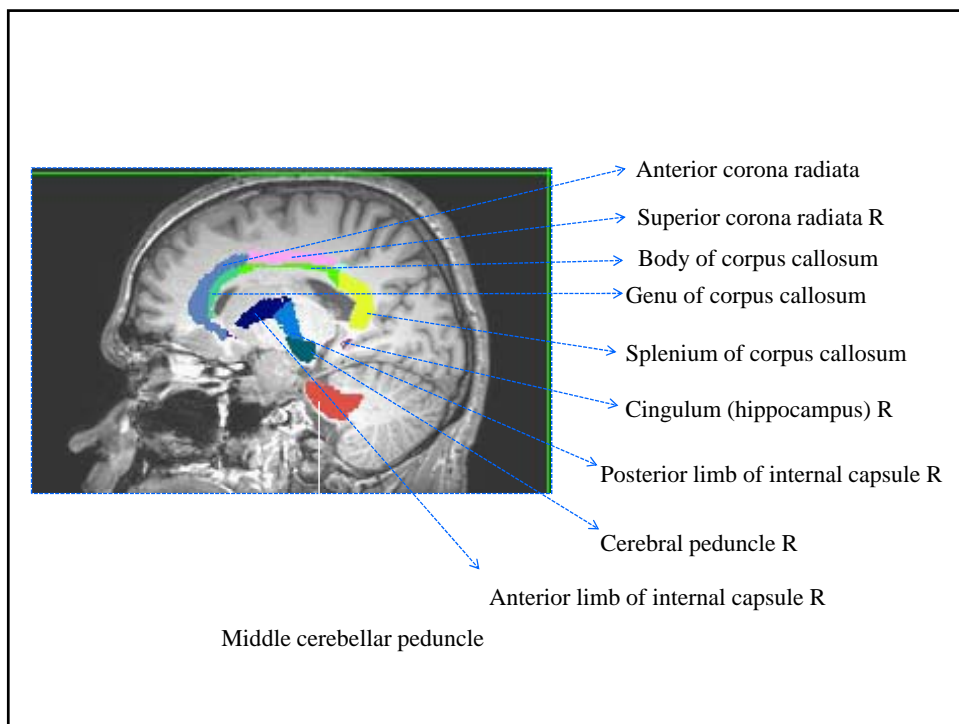
External capsule L

Posterior limb of internal capsule L

Retrolecticular part of internal capsule L

Superior longitudinal fasciculus L

Posterior thalamic radiation (include optic radiation) L



### Automated FA measurements

index	label	FA Value	Index	Label	FA Value
1	Middle cerebellar peduncle	0.348497	31	Sagittal stratum (include inferior longitudinal fasciculus and inferior fronto-occipital fasciculus) R	0.447041
2	Pontine crossing tract (a part of MCP)	0.414859	32	Sagittal stratum (include inferior longitudinal fasciculus and inferior fronto-occipital fasciculus) L	0.440027
3	Genu of corpus callosum	0.404761	33	External capsule R	0.322001
4	Body of corpus callosum	0.325766	34	External capsule L	0.333932
5	Splenium of corpus callosum	0.52199	35	Cingulum (cingulate gyrus) R	0.177297
6	Fornix (column and body of fornix)	0.373117	36	Cingulum (cingulate gyrus) L	0.154754
7	Corticospinal tract R	0.489382	37	Cingulum (hippocampus) R	0.227064
8	Corticospinal tract L	0.467688	38	Cingulum (hippocampus) L	0.226276
9	Medial lemniscus R	0.534683	39	Fornix (cres) / Stria terminalis (can not be resolved with current resolution) R	0.45711
10	Medial lemniscus L	0.544942	40	Fornix (cres) / Stria terminalis (can not be resolved with current resolution) L	0.432283
11	Inferior cerebellar peduncle R	0.277768	41	Superior longitudinal fasciculus R	0.346349
12	Inferior cerebellar peduncle L	0.289317	42	Superior longitudinal fasciculus L	0.346567
13	Superior cerebellar peduncle R	0.33122	43	Superior fronto-occipital fasciculus (could be a part of anterior internal capsule) R	0.333865
14	Superior cerebellar peduncle L	0.351684	44	Superior fronto-occipital fasciculus (could be a part of anterior internal capsule) L	0.300206
15	Cerebral peduncle R	0.468039	45	Uncinate fasciculus R	0.433751
16	Cerebral peduncle L	0.455127	46	Uncinate fasciculus L	0.461698
17	Anterior limb of internal capsule R	0.440927	47	Tapetum R	0.588981
18	Anterior limb of internal capsule L	0.40953	48	Tapetum L	0.610701
19	Posterior limb of internal capsule R	0.477165			
20	Posterior limb of internal capsule L	0.487003			
21	Retrolenticular part of internal capsule R	0.492149			
22	Retrolenticular part of internal capsule L	0.502794			
23	Anterior corona radiata R	0.336596			
24	Anterior corona radiata L	0.377241			
25	Superior corona radiata R	0.44589			
26	Superior corona radiata L	0.399122			
27	Posterior corona radiata R	0.393846			
28	Posterior corona radiata L	0.385009			
29	Posterior thalamic radiation (include optic radiation) R	0.462773			
30	Posterior thalamic radiation (include optic radiation) L	0.492928			



Product Line  
Review  
(PLR)  
Meeting

Medical  
Imaging  
Technologies

12 June 2012

23

## Software components

- XNAT
- FSL
- DTI Prep
- NINDS/DoD TBI Common Data Elements



Product Line  
Review  
(PLR)  
Meeting

Medical  
Imaging  
Technologies

12 June 2012

24

## XNAT

- XNAT is an open source imaging informatics platform, developed by the Neuroinformatics Research Group at Washington University. It facilitates common management, productivity, and quality assurance tasks for imaging and associated data. XNAT is extensible for use in a wide range of imaging-based projects.
  - <http://xnat.org/>
  - References:
    - Marcus, D.S., et al. (2007) **The Extensible Neuroimaging Archive Toolkit (XNAT): An informatics platform for managing, exploring, and sharing neuroimaging data.** Neuroinformatics 5(1): 11-34.
    - Marcus, D.S., et al. (2005) **XNAT: A Software Framework for Managing Neuroimaging Laboratory Data.** Organization for Human Brain Mapping Annual Meeting.



## FMRIB Software Library

FSL 4.1.9

[intro](#) - [list of tools](#) - [what's new](#) - [documentation, support, tutorials & training](#)  
[download](#) - [patches](#) - [example data](#) - [contributors](#) - [FSL & other software](#) - [licence](#)


FSL is a comprehensive library of analysis tools for FMRI, MRI and DTI brain imaging data. FSL is written mainly by members of the [Analysis Group, FMRIB, Oxford, UK](#). FSL runs on Apple and PCs (Linux and Windows), and is very easy to install. Most of the tools can be run both from the command line and as GUIs ("point-and-click" graphical user interfaces).

To quote the relevant references for FSL tools you should look in the individual tool's manual page (or the Analysis Group [publications page](#)), and also please reference the FSL overview papers:

- 1) M.W. Woolrich, S. Jbabdi, B. Patenaude, M. Chappell, S. Makni, T. Behrens, C. Beckmann, M. Jenkinson, S.M. Smith. Bayesian analysis of neuroimaging data in FSL. *NeuroImage*, 45:S173-186, 2009.
- 2) S.M. Smith, M. Jenkinson, M.W. Woolrich, C.F. Beckmann, T.E.J. Behrens, J.M. De Luca, I. Drobnjak, D.E. Flitney, R. Níaz, J. Saunders, J. Vickers, Y. Zhang, P.M. Matthews. Advances in functional and structural MR image analysis and implementation as FSL. *NeuroImage*, 23(S1):208-219, 2004.

The UK EPSRC is the largest provider of funding for the FMRIB Analysis Group. We are also very grateful for significant financial support from the [BBSRC](#), [GlaxoSmithKline CIC](#) and [Pfizer UK](#).

What's in FSL - see the [list of tools](#).



FSL

The Oxford Centre for Functional MRI of the Brain

Imaging Technologies

12 June 2012

CAMINO

25 June 2012

Imaging Group  
College London

### Camino

Diffusion MRI toolkit

Recent Changes - Search:

---

View Edit History Print

#### User Guide and Installation


Camino is a fully featured toolkit for Diffusion MR processing and reconstruction, including diffusion tensor techniques, tractography and advanced algorithms for resolving non-Gaussian diffusion profiles, the so-called fibre-crossing problem. Camino is written entirely in Java, and is an open source development project, meaning that anyone can contribute to the project.

This document is a brief introduction to the Camino toolkit, the philosophy behind it and a jumping-off point for starting to use Camino in your own projects. We start by discussing the installation of Camino, including installation under Windows using Cygwin, and then discuss building and testing the toolkit and conclude with some simple ways to use Camino. Here we assume no prior knowledge of the systems side of things at all and (hopefully) will explain enough so that the remainder of the case-studies included on this website will be readily accessible for more complicated uses of Camino.

#### Installing Camino

Camino can be installed under Linux/Unix, Mac OS X and Windows. For more detailed instructions and requirements, click on the links below:

[Installing Camino in Linux/Unix](#)  
[Installing Camino in Windows](#)  
[Installing Camino in OS X](#)



**Product Line Review (PLR) Meeting**

Medical Imaging Technologies

12 June 2012

26

# FSL

- FSL is a comprehensive library of analysis tools for FMRI, MRI and DTI brain imaging data. FSL is written mainly by members of the Analysis Group, FMRIB, Oxford, UK.
- <http://www.fmrib.ox.ac.uk/fsl/>
- References:
  - 1) M.W. Woolrich, et al. **Bayesian analysis of neuroimaging data in FSL**. *NeuroImage*, 45:S173-186, 2009.
  - 2) S.M. Smith, et al. **Advances in functional and structural MR image analysis and implementation as FSL**. *NeuroImage*, 23(S1):208-219, 2004.



Product Line  
Review  
(PLR)  
Meeting

Medical  
Imaging  
Technologies

12 June 2012

27

## DTI Prep

- DTIPrep performs a "Study-specific Protocol" based automatic pipeline for DWI/DTI quality control and preparation. This is both a GUI and command line tool.
- The configurable pipeline includes:
  - Dicom to NRRD converting
  - Image information checking
  - Diffusion information checking
  - Slice-wise intensity artifact checking
  - Interlace-wise venetian blind artifact checking
  - Baseline averaging
  - Eddy-current and head motion artifact correction
  - Motion artifact checking
- Source: Neuroimaging Informatics Tools and Resources Clearinghouse (NITRC)
  - <http://www.nitrc.org/projects/dtiprep/>



Product Line  
Review  
(PLR)  
Meeting

Medical  
Imaging  
Technologies

12 June 2012

28

## Data Formats

- **DICOM** – imaging industry interchange format
- **NRRD - Nearly Raw Raster Data**
  - Nrrd is a library and file format designed to support scientific visualization and image processing involving N-dimensional raster data.
  - <http://teem.sourceforge.net/nrrd>
- **NifTI - Neuroimaging Informatics Technology Initiative**
  - NifTI-1 is a widely used data format, originally developed by an NIH-sponsored working group to promote interoperability of functional neuroimaging software tools, especially fMRI.
  - <http://nifti.nimh.nih.gov/nifti-1/>



Product Line  
Review  
(PLR)  
Meeting

Medical  
Imaging  
Technologies

12 June 2012

29

## Project Team

- University of Chicago
  - Michael Vannier
  - Jia-Hong Gao
  - Xia Jiang
  - Greg Karczmar
- VA Center of Excellence (Waco, TX)
  - Texas Tech Univ Medical School
  - Scott & White Clinic
  - (Formerly UIChicago)
  - Deb Little
- Computation Institute
  - Univ of Chicago / ANL
  - Ian Foster
  - Steve Tuecke
  - Rachana Ananthakrishnan
  - Kyle Chard
  - Farid Dahi
  - Gordon Kindlmann



Product Line  
Review  
(PLR)  
Meeting

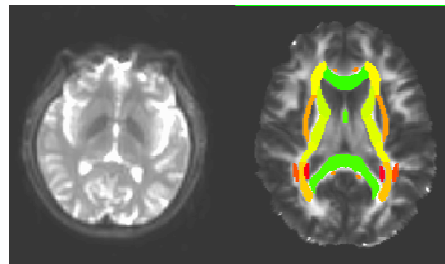
Medical  
Imaging  
Technologies

12 June 2012

30

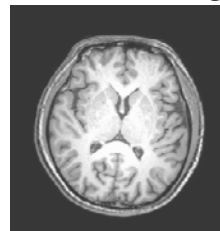
### DTI Protocol

- Number of diffusion gradient directions = 41
- Number of b = 0 images: 5
- b value = 1000
- TR/TE = 8773 ms/52 ms
- Flip angle = 90°
- FOV = 250 x 250 x 146 mm<sup>3</sup>
- Matrix size = 96 x 96
- Slice number = 56
- Slice gap = 0
- Resolution = 2.6 x 2.6 x 2.6 mm<sup>3</sup>
- Sense factor = 2
- **Total scan time = 7 min**



### High resolution 3D T1 weighted anatomical image

- FOV = 256 x 256 x 146 mm<sup>3</sup>
- Resolution = 1 x 1 x 1 mm<sup>3</sup>
- TR/TE = 10 ms/4.6 ms
- Flip angle = 8°
- **Total scan time = 5 min**





Product Line  
Review  
(PLR)  
Meeting

Medical  
Imaging  
Technologies

12 June 2012

31

## Validation Strategy

Many published studies on D-MRI of TBI have produced results – analyzed only once

Test automated tools – will they reproduce the published results?

Repository with integrated tools enables secondary analyses – testing with NDAR, Pediatric brain MRI study, ADNI and related datasets

Plan to test system with FITBIR – when available



Product Line  
Review  
(PLR)  
Meeting

Medical  
Imaging  
Technologies

12 June 2012

32

### DTI Protocol

- Number of diffusion gradient directions = 41
- Number of b = 0 images: 5
- b value = 1000
- TR/TE = 8773 ms/52 ms
- Flip angle = 90°
- FOV = 250 x 250 x 146 mm<sup>3</sup>
- Matrix size = 96 x 96
- Slice number = 56
- Slice gap = 0
- Resolution = 2.6 x 2.6 x 2.6 mm<sup>3</sup>
- Sense factor = 2
- **Total scan time = 7 min**

### High resolution 3D T1 weighted anatomical image

- FOV = 256 x 256 x 146 mm<sup>3</sup>
- Resolution = 1 x 1 x 1 mm<sup>3</sup>
- TR/TE = 10 ms/4.6 ms
- Flip angle = 8°
- **Total scan time = 5 min**

## DTI voxel-wise correlation (human brain) – Intra-day

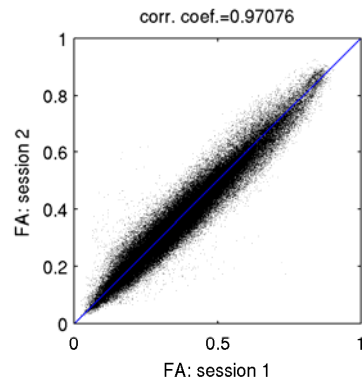


Fig.1. Intraday reproducibility of FA (for all voxels in the 48 white matter ROIs)

Fractional Anisotropy (FA)

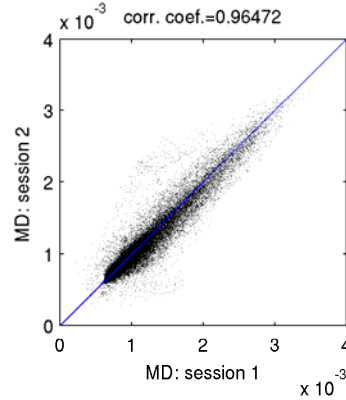


Fig.2. Intraday voxel-wise reproducibility of MD (for all voxels in the 48 white matter ROIs)

Mean Diffusivity (MD)

## DTI voxel-wise correlation (human brain) – Inter-day

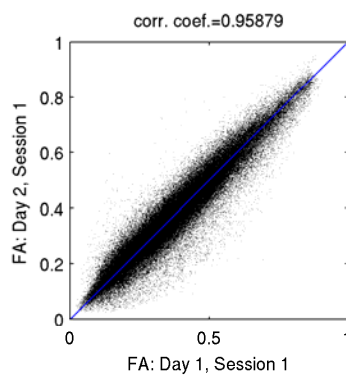


Fig.3. Interday reproducibility of FA (for all voxels in the 48 white matter ROIs)

Fractional Anisotropy (FA)

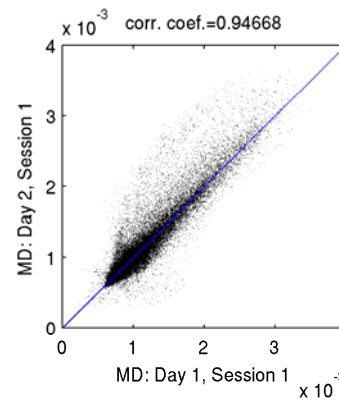


Fig.4. Interday voxel-wise reproducibility of MD (for all voxels in the 48 white matter ROIs)

Mean Diffusivity (MD)



International Neuroimaging  
Data-Sharing Initiative



Open science initiatives are transforming the neuroimaging community. Researchers who once struggled to obtain 20-30 datasets now have unrestricted access to thousands of scans, including data obtained from developing, aging and clinical populations.



CHILD MIND  
INSTITUTE

The International Neuroimaging Data-sharing Initiative (INDI) is now sponsored by the Child Mind Institute ([childmind.org](http://childmind.org)).

# FITBIR

## Federal Interagency Traumatic Brain Injury Repository

Matthew J. McAuliffe, PhD  
Chief, Biomedical Imaging Research  
Services Section (BIRSS)  
NDAR Project Manager  
Co-director FITBIR project  
[Matthew.McAuliffe@nih.gov](mailto:Matthew.McAuliffe@nih.gov)

301 594-2432 desk

240 839-0076 cell

Web: [mipav.cit.nih.gov](http://mipav.cit.nih.gov)



# FITBIR

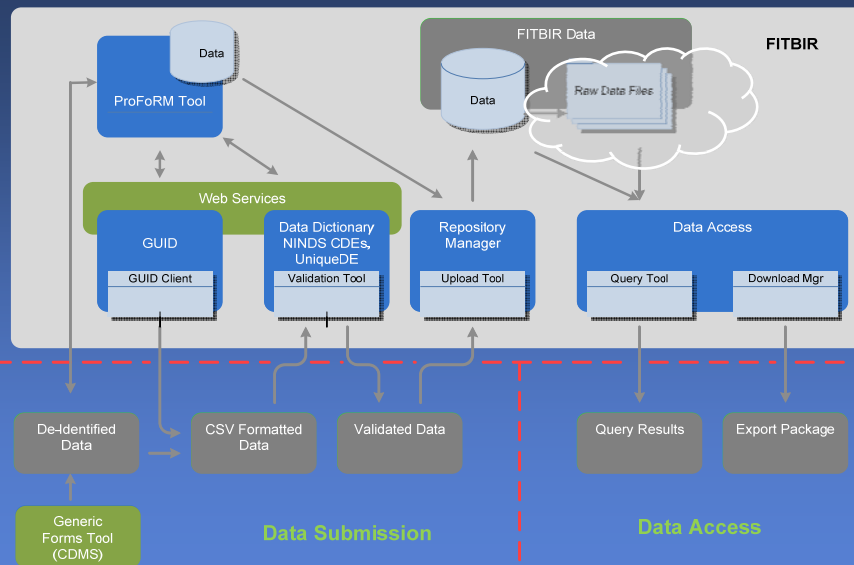
The FITBIR is a collaborative biomedical *informatics system* to support research in Traumatic Brain Injury to accelerate scientific discovery and treatment.

FITBIR mission goals:

1. **Development of standards and policies** to enable cross site meta-analysis and data comparisons (i.e. NINDS TBI **CDEs, GUID**)
2. **Central/federated** repository and portal for **phenotypic, genomic, and imaging data**.
3. Promotion for the **sharing of quality research data** throughout the TBI research community
  - a. Attribution for shared data
  - b. Timing of sharing data
4. Deployment of useful **tools** for community adoption

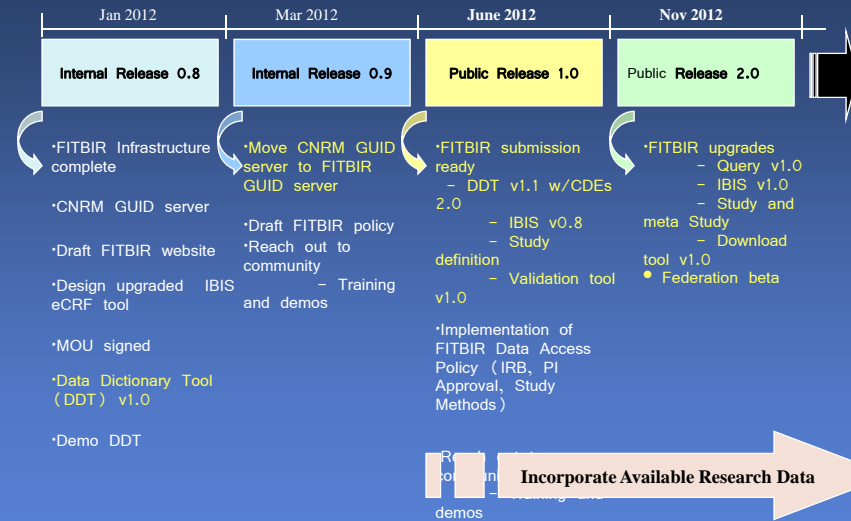


# FITBIR





## FITBIR Roadmap



**Draft – June 2012**



Product Line  
Review  
(PLR)  
Meeting

Medical  
Imaging  
Technologies

12 June 2012

Federal Interagency Traumatic Brain  
Injury Research Informatics System  
(FITBIR)

Policy Document



## D-MRI Data Acquisition & Quality Control

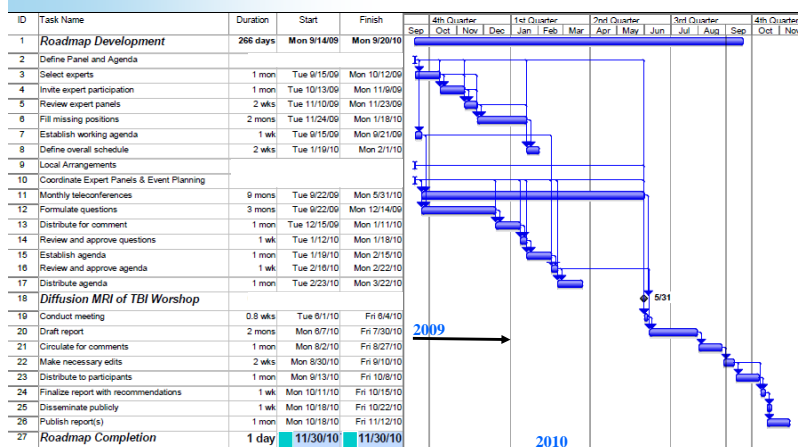
### Research/Development Timeline

Product Line  
Review  
(PLR)  
Meeting

Medical  
Imaging  
Technologies

12 June 2012

41



Product Line  
Review  
(PLR)  
Meeting

Medical  
Imaging  
Technologies

12 June 2012

42

### Successes to Date

New D-MRI data acquisition schemes and protocols for clinical MRI system (Philips)

On-line repository and integrated software analysis tools are available

Reproducibility testing – of parcellated brain regions – using automated tools



Product Line  
Review  
(PLR)  
Meeting

Medical  
Imaging  
Technologies

12 June 2012

43

## Challenges

Access to datasets is difficult – perhaps FITBIR will solve this

Site qualification and quality control may become important



Product Line  
Review  
(PLR)  
Meeting

Medical  
Imaging  
Technologies

12 June 2012

44

## What's Next

Plan an international workshop with software tool developers with D-MRI expertise

Unique aspect is to attract interest focused on D-MRI of TBI (rather than normal brain white matter) – so the challenges of TBI can be addressed

Availability of FITBIR as a federated TBI data archive necessitates integration of software tools to facilitate analysis that realizes it's potential – we're working to address this need



Product Line  
Review  
(PLR)  
Meeting

Medical  
Imaging  
Technologies

12 June 2012

45

## Compare Competing Solutions

What relevant ongoing solutions are being pursued by others?

- Many groups have their own software infrastructure for image analysis

Describe the market(s), if applicable:

- No commercial offering in this area
- Potential market for evaluation of TBI datasets obtained with DTI – many scanners, but few analysis sites



Product Line  
Review  
(PLR)  
Meeting

Medical  
Imaging  
Technologies

12 June 2012

46

## Intellectual Property / Publications Deriving from this Project

List any Confidentiality Agreements – None



Patents Filed - None

List Invention Disclosures Submitted – None

List all Publications deriving from the project:

**A Tamhane, K Arfanakis, M Anastasio, X Guo, M Vannier, JH Gao.** "Rapid PROPELLER-MRI: A Combination of Iterative Reconstruction and Under-Sampling", Journal of Magnetic Resonance Imaging, in press.

**M. Vannier, et al. Diffusion MRI of traumatic brain Injury roadmapping project**, CARS 2010 annual meeting, Geneva, 26 June 2010. Published in Int J CARS (2010) 5 (Suppl 1):S39-S44.

Product Line  
Review  
(PLR)  
Meeting



Medical  
Imaging  
Technologies

12 June 2012

47

## Transition/ Business/ Marketing Plan

Describe plan, if applicable

Product Line  
Review  
(PLR)  
Meeting

Medical  
Imaging  
Technologies

12 June 2012

48

## Project Funding

<u>Current Budget</u>	<u>Expended Funds</u>	<u>%</u>
\$972,637	\$989,893	60%

UIC subcontract was terminated after PI departed.

**Other Funding if applicable: None**



Product Line  
Review  
(PLR)  
Meeting

Medical  
Imaging  
Technologies

12 June 2012

49

## Additional Project Information

**Lab/Company/Group: University of Chicago**

**Principal Investigator: Dr. Michael Vannier**

**Government COR: Dr. Anthony Pacifico**

**Government Project Officer: Laurie Haines**

**Contract Instrument: Cooperative Agreement**

**Period of Performance: 14 September 2009 – 13  
October 2012**

**Contract Specialist:**

**EDMS# : 3906**

**Contract #: W81XWH0920102**

**\*\* To Be Completed by  
COR or Project Officer**

## Appendix 11:

Xia Jiang, et al. Slice Timing  
Correction in Volume  
Selective z-shim fMRI  
Acquisition. Organization for  
Human Brain Mapping,  
Beijing, CN (2012).



## Slice Timing Correction in Volume Selective z-shim fMRI Acquisition

### Presented During:

Wednesday Poster Stand-By Session

Wednesday, June 13, 2012: 1:30 PM - 3:30 PM

Room: Plenary Hall, Level 4

### Poster No:

588

### On Display:

Wednesday, June 13 & Thursday, June 14

### Authors:

Xia Jiang<sup>1</sup>, Xiaodong Guo<sup>1</sup>, Fang Zhu<sup>1</sup>, Michael Vannier<sup>1</sup>, Jia-Hong Gao<sup>1</sup>

### Institutions:

<sup>1</sup>Brain Research Imaging Center and Department of Radiology, University of Chicago, Chicago, IL

### Poster Presenter:

*Xia Jiang* - Contact Me  
University of Chicago  
Chicago, United States

### Introduction:

Susceptibility-induced magnetic field gradient caused by air-tissue interface can lead to severe MRI signal loss at orbitofrontal cortex (OFC) and inferior temporal regions in a gradient-echo EPI scans (Fig. 1a). One way to recover such signal loss, termed the z-shim technique (Frahm 1988), is to acquire additional images with a compensation gradient, and then combine these images (referred to as ZS images below) with the original images (referred to as NZS images below). An overlooked problem with this method is that the ZS image and the corresponding NZS image are acquired at slightly different times in the volume selective z-shim technique (Du, et al., 2007), which could lead to lowered statistical power in fMRI studies if these two images are combined before performing slice timing correction (STC). In this study, we will make quantitative assessment of the potential problem in functional maps associated with STC performance.

### Methods:

Simulation was performed by artificially adding activity to resting state fMRI scan. The fMRI scan was acquired from one adult subject at 3 T using a gradient EPI sequence with TR/TE = 2 s/30 ms, voxel size = 2.85 x 2.85 x 5 mm<sup>3</sup> and 400 time points. A volume selective z-shim scheme (Du et al., 2007) was employed. Twenty-eight slices were prescribed to cover the whole brain and z-shim was performed only for 4 of the slices that cover the OFC region. During each TR, these 4 slices were first acquired without compensation gradient at the center of TR (NZS), and then acquired again with the compensation gradient at the end of the TR (ZS), leading to a time shift of 1 sec between the NZS and ZS images. A 2% of signal increase was added to two spherical ROIs at OFC and visual area (Fig. 1d). The latter served as control. The signal time course was generated from an event related experimental design convolved with the canonical hemodynamic response function. The interstimulus interval (ISI) was set to be 4s, 8s, 12s and 16s. The stimulus onsets were jittered according to a uniform distribution within 50% of ISI (Sladky et al., 2011). The data were then processed based on three schemes: I, without STC, II, STC after image combination and III, STC before image combination. STC was performed with a sinc interpolation using AFNI (Cox 1996). After this step, all data were motion corrected, spatially smoothed with a FWHM = 5mm Gaussian kernel and analyzed using the general linear model (GLM).

Imaging Methods BOLD fMRI 6365  
Jiang 588 WTh Wednesday, June 13, 2012

Jiang, X, et al. (2012). Slice Timing Correction in Volume Selective z-shim fMRI Acquisition. Poster presented at the 18th Annual Meeting of the Organization for Human Brain Mapping, Beijing, China.

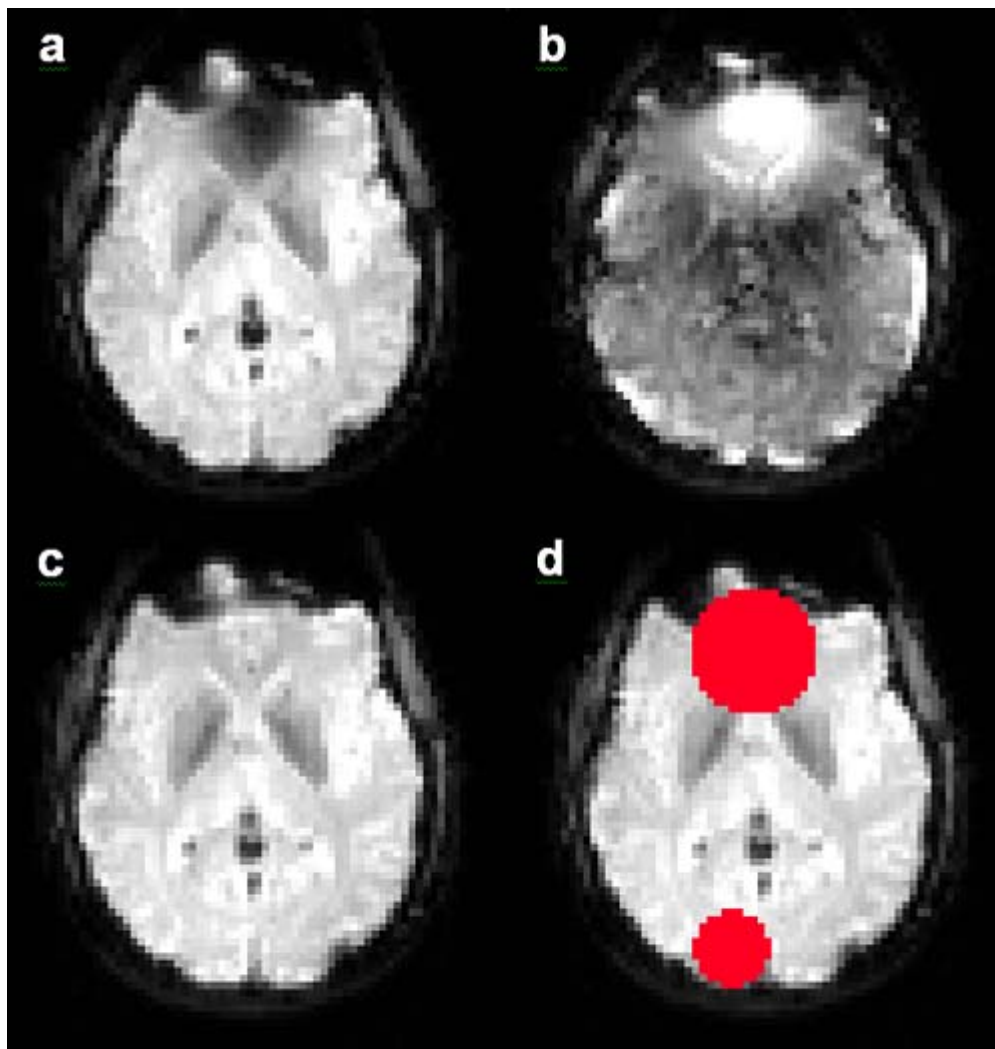


**Figure 1.** (a) and (b): a representative slice at OFC level acquired without and with the z-shim compensation gradient. (c): Combined image from (a) and (b). (d): Two ROIs in which simulated activity was added to the raw signal.

#### Results:

The signal loss due to the susceptibility gradient is clearly visible in Fig. 1a and z-shim effectively recovered the signal loss (Fig. 1c). The t-static maps obtained from the three scenarios for ISI = 8s are shown in Fig. 2 at  $p < 0.001$  level (uncorrected). Schemes I and II successfully detected most activation in both ROIs, but missed a few voxels at the OFC, where the signal loss is most severe. Scheme III correctly detected activation in those voxels, and also showed a general improvement in t-value in the ROI at OFC. Fig. 3 shows the improvement in the fitted coefficient beta from the GLM by comparing scheme III to scheme II. A clear increase in beta can be seen at the signal loss region. On the other hand, only small improvement is seen in ROI at visual area and at the edge of the ROI at OFC. This is expected because performing STC before combination most benefited the ZS slices, not the NZS slices. And in the signal loss region, the majority of the signal comes from the NZS slices, while in the rest of the image, signal mostly comes from the NZS slices (Fig. 1 a and b). For all ISIs, significant improvement in beta was found in the signal loss region (Table I).

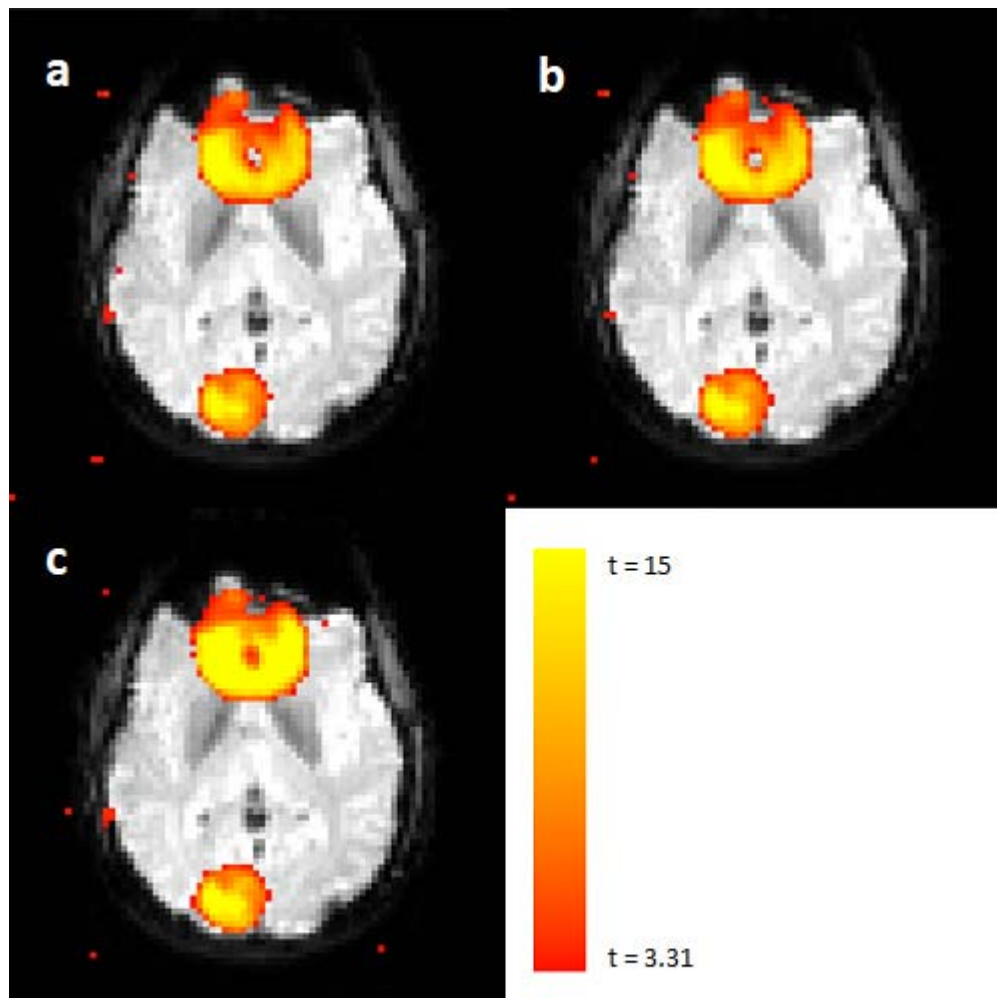


**Figure 2.** t-static map obtained from the GLM analysis. (a): No STC performed. (b): STC was performed after image combination. (c): STC was performed before image combination. All t maps were thresholded at  $p < 0.001$  level (uncorrected).

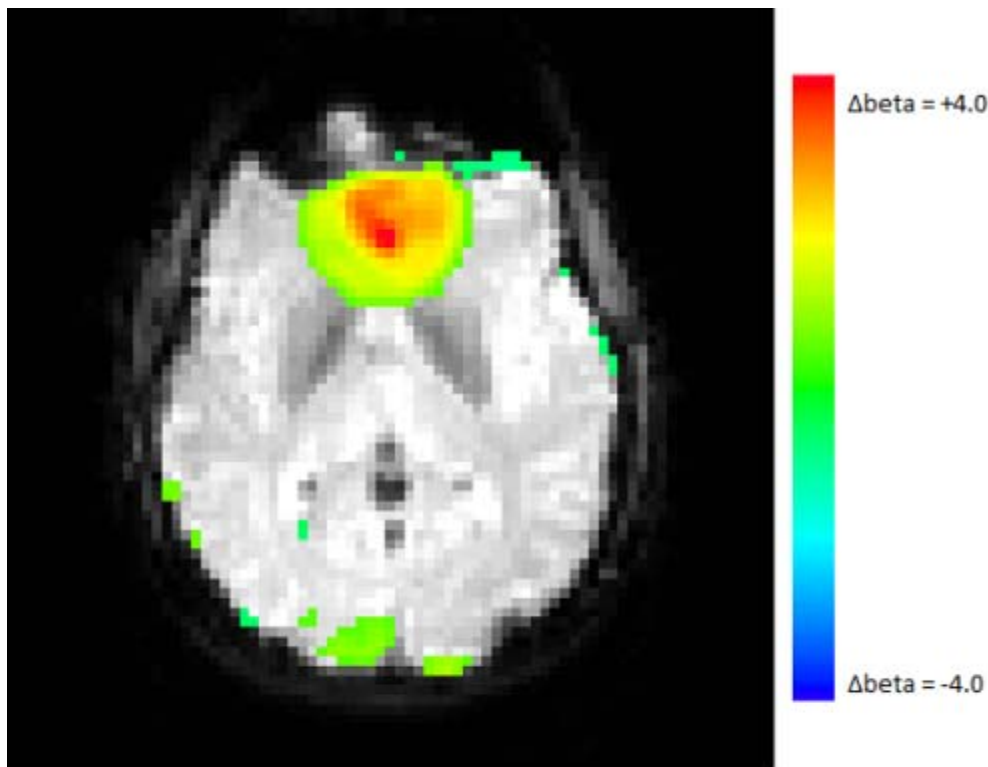


**Figure 3.** Comparison between scheme III and II for ISI = 8 s. Color map corresponds to improvement in the fitted coefficient beta, and only change greater than 0.5 is shown. Significant increase in beta was seen in the ROI at OFC by performing STC before image combination. Only slight increase was found in the ROI at visual area.

**Table I.** Percentage increase in beta in the signal loss region by performing STC before image combination, compared to performing STC after image combination.

ISI	4 ± 2 s	8 ± 4 s	12 ± 6 s	16 ± 8 s
% change in beta	30 ± 8	73 ± 38	25 ± 22	37 ± 11

#### Conclusions:

The z-shim technique effectively recovers signal loss at OFC in a time efficient way in fMRI studies, and the statistical power in detecting activation areas can be further improved if STC is performed before image combination, especially for event-related designs.

#### Imaging Methods:

BOLD fMRI

#### Abstract Information

#### References

- Cox RW (1996) AFNI: software for analysis and visualization of functional magnetic resonance neuroimages. *Comput Biomed Res* 29,162-173.
- Du Y.P., Dalwani M., Wylie K., Claus E., Tregellas J.R. (2007), Reducing susceptibility artifacts in fMRI using volume-selective z-shim compensation, *Magnetic Resonance in Medicine*, 57(2), 396-404.
- Frahm J., Merboldt K.D., Hänicke W. (1988), Direct FLASH MR imaging of magnetic field inhomogeneities by gradient compensation, *Magnetic Resonance in Medicine*, 6(4), 474-80.
- Sladky R., Friston J.K., Tröstl J., Cunningham R., Moser E., Windischberger C. (2011), Slice-timing effects

and their correction in functional MRI, *NeuroImage* 58, 588–594.

## Appendix 12.

Xia Jiang, et al. Partial  
Volume Effect in Diffusion  
Tensor Imaging: a Phantom  
Study (manuscript)

# **Partial Volume Effect in Diffusion Tensor Imaging: a Phantom Study**

**Xia Jiang, Kyle Chard, Jia-Hong Gao, Michael Vannier**

## **Introduction**

Diffusion Tensor Imaging (DTI), originally proposed by Basser et al. (1994), takes advantage of hindered water molecule diffusion perpendicular to the axons, compared to diffusion parallel with the axons, in the brain white matter. DTI measurements have been shown to reflect changes in the white matter related to aging (Johns 2006, Bastin et al. 2010, Yassa et al. 2010), various psychiatric disorders (Lim and Helpner 2002, Kanaan et al. 2005, Bozzali et al. 2002, Fellgiebel et al. 2004), and brain injury (Arfanakis et al. 2002, Bendlin et al. 2008). A well known confounding factor in DTI is the partial volume effect (PVE), where intra-voxel tissue inhomogeneity degrades DTI measurements (Alexander et al. 2001, Pfefferbaum and Sullivan 2003). Yet this effect is not commonly considered in most studies employing DTI. A previous study (Vos et al. 2011) examined the impact of PVE on DTI metrics extensively using simulated fiber bundles, and found that DTI metrics correlated with fiber bundle volume, orientation and curvature. This work aims to verify some of the findings by the above mentioned paper in a DTI phantom, and demonstrate the effect of sampling grid position and voxel size on fractional anisotropy (FA) and mean diffusivity (MD).

## **Methods**

### **Experiment 1**

Voxels affected by the PVE have signal contributions from more than one tissue types, hence the relative position of the voxel and the tissue boundary would affect the resultant DTI metrics. Such "gridding effect" has been previously described by Vos et al. (2011) based on theoretical simulations. This experiment aims to verify this effect in phantom by shifting the DTI acquisition sampling grid.

### **DTI phantom**

The DTI phantom (Brain Innovation BV) was a 16-cm-diameter sphere filled with  $\text{MnCl}_2 \cdot 4\text{H}_2\text{O}$  solution to mimic human white matter  $T_2$ . Submerged in the solution were 12 cylindrical fiber bundles, each consisting of 10,000 parallel polyester to mimic white matter anisotropy through restricted diffusion. The fibers were  $\sim 14$  cm long and  $\sim 7$  mm in diameter.

### **Data acquisition**

DTI data were acquired on a Philips Achiva 3.0 T MRI scanner using single-shot spin-echo EPI sequences with an isotropic resolution of 2.6 mm. 41 diffusion encoding directions and a b-value



of 1000 was used, with 5  $B_0$  images and a parallel imaging (SENSE) factor of 2. The time for each DTI scan was about 7 minutes. To test the "gridding effect", 11 DTI scans were made with identical parameters, except that the sampling grid was shifted in the slice selection direction by 1/10 of a voxel for each scan, so that in the last scan, the grid was moved by exactly 1 voxel from the first scan. A structural image of the phantom was acquired using a  $T_1$ -weighted 3D rapid acquisition with refocused echoes (RARE) sequence with  $TR/TE = 9.6 \text{ ms}/4.6 \text{ ms}$ .

### **Image processing**

DTI images were processed using the diffusion toolbox in the FSL software package. First, eddy current correction was performed on the raw images. In order to compare the results from different scans, the eddy-current-corrected images were then registered to a common  $T_1$ -weighted structural image using the linear registration tool in FSL with 9 degrees of freedom. This step also served to resample the data to a higher resolution (1 mm) grid. Tensor fitting was then performed on the registered images and FA and MD were calculated. Regions of interest (ROIs) were manually drawn on the  $T_1$  image to cover each of the fiber bundles for calculation of ROI-averaged FA and MD.

## **Experiment 2**

In this experiment, we test the effect of spatial resolution on DTI metrics. The assumption is that at higher resolution, a lower ratio of voxels is affected by the PVE, and quality of DTI measurements should improve.

### **Data acquisition**

The same phantom and DTI protocol as in Experiment 1 was used, except that seven different isotropic spatial resolutions were used, from 1.4 mm to 3.2 mm with 0.3 mm interval. The seven DTI scans were performed with the phantom staying in the same position. Then the phantom was shifted to a slightly different position and orientation, and another seven scans were made. This process was repeated for four times to evaluate the variability between scans.

### **Image processing**

The same image processing steps as in Experiment 1 were used.

## Results

### Experiment 1

Fig. 1 (b) and (c) shows voxel-wise FA and MD as functions of sampling grid position. Shown here are 8 voxels across a fiber bundle, marked by the red line segment in Fig. 1(a). And the direction of grid shifting is indicated by the white arrow in Fig. 1(a). The effect of grid position on FA and MD at ROI level is shown in Fig. 2 (a) and (b).

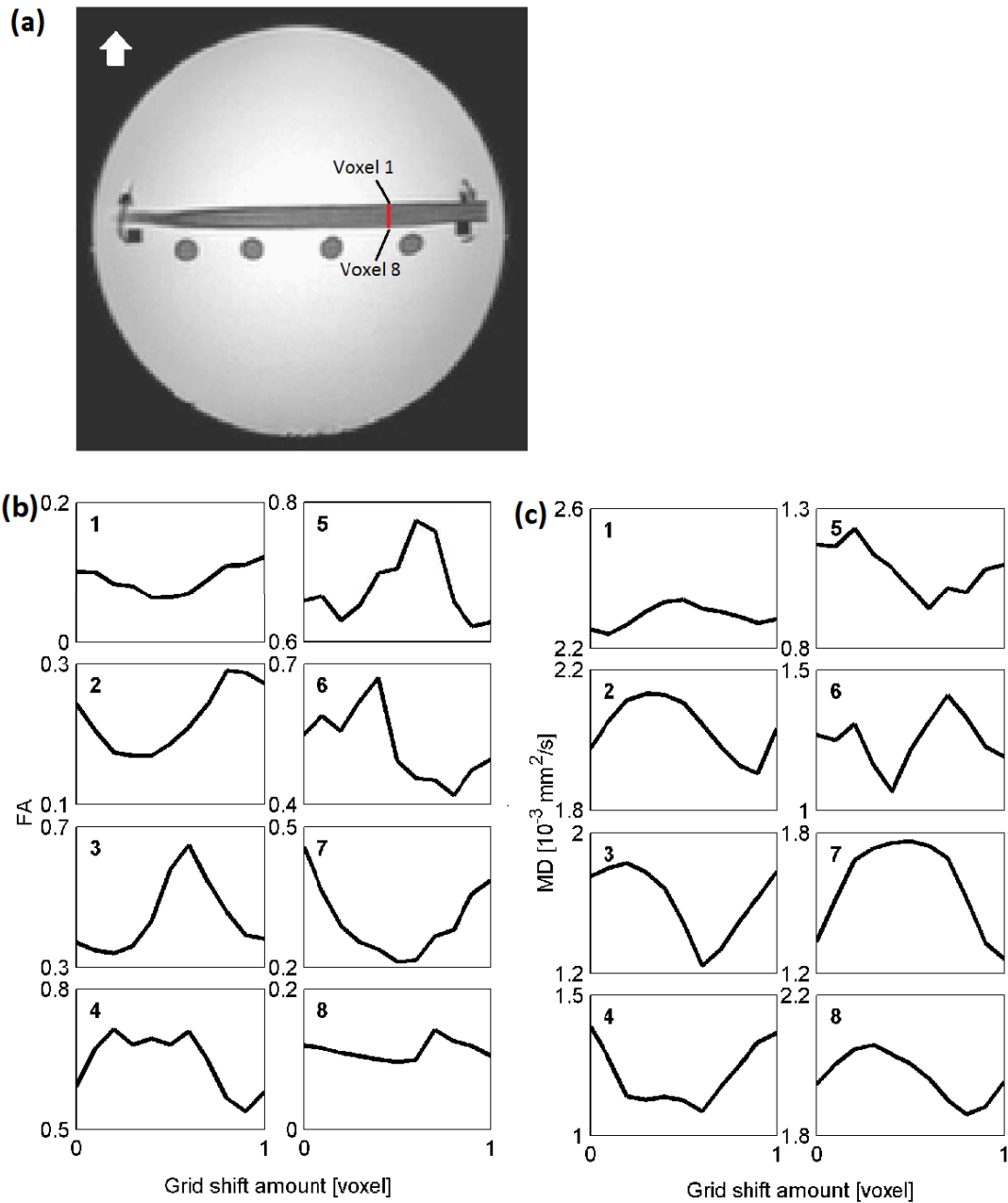


**Figure 1.** Effect of shifting sampling grid at voxel level. (a) A  $T_1$  structural image of the DTI phantom with 1 mm isotropic resolution. The red line segment marks 8 voxels across the fiber bundle for which FA and MD are shown in (b) and (c) respectively. (b) FA as a function of sampling grid position. (c) MD as a function of sampling grid position. The numbers 1-8 in (b) and (c) correspond to the voxel number as is marked in (a).

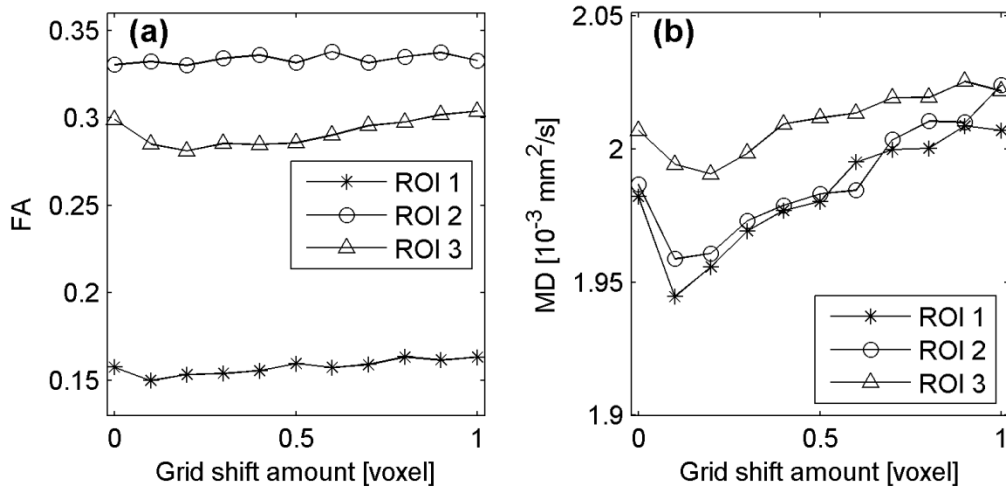


**Figure 2.** Effect of shifting sampling grid at ROI level. The FA (a) and MD (b) averaged over three orthogonally aligned fiber bundles are shown as functions of grid shift. The ROIs 1-3 corresponded to fibers aligned in the slice selection, phase encoding and frequency encoding directions respectively.

## Experiment 2

FA and MD measurement as a function of acquisition voxel size is given in Fig. 3. Shown here are ROI-averaged values in one representative fiber bundle measured over 4 sessions.

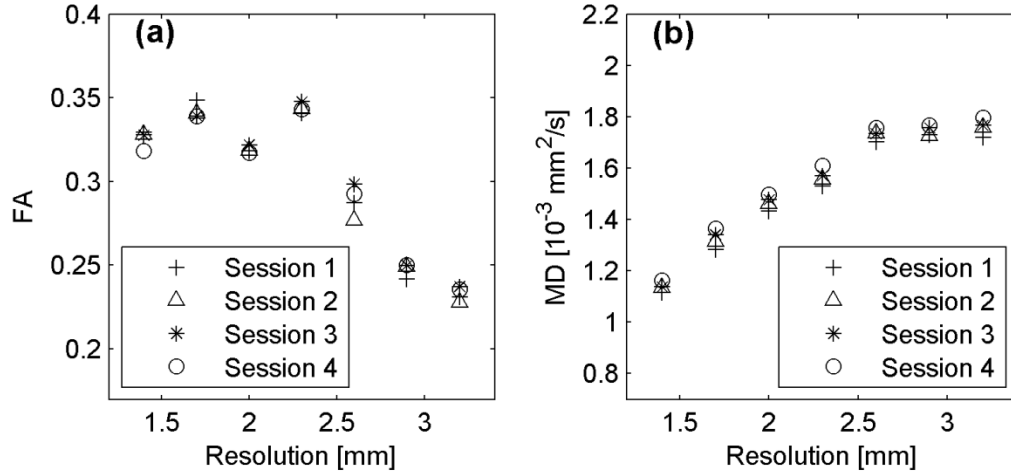


**Figure 3.** ROI-wise FA (a) and MD (b) as functions of spatial resolution. Seven isotropic resolutions were used in DTI acquisition, from 1.4 mm to 3.2 mm with 0.3 mm interval. And measurements were repeated over 4 sessions.

## Discussions and Conclusions

In experiment 1, both FA (Fig.1(b)) and MD (Fig.1(c)) showed strong dependence on grid position at voxel level, confirming the simulation results in previous work (Vos et al. 2011). The value of FA and MD returned to close to their original values as the shifting amount became exactly one voxel, as is expected. Comparing Fig 1 (b) and (c), it can be observed that FA and MD showed a clear anti-correlation, which can be readily explained by the fact that when more solution is included in a PVE voxel, the solution will reduce the voxel's FA and increase its MD. Shifting grid position may change FA by as much as 100% and MD by as much as 50% in our phantom at voxel level. However, since the extreme values in each voxel are reached at different grid positions (Fig 1 (b) and (c)), this effect tends to cancel out and becomes much less significant at ROI level (Fig. 2), where FA variation is less than 8% and MD variation is less than 5%.

In experiment 2, the measured FA was more consistent at higher resolutions and decreased with voxel size at lower resolution. Clearly at lower resolutions PVE becomes more prominent, and contributions of signal from outside the fiber bundles caused average FA to drop. The resolution threshold beyond which FA measurement began to drop was 2.3 mm, which was about 1/3 of the diameter of the fiber bundles. MD, on the other hand, increased almost linearly with voxel size up until 2.6 mm, and remained at about the same level for greater voxel sizes. These conclusions are parallel to previous findings (Vos et al. 2011) that FA increases with and MD decreases with the volume of fiber bundle, as reduction of voxel size can be viewed as a relative increase in

bundle volume, if the fiber bundle is considered to be homogeneous and the difference in signal to noise ratio is ignored. The variation of DTI metrics at ROI-level among the 4 sessions (standard deviation divided by mean) was about 2-4% for FA and 1-2% for MD , and did not show clear evidence of improvement at higher resolutions.

In conclusion, we have confirmed some previous simulation results on PVE (Vos et al. 2011) by showing that in a diffusion phantom, (1) the position of the sampling grid can have significant impact on DTI metrics at voxel level, but becomes less important at ROI level. Therefore the "gridding effect" may be safely ignored if only ROI level metrics are used in analysis. (2) FA decreases with, while MD increases with, voxel size. Therefore higher resolution could help improve the accuracy of both FA and MD measurements, which of course will be restricted by acquisition time in reality. But it should be kept in mind, when interpreting DTI data, that FA is likely to be underestimated while MD overestimated, especially for thinner fiber bundles. It should be pointed out that in this study, the effect of fiber crossing was not considered due to the limitation of the phantom. In reality this effect will further add to the PVE and degrade DTI measurements.

## **References**

- Jones et al 2006 - Age effects on diffusion tensor magnetic resonance imaging tractography measures of frontal cortex connections in schizophrenia. *Hum. Brain Mapp.* 27 (3), 230–238. 2006.
- Bastin et al. 2010 - Quantifying the effects of normal ageing onwhitematter structure using unsupervised tract shape modelling. *Neuroimage* 51 (1), 1–10.
- Yassa et al. 2010 - Ultrahigh-resolution microstructural diffusion tensor imaging reveals perforant path degradation in aged humans in vivo. *Proc Natl Acad Sci U S A.* 2010 Jul 13;107(28):12687-91.
- Lim and Helpert 2002 - Neuropsychiatric applications of DTI - a review. *NMR Biomed.* 2002 Nov-Dec;15(7-8):587-93.
- Kanaan et al. 2005 - Tract-specific anisotropy measurements in diffusion tensor imaging. *Psychiatry Res.* 2006 Jan 30;146(1):73-82.
- Bozzali et al. 2002 - Quantification of brain gray matter damage in different MS phenotypes by use of diffusion tensor MR imaging. *AJNR Am J Neuroradiol.* 2002 Jun-Jul;23(6):985-8.
- Fellgiebel et al. 2004 - Ultrastructural hippocampal and white matter alterations in mild cognitive impairment: a diffusion tensor imaging study. *Dement Geriatr Cogn Disord.* 2004;18(1):101-8.
- Arfanakis et al. 2002 - Diffusion tensor MRI in temporal lobe epilepsy. *Magn Reson Imaging.* 2002 Sep;20(7):511-9.
- Bendlin et al. 2010 - White matter in aging and cognition:a cross-sectional study of microstructure in adults aged eighteen to eighty-three. *Dev. Neuropsychol.* 35 (3), 257–277.
- Alexander et al. 2001 - Alexander, A.L., Hasan, K.M., Lazar, M., Tsuruda, J.S., Parker, D.L., 2001. Analysis of partial volume effects in diffusion-tensor MRI. *Magn. Reson. Med.* 45 (5), 770–780.
- Pfefferbaum and Sullivan 2003 - Increased brain white matter diffusivity in normal adult aging: relationship to anisotropy and partial voluming. *Magn Reson Med.* 2003 May;49(5):953-61.
- Vos et al 2011 - Vos SB, Jones DK, Viergever MA, Leemans A. Partial volume effect as a hidden covariate in DTI analyses. *Neuroimage.* 2011 Apr 15;55(4):1566-76.